FUNCTIONAL CHARACTERIZATION OF ODORANT RECEPTORS IN DISEASE VECTOR MOSQUITOES

By

Patrick L. Jones

Dissertation

Submitted to the Faculty of the

Graduate School of Vanderbilt University

in partial fulfillment of the requirements

for the degree of

DOCTOR OF PHILOSOPHY

in

Biological Sciences

May, 2011

Nashville, Tennessee

Approved

Dr. Lawrence J. Zwiebel

Dr. Kendal S. Broadie

Dr. Brandt F. Eichman

Dr. Aurelio Galli

Dr. Douglas G. McMahon

For My Parents,

Kathleen and Kevin

ACKNOWLEDGEMENTS

First and foremost, I would to thank the Bill and Melinda Gates Foundation for their dedication to solving problems in global health. Without their generous financial support these works would not have been possible. In addition, these works would not have been possible without the guidance and help of my fellow lab members, our collaborators, and the greater Vanderbilt community. I would like to thank my committee members, my chair Dr. Douglas C. McMahon, Dr. Kendal S. Broadie, Dr. Brandt F. Eichman, and Dr. Aurelio Galli for being available at all times over the years and helping me grow as a scientist. Thank you to the department of Biological Sciences members and support staff, which have always been available and provided great assistance over the years.

The Zwiebel lab has been my extended family over the years, and I would like to thank everyone for making this a great place to work and to put in long hours. I would like to thank Zhen Li for her sense of humor and for always being there to help whenever I needed it. I would also like to thank Chao Liu and Willi Honneger for being critical scientists and always adding to every discussion. Greg Pask, Jason Pitts, and David Rinker have been not only fantastic collaborators, but also great friends to me. I will cherish these friendships always. David Rinker was a driving force for the next-generation sequencing projects in the lab and laid the groundwork for high throughput screening and analysis, without which many of the described studies would not have been possible. Greg Pask has brought his skills of patch clamping to the lab and has been instrumental in progressing many research projects. Jason Pitts was instrumental in teaching me almost everything I know about molecular cloning, I would not be the scientist I am today were it not for his tutelage.

I would also like to thank the past and present members of the Zwiebel lab for their mentorship and friendship including Gray Camp, Poornima Murthi, Michael Rutzler, Lujuan Sun, Guirong Wang, and Pingxi Xu. Dr. Jonathon Bohbot was my bench mentor upon joining the lab and was a great collaborator on my first publication. Most importantly, I would like to thank Dr. Zwiebel. He has fostered an intense desire to question standing hypotheses and to push the field forward. He has always let me pursue my interests and has shaped me as a scientist. I am most grateful for everything his mentorship has encompassed.

I would like to thank the many friends I have made in Nashville, who have made the last few years memorable. My brother Christopher and my sister Emily have always provided the most encouraging words and “wisdom”. Last but not least, I would like to express my deepest gratitude to my loving parents, Kathleen and Kevin, who have always had unwavering confidence in me. I love you all dearly.

TABLE OF CONTENTS

LIST OF TABLES

Tables Page

CHAPTER II

CHAPTER IV

Table S1. is available by request only to Dr. Laurence J. Zwiebel.

LIST OF FIGURES

CHAPTER IV

CHAPTER V

LIST OF ABBREVIATIONS

AgOr	*An. gambiae* odorant receptor
AgObp	*An. gambiae* odorant binding protein
AgGr	*An. gambiae* gustatory receptor
CO_2	Carbon Dioxide
Cp	Capitate Peg
cRNA	Complementary RNA
HEK	Human Embryonic Kidney cell
DEET	N,N-diethyl-3-methylbenzamide
GPCR	G-protein coupled receptor
ORN	Olfactory Receptor Neuron
OSN	Olfactory Sensory Neuron
ORco	Odorant Receptor Co-Receptor
RT-PCR	Reverse-transcriptase polymerase chain reaction
SSR	Single sensillum Recording
TRP	Transient Receptor Potential
VUAA	Vanderbilt University Allosteric Agonist

CHAPTER I

INTRODUCTION

Disease Transmission in Vector Mosquitoes

Mosquito borne pathogens such as those causing yellow fever, dengue fever, and malaria constitute the largest threats to public health throughout most of the world (reviewed in Gardner and Ryman, 2010; Mackenzie, Gubler and Petersen, 2004, Snow et al., 2005). Malaria is by far the most devastating vector-borne disease and has significant consequences on the health and economy of affected nations, most of which are exceedingly poor (Sachs and Malaney, 2002). Eighty-seven countries are now classified as endemic for malaria, with more than 50% of the global population at risk (WHO, World Malaria Report 2010). Greater than 300-million human malaria cases are reported annually, which result in over 1 million deaths (Snow et al., 2005). In countries with a high disease burden, the estimated annual economic toll is a 1.3% growth penalty in gross domestic product (WHO, World Malaria Fact Sheet N94, 2010). While there are a number of mosquito species capable of transmitting human malaria, *An. gambiae* is the principal vector in Afro-tropical regions.

An. gambiae are hematophagous insects, and females require a blood-meal for completion of the gonadotrophic cycle (Clements, 1992). The degree to which a female mosquito prefers a human blood-meal is

termed anthropophily; conversely preference toward other animals is termed zoophily. This anthropophily serves as the foundation for transmission of the four species of *Plasmodium* responsible for human malaria (reviewed in Zwiebel and Takken, 2004). Malaria transmission occurs when a female bites an infected individual and acquires a parasite, which then matures within the mosquito and is passed on during a subsequent blood-meal. The process of pathogen transmission is analogous for females of a related sub-order of mosquitoes, the culicines, which includes the west nile virus vector, *Culex pipiens quinquefasciatus,* and the yellow fever virus vector, *Aedes aegypti*. It has been postulated that the anthropophilic tendencies of a mosquito species are largely dependent on the tuning of their olfactory system (Takken and Knols, 1999; Zwiebel and Takken, 2004).

Chemical Ecology and Mosquito Behavior

In insects, olfaction is an integral component of environmental information processing, and olfactory cues dictate, in large part, a diverse range of behaviors (Gillot, 2005). These behaviors include predator avoidance and kin selection as well as the locating oviposition sites, mates, and food sources (Hildebrand and Shepherd, 1997). While all mosquito species and sexes are known to take nectar-based sugar meals, only females of the anopheline and culicine lineages will take a blood-meal (Clements, 1992). Furthermore, only a subset of these females will seek a human host.

Some species, such as *An. gambiae* are highly anthropophilic, and seldom take alternative blood-meals (Takken and Knols, 1999).

The host-seeking behavior of female *An. gambiae* is principally dictated by the sensory modality of olfaction, although thermosensation and vision have also been implicated (Takken and Knols, 1999). In lab and field experiments, mosquitoes are attracted to airborne human volatiles from a distance, and respond even after the physical presence of the host has been removed, strongly supporting the role of chemosensation in host-seeking (reviewed in Takken and Knols, 1999). The host-seeking response is a complicated behavioral process, which is dependent on circadian and physiological states. Females in search of a blood meal are activated by odors at a distance, and then orient themselves to the source of the odor dependent on air turbulence and wind direction (Takken and Knols, 2010). Attraction is generally not induced by the presence of a unitary odorant, but rather by a collection of semiochemicals (Takken and Knols, 1999; Zwiebel and Takken, 2004, Smallegane et al., 2005).

The diversity of human skin volatiles is estimated to be 350 compounds, but it is not expected that all play a role in host-seeking (Bernier et al., 2000). The exact odors required to elicit a full host-seeking response in *An gambiae* have not been defined, but responses to multiple compounds including small-chain carboxylic acids, ammonia, and 1-octen-3-ol, a volatile component of human sweat have been demonstrated both

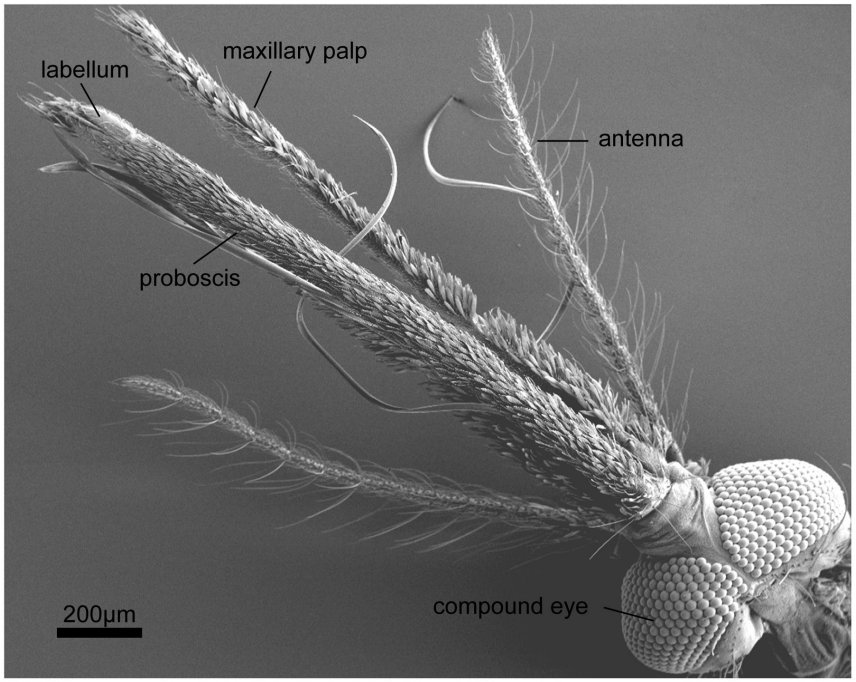

Figure 1. Head of a female *An. gambiae* mosquito. Indicated are the three principal olfactory organs; the antennae, maxillary palps, and proboscis (Pitts and Zwiebel, 2006).

behaviorally and electrophysiologically (Cork and Park, 1996; Hall et al., 1984; Meijerink, Braks and Loon, 2001; Meijerink et al., 2000, Qiu et al, 2006). Attractive odors are produced not only by the host, but also by bacteria present upon the skin (reviewed in Smallegange, Verhulst and Takken, 2011). In addition to volatile organic compounds, many mosquito species are activated or attracted by carbon dioxide and heat, which act as synergistic attractants (Bowen, 1991; Mboera and Takken, 1997; Takken & Knols, 1999). In addition to host-seeking, odorants play a role in oviposition. Various indoles, phenols and carboxylic acids are oviposition-site attractants for gravid female mosquitoes (Bentley et al., 1979; Kyorku et al., 1990, Millar et al., 1994; Allan and Kline 1998; Blackwell and Johnson, 2000; Sumba et al., 2004).

Ultrastructure of Mosquito Olfactory System

The mosquito olfactory system is found on the three sexually dimorphic organs projecting from the head; the antennae, the maxillary palps, and the proboscis (McIver, 1982). The olfactory apparatus is contained within sensilla, microscopic hairs found on each of these organs that contain the dendrites of sensory neurons. Sensilla are porous extensions of the cuticle and are subdivided into categories based on properties of information detection: mechano-, thermo-, or chemosensory. The wall of each sensilla encloses the neuron in sensillar lymph, an aqueous solution that bathes the neuron. In the case of olfaction, the detection of volatile chemicals by

an olfactory sensory neuron (OSN) requires that odorants first pass through pores located on the sensillar cuticle, travel through the sensillar lymph, and finally contact chemosensory receptors present on the dendrite surface (Rutzler and Zwiebel, 2005).

Mosquito species possess 5 types of olfactory sensilla. These sensilla vary in the number of innervating OSNs and in their basic cuticle ultrastructure. Different sensilla types respond to divergent classes of odorants, but in some cases, sensitivities overlap between sensilla types. The most stereotypic sensilla type is the club-like capitate peg (Cp) sensilla, which is only found on the maxillary palp. The maxillary palp is a sexually dimorphic olfactory organ that is the principal appendage for carbon dioxide (CO_2) and 1-octen-3-ol detection in *An. gambiae* (Lu et al., 2007). There are approximately 70 Cp sensilla found on the *An. gambiae* female MP, and the Cp's are not found upon any other organ. Contained within the club-like Cp sensilla are three neurons, two of which respond to human host odors, while the lamellate third neuron responds to carbon dioxide.

The antenna is by far the most complex olfactory organ, and contains 2 known olfactory sensilla types; the trichoid and grooved peg (GP) sensilla, (McIver, 1982). In *Anopheles gambiae* females, these sensilla types are non-uniformly distributed across the 13 antennal segments and their expression is not stereotypic. The distal 3 segments of the antennae are highly enriched for GP sensilla, which are activated by

some of the most attractive human odors, such as lactic acid and ammonia (Qiu et al., 2006). The molecular basis for this activation is currently unknown.

The least well understood chemosensory organ is the labellum, which is found at the end of the proboscis. As in other dipterans, the labellum is principally a gustatory organ, consistent with the proboscis' role in both nectar- and blood-feeding (Clements, 1999). Upon the labellum are trichoid sensilla, which respond to a variety of human orders including butylamine and several ketones (Kwon et al., 2006).

Insect Chemosensory Receptors

Chemoreception of olfactory cues utilizes at least two, and possibly more, families of cell-surface receptor proteins, which are expressed on OSN's. Recently, an insect-specific family of ionotropic glutamate receptors was discovered, which are distinct from, but related to the NMDA, AMPA, and kainite receptors and were thus named ionotropic receptors (*Irs*) (Benton et al., 2009). IRs respond to a small class of acidic odors and are expressed in the coeloconic sensilla. Relatively little is known about the IRs in comparison to the classical odorant receptors (ORs), which decode most olfactory information (Qiu et al., 2006; Benton et al., 2009; Carey et al., 2010; Wang et al., 2010). ORs and IRs are expressed in independent OSNs, and there is currently no evidence to suggest that they are co-

expressed in the same sensilla. In addition the ORs are expressed at higher levels and on a much broader scale than the IRs (Pitts et al., 2011)

Upon their discovery in *Drosophila melanogaster*, insect ORs were classified as 7-transmembrane (TM) G-Protin coupled receptors (GPCRs), like their mammalian counterparts (Clyne et al., 1999; Vosshall et al., 1999, reviewed in Mombaerts 1999). Insect ORs, however, bear no resemblance at the amino acid level to GPCRs, and have an inverse GPCR topology, possessing an intracellular C-terminus and an extracellular N-terminus (Benton et al., 2006). In addition, more recent data suggests that insect ORs do not signal through g-protein based mechanisms and instead form heteromeric ion channel complexes (Wistrand, Kall, Sonnhammer, 2006; Smart et al., 2008; Sato et al., 2008; Jones et al., 2011). A functional OR complex consists of a conventional odorant binding OR and a highly-conserved, broadly expressed and obligate OR co-receptor (ORco) (Neuhaus et al., 2005, Benton et al., 2006). The ORco is required for trafficking to the dendritic membrane as well as proper signal transduction (Benton et al., 2006). Each OSN expresses only a single conventional OR and ORco, with rare exception, and as a result follows the same one OR: one ORN architecture found in mammals (Dobritsa et al., 2003; Mombaerts, 2004). Recently, it was shown that the ORco can form a stand-alone ion channel capable of functional agonism by a synthetic agonist, although the *in vivo* implications of this are still unknown (Jones et al., 2011). When an OR is

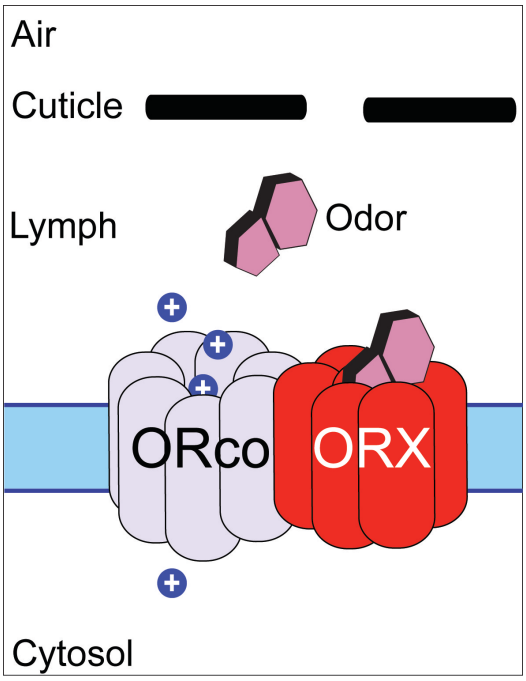

Figure 2. Current model of Insect Odorant Receptor Signaling. An odorant passes into the aqueous sensillar lymph from the air and interacts with a conventional ORx, which upon successful binding, ionotropically gates the ORco. ORco gating results in an influx of non-selective cations (Sato et al., 2008; Wicher et al., 2008; Jones et al., 2011)

heterologously expressed without an ORco, there is no discernible odorant-induced signal (Larrson et al., 2004; Sato et al., 2008; Wang et al., 2010)

The OR family of *An. gambiae* is remarkably divergent, consistent with the requirement to sense a diverse set of odorant ligands specific to their ecological niche (Hill et al., 2002). Between insect taxa there is also relatively little OR conservation, with one notable exception, the Orco, which is both genetically and functionally conserved (Krieger et al., 2003; Jones et al., 2005). When comparing the ORco between two mosquito species, *An. gambiae* and *Ae. Aegypti*, it is 87% identical (Bohbot et al, 2007). There are 76 conventional ORs in *An. gambiae* (*AgOrs*) and these bind the odorant either alone or with the help of the ORco and provide coding specificity to each complex (Hill et al., 2002). Upon odor binding, it is hypothesized that the OR then ionotropically gates the ORco, causing a non-selective influx of cations, depolarizing the neuron (Sato et al., 2008; Wicher et al., 2008; Jones et al., 2011). Using various heterologous methods, the tuning of greater than 50% of AgORs has been determined (Lu et al., 2007; Carey et al., 2010; Wang et al., 2010). The odor coding capacity (odor space) of *An. gambiae* has proven to be quite extensive, with each OR occupying a defined, but at times overlapping odor space, with varying specificities (Carey et al., 2010; Wang et al., 2010)

Peripheral Proteins in Insect Chemosensation

It has yet to be determined how the principally hydrophobic odorants known to elicit responses from ORNs, pass through the aqueous sensillum lymph and physically contact the ORs on the dendrite surface (Qiu et al., 2006). A family of odorant binding proteins (*Obps*), first characterized in the moth *Antheraea polyphemus,* are hypothesized to act, in part as shuttle proteins across this aqueous barrier and thus enhance the sensitivity of volatile chemosensation (Vogt and Riddiford, 1981).

OBPs comprise a family of small, soluble proteins, which are secreted into the sensillar lymph of insects by non-neuronal accessory cells located at the base of the sensilla (Galindo and Smith, 2001; McKenna et al., 1994). While the precise role and mechanism of OBP function in insect systems has yet to be fully determined, it has been shown that OBPs are required for normal olfactory signal transduction in a subset of ORNs tested (Kim and Smith, 2001). OBPs are not, however, an absolute requirement for olfactory signal transduction in all cases, as OR response profiles in heterologous expression systems, which lack endogenous, con-specific, and in some cases any OBPs, closely mirror odorant responses from *in vivo* data (Hallem et al., 2004; Lu et al., 2007, Carey et al., 2010, Wang et al., 2010; Bohbot et al., 2011). While multiple hypothesis have been put forward to describe the role of OBPs, at the forefront lies the belief that OBPs function to facilitate the interaction of a

hydrophobic ligand with an OR by acting as an odorant shuttle/chaperone from the air/lymph interface to the ORN dendrite.

Insect Repellents

The molecular basis of repellent action remains largely unknown, and the few reports that describe repellent targets remain highly controversial. Reports have suggested that rather than acting as a direct repellent, DEET, the benchmark standard for repellents, antagonizes the ORco, and as result, masks the presence of human odors (Ditzen et al., 2008). Subsequently, others showed that the experimental design used in this study was flawed, and that DEET triggers an aversive through the bimodal activation of a subset of ORNs and through the agonism of specific Gustatory Receptors (GRs; Syed and Leal, 2008; Xia et al., 2008; Liu et al., 2010; Lee, Kim, and Montell, 2010). Citronella is the only other repellent with at least a partially defined molecular target. Citronella was shown to target a Transient Receptor Potential (TRP) channel responsible for heat detection in dipterans. Citronella, in ways that are still not entirely clear, targets a TRPA1 dependent pathway, and triggers an avoidance response (Katz, Miller and Hebert, 2008; Kwon et al., 2010). In addition, citronella also targets an ORco dependent pathway, although the conventional OR targets have yet to be defined (Kwon et al., 2010).

Despite its widespread use, DEET has demonstrated toxicity problems, minimal efficacy against some vector mosquito species, and decreasing

consumer acceptance (reviewed in Paluch, Barholomay and Coats, 2010). For these reasons, there is widespread interest in developing next generation insect repellents, which would demonstrate increased efficacy, longer half-lives, and greater use compliance.

Olfactory Processing

Insects, like vertebrates, use *cross-fiber* (combinatorial) coding to encode the wide breadth of chemical information encountered (reviewed in Smith and Getz, 1994). As a result, each OR responds to more than one ligand, and one ligand can activate more than one OR. However, there are instances of labeled-line olfactory coding, although these are likely to be pheromone-specific (Anton and Hansson, 1995; Roche-King et al., 2000; Datta et al., 2008). Sensation of an odorant is transmitted from the periphery to higher brain centers through an OSN. The axon of a bipolar OSN terminates on a dense cluster of neurons and glia, known as a glomerulus, in the antennal lobe (AL). In *Drosophila,* OSNs expressing the same OR converge on the same, stereotypic glomerulus in virtually all cases (Laissue et al., 1999; Vosshall, Wong and Axel, 2000; Fishilevich and Vosshall 2005; Cuotu, Alenius and Dickson, 2005). As a result, a given glomerulus receives direct olfactory input for a limited set of odorants, which must interact with the corresponding OR. However, there is also a complex network of excitatory and inhibitory horizontal interglomerular connections, which relate chemical information from other

ORs via local neurons (reviewed in Vosshall and Stocker, 2007; and Masse et al., 2009; Olsen and Wilson, 2008).

Glomerular input is integrated into the electrical activity of the projection neurons (PNs), which send axons to the mushroom body and the lateral horn (reviewed in Vosshall and Stocker, 2007). The mushroom body is involved in long-term associative learning and memory, while the lateral horn is involved in experience-independent, immediate odor-decoding (reviewed in Masse et al., 2009). Information concerning olfactory processing at levels higher than these brain centers, however, is extremely limited. How olfactory signals are integrated in higher brain centers and ultimately dictate behaviors such as host seeking and oviposition are still largely unknown.

Significance of the Proposed Study

These studies have sought to define the expression and function of a subset of disease vector mosquito odorant receptors. As olfaction in mosquitoes is a principal determinant in dictating disease transmission behaviors, the ability to disrupt OR-based chemosensation would serve to reduce the vectorial capacity for *An. gambiae* and other medically important insects. The work described here not only strengthens the paradigm of insect olfaction, but demonstrates proof of concept for new compounds with broad implications for agricultural pest and disease vector control.

CHAPTER II

CONSERVATION OF INDOLE RESPONSIVE ODORANT RECEPTORS IN MOSQUITOES REVEALS AN ANCIENT OLFACTORY TRAIT

Preface

The following publication by Jones et al. appeared in *Chemical Senses* (*Chem Senses* **36(2)** 149-160 (2011)). My contribution to this work included writing portions of the manuscript, creation and functional verification of cell lines AgOR10, AaOR10, AgOr2, AaOr2 and AaOR9. I was responsible for all of the odor tuning studies, and for the AxOR concentration response curves.

Introduction

In many parts of the world, a diverse spectrum of blood-feeding mosquitoes present a serious challenge to the economic and physical well being of human populations; each year, hundreds of millions of people contract mosquito-borne diseases including malaria, Dengue, lymphatic filiariasis, Rift Valley, West Nile, Chikungunya and other maladies (Snow et al*.,* 2005; Weissenbock et al*.,* 2009). The vectors for the majority of these disease-causing agents belong to the Anophelinae and the Culicinae sub-families, which include *Aedes aegypti*, *Culex pipiens quinquefasciatus* and the malaria vector mosquito, *Anopheles gambiae sensu stricto*.

In spite of distinct evolutionary histories, these species share a number of general properties insofar as life cycle (Clements, 1999). The need to efficiently meet these complex ecological demands is, in part, the task of the mosquitoes sensory systems that acquire and process a wide array of environmental information pertaining to mating, resource acquisition and other aspects of the ecological niches occupied by these mosquitoes. Olfaction in particular, is a central component of this system as it facilitates nectar feeding (Davis, 1977; Foster and Hancock, 1994) and mating (Cabrera and Jaffe, 2007) as well as female specific behaviors including host seeking, blood-feeding (Takken, 1991) and oviposition (Bentley and Day, 1989).

The general ultrastructure of the olfactory apparatus of mosquitoes is largely conserved, as is the qualitative and quantitative characteristics of olfactory sensilla (McIver, 1982; Pitts and Zwiebel, 2006). At a physiological level, mosquitoes and other blood-feeding arthropods exhibit overlapping receptive fields for many aromatic compounds such as indole (Blackwell and Johnson, 2000; Jeanbourquin and Guerin, 2007; Harraca et al*.,* 2009), 3-methyl-indole (sometimes referred to as skatole; Mboera et al*.,* 2000; Jeanbourquin and Guerin, 2007; Harraca et al*.,* 2009) and 4-methyl-phenol (4-MP; sometimes referred to as p-cresol; Blackwell and Johnson, 2000; Jeanbourquin and Guerin, 2007; Harraca et al*.,* 2009; Bentley et al*.,*1979). A variety of sensory modalities mediate the oviposition behavior of mosquitoes (O'Gower, 1963). Olfaction plays a

central role in facilitating both attraction to specific aqueous sites as well as stimulation of egg-laying behavior itself (Lindh et al*.,* 2008; Ponnusamy et al*.,* 2008). Indole and 4-MP are both derived from bacterial degradation (Isenberg and Sundheim, 1958; Lindh et al*.,* 2008) of tryptophan (Elgaali et al*.,* 2002) and tyrosine (Curtis et al*.,* 1976), respectively. Indole is also a by-product of a wide variety of plants (Frey et al*.,* 2000; Schmelz et al*.,* 2003). An odor blend consisting of phenol, 4-MP, 4-ethylphenol, indole and 3-methylindole from grass infusion attracts female *Culex quinquefasciatus* (Millar et al*.,* 1992; Du and Millar,1999). Of these, 3-methylindole alone mediates long-range attraction in several culicine species. Other aromatics such as 4-MP, a compound found in hay infusion (Bentley et al*.,* 1979; Millar et al*.,* 1992) and human-sweat (Cork and Park, 1996) also play an important role as an oviposition attractant for various mosquito genera including *Aedes*, *Culex* and *Anopheles* (Bentley et al., 1979; Blackwell and Johnson, 2000; Poonam et al., 2002).

In order to examine evolutionary aspects of odor sensitivity in vector mosquitoes, we have focused on a subset of their olfactory repertoire that defines precise ecological niches. Aromatics and heterocyclics occupy a large portion of the characterized odor space of *An. gambiae* (Carey et al., 2010; Wang et al., 2010) and play a role in attracting mosquitoes from various lineages in the context of host detection (Cork and Park 1996; Takken et al. 2001), larval behavior (Xia et al. 2008) and oviposition (Du and Millar 1999; Lindh et al. 2008). Indole,

in particular is an aromatic heterocyclic organic compound that elicits strong responses in adult antennal trichoid sensilla of *An. gambiae* (Blackwell and Johnson 2000; Meijerink et al. 2000; Qiu et al. 2006) and activates olfactory receptor neurons (ORNs) in *Ae. aegypti* (Siju et al. 2010), *Cx. quinquefasciatus* (Hill et al., 2009, Syed and Leal 2009) and *Cx. tarsalis* (Du and Millar 1999).

At a molecular level, mosquito olfactory signal transduction begins on the surface of ORN dendrites that lie within antennal, labellar and maxillary palp sensilla. Although the precise mechanisms underlying this process are still emerging (Sato et al. 2008; Wicher et al. 2008), it is clear that odorant receptors (ORs) play a significant, if not central role. As is the case for all insect systems, mosquito ORs form heteromeric complexes of unknown stoichiometry, consisting of at least one conventional and one non-conventional OR (Benton et al. 2006). Conventional ORs are thought to be the ligand binding components of the complex while the non-conventional OR is necessary for the proper function of this assembly (Rutzler and Zwiebel 2005; Benton et al., 2006). Mosquito and other insect ORs, are encoded by large and highly divergent gene families that are unrelated to vertebrate ORs (Mombaerts 1999; Benton et al. 2006).

The characteristic divergence of insect ORs is likely to reflect rapid changes in ecological and other life cycle considerations that help to drive speciation (Clark et al., 2007; Guo and Kim 2007; McBride 2007; Gardiner

et al., 2008; de Bruyne et al., 2010). Indeed, a phylogenetic comparison between conventional *Ae. aegypti* and *An. gambiae Or* genes demonstrate that with the exception of a subset of 12 *Aedes/Anopheles* presumably orthologous *Or* pairs most of the predicted proteins encoded by these genes share less than 20% amino-acid identity (Bohbot et al. 2007). This high level of divergence among conventional OR proteins may reflect both the evolutionary distance (Krzywinski et al. 2001a) and the diversity of chemical signals encountered by each species. As would be expected, genes encoding mosquito *Or7* proteins, the ortholog of the non-conventional *Drosophila melanogaster Or83b* (*DOr83b*) which is the requisite functional partner of most conventional ORs (Larsson et al., 2004) are extremely conserved at both the amino-acid sequence (Melo et al., 2004; Xia and Zwiebel 2006; Bohbot et al., 2007) and functional levels (Jones et al. 2005).

Beyond the *Or83b/Or7* orthologous group, the most closely related group of ORs between *Ae. aegypti* and *An. gambiae* is represented by the OR2/OR10 clade which shares an average of 69% or greater amino-acid identity (Bohbot et al., 2007). Recently, conserved members of the OR2/OR10 clade have been identified in the southern house mosquito *Culex pipiens quinquefasciatus* (Pelletier et al., 2010b). When viewed within the overall context of *Or* gene divergence, it is evident that strong selective pressure has maintained the high level of sequence conservation within the OR2/OR10 clade. This could arise from shared ecological

constraints that require a set of common olfactory responses that predate the Anophelinae/Culicinae split ~150 million years ago (Krzywinski et al., 2001a). A prediction of this hypothesis would be that OR2/OR10 would share similar activation profiles between *Ae. aegypti* and *An. gambiae* and moreover, that additional members of this gene subfamily are present in the olfactory repertoire of other mosquito species.

To examine this question, we have used heterologous expression in two distinct systems to functionally characterize the odorant response profiles of OR2/OR10 members from *Ae. aegypti* and *An. gambiae*. These studies establish broad and commonly held functional relationships between the OR2/OR10 clade's amino-acid sequence and its odorant response profiles. We have also identified OR2/OR10 homologs from additional mosquito species across variable evolutionary distances. From a biological perspective, the functional conservation of the OR2/OR10 clade in both zoophilic and anthropophilic mosquitoes suggests that while the role of this group of ORs is not strictly associated with host selection, it is nonetheless crucial within the entire family of Culicidae. These studies provide an example of how comparative studies can inform our understanding of the role of ORs in the evolution of chemosensory pathways as well as reveal structure-function relationships of OR proteins in mosquito vectors.

Materials and Methods

Mosquito Rearing

Ae. aegypti (Costa Rica strain), *An. gambiae sensu stricto* (Suakoko strain), *Anopheles quadriannulatus* and *Anopheles stephensi* were reared as described in Fox et al., 2001. *An. gambiae* (SUA2La; MRA765), *An. quadriannulatus* (SUAQUA; MRA-761) and *An. stephensi* (IV; MRA-314) were provided by The Malaria Research and Reference Reagent Resource Center (MR4). For stock propagation, 4- to 5-day-old female mosquitoes were blood-fed for 30–45 min on anesthetized mice, following the guidelines set by Vanderbilt Institutional Animal Care and Use Committee.

Molecular Cloning

AqOr2 and AsOr2 cloning

PCR templates were prepared from 908 hand-dissected female antennae of *Anopheles quadriannulatus* and 561 hand-dissected female antennae of *Anopheles stephensi* mosquitoes. Collected tissues were used to generated total RNA using the RNeasy (Qiagen, Valencia, CA) protocol followed by cDNA synthesis using the BD Smart Race cDNA Amplification Kit (BD Biosciences Clontech) generating 5' and 3' cDNA pools. The same two degenerate primers and amplification protocols described above were used in subsequent PCR amplifications. Full length *AqOr2* cDNA were obtained using RACE amplifications in a GeneAmp

PCR system 9700 (Applied Biosystems, Foster City, CA) under conditions as described in the BD Smart Race cDNA Amplification Kit and with Adaptor primer Universal Primer Mix (UPM) and *AqOr2* specific RACE primers— 3' RACE primer 1: TTCACCAGCTTCTACGCGACCTG and 5' RACE primer 2: CAGCAGTGCGCACAGCATCATC. A second, nested PCR RACE amplification was carried out using *AqOr2* specific RACE primers—3' RACE primer 3: TCGTCCAGATAGCGGCCCTAAAGC and 5' RACE primer 4: CAGCAGTGCGCACAGCATCATC both with UPM. All experimental-specific PCR products were gel-purified using QIAquick gel extraction reagents (Qiagen, Valencia, CA), cloned into the pCRII-TOPO cloning vector (Invitrogen, Carlsbad, CA) and subsequently sequenced in the DNA Core Facility at Vanderbilt University. The same procedure was applied for *AsOr2* using the following RACE primers— 3' RACE primer 1: GTTCACCAGCTTCTACGCGACCTG and 5' RACE primer 2: CACAGCATCATCCCGAACGACAAG. A second, nested PCR RACE amplification was carried out using AsOr2 specific RACE primers—3' RACE primer 3: ACTCTGTTCGCCGAGCTGAAGGAG and 5' RACE primer 4: TCGAGCAAACACAGATGGGTGACG both with UPM. The complete nucleotide sequences has been deposited to GenBank (accession numbers: FJ008067, FJ008068, FJ008071 and FJ008072).

AqOr10 and AsOr10 cloning

AqOr10 and *AsOr10* were amplified from the same cDNA pools as

described above using the following two degenerate primers: Forward primer 5'-CCTGTACCGGGCCTGGGGNAAVAT-3' and reverse primer 5'-GAGGCGTTCAGCAGGGACTGRAACATYTC-3'. The PCR products were gel-purified using QIAquick gel extraction reagents, cloned into the pCRII-TOPO cloning vector and subsequently sequenced in the DNA Core Facility at Vanderbilt University. 5' and 3' missing fragments for *AqOr10* and *AsOr10* were amplified from the cDNA pools using the Advantage® 2 Polymerase Mixes and PCR Kit (Clontech) combined with touchdown PCR following the manufacturer procedure. RACE primers for *AqOr10* included— 3' RACE primer 1: AACGAGGTGCGGGAGGAAAGC and 5' RACE primer 2: TTGATCTGCACCAGCCCGAACAG. A second, nested PCR RACE amplification was carried out using *AqOr10* specific RACE primers—3' RACE primer 3: ACCGTGGCTGAATGTGGATGAAAC and 5' RACE primer 4: GCCAGGTTGGAGATGGACAGGAAG both with UPM. RACE primers for *AsOr10* included— 3' RACE primer 1: ACGAGGTGCGTGAGGAAAGCATGG and 5' RACE primer 2: CGAACAGCGTGCTCGAGGTGAA. A second, nested PCR RACE amplification was carried out using AsOr10 specific RACE primers—3' RACE primer 3: ACAGTGGACCGTGGCTCAATGTGG and 5' RACE primer 4: GAAGTGGGCCCGTTTGGTGTACG both with UPM. In all cases, cDNA and genomic DNA sequences were amplified, cloned and sequenced. Full-length cDNA and genomic clones were obtained using gene specific primers and nucleotide sequences have been deposited to

GenBank (accession numbers: FJ008069, FJ008070, FJ008073 and FJ008074).

Receptor Expression in *Xenopus laevis* Oocytes and Two-Electrode Voltage-Clamp Electrophysiological Recording

Full-length coding sequences of *AaOr2*, *AaOr9*, *AaOr10*, *AgOr2* and *AgOr10* were PCR amplified from antennal cDNA. PCR were first cloned into pENTR/D-TOPO (Invitrogen) and then subcloned into pSP64DV by means of the Gateway LR reaction (Lu et al., 2007). Complementary RNA (cRNA) was synthesized from linearized vectors using the mMESSAGE mMACHINE SP6 kit (Ambion). Mature healthy oocytes (stage V–VII) were treated with 2 mg／mL collagenase S-1 in washing buffer [96 mm NaCl, 2 mm KCl, 5 mm MgCl2 and 5 mm HEPES (pH 7.6)] for 1–2 h at room temperature. Oocytes were later microinjected with ~28 nL cRNA. After injection, oocytes were incubated for 3-5 days at 18°C in 1 X Ringer's solution [96 mm NaCl, 2 mm KCl, 5 mm MgCl2, 0.8 mm CaCl2 and 5 mm HEPES (pH 7.6)] supplemented with 5% dialyzed horse serum, 50 mg／mL tetracycline, 100 mg／mL streptomycin and 550 mg／mL sodium pyruvate. Whole-cell currents were recorded from the *Xenopus* oocytes injected with corresponding cRNAs by using a two-electrode voltage clamp as described in Lu et al., 2007. The data was first analyzed using Clampfit. A Tukey multiple comparison test ($P < 0.001$) was used to compare the mean EC_{50} values of each OR-odorant couple.

Cell Culture and Ca^{2+} Fluorometry

To create a cell culture expression vector capable of co-expressing AgOR7 in conjunction with a conventional ORx, pcDNA5/FRT/TO (Invitrogen) was modified to create two individual expression cassettes each under the control of separate CMV/TetO2 promoters and BGH poly-adenylation signals. Flp-In™ T-REx™ 293 cell lines (Invitrogen) were transfected with the modified pcDNA5 plasmid along with POG44 (a plasmid encoding FLP recombinase) to facilitate site-specific recombination. Stable cell lines were selected using Hygromycin B (Invitrogen). Cells were maintained in DMEM (Invitrogen) supplemented with 10% Tetracycline-free FBS (HyClone).

For the fluorometric measurements of Ca^{2+} mobilization, stable lines expressing OR7/ORX were seeded at 20,000 cells/well in black wall, poly-lysine coated 384-well cell culture plates (Greiner) and treated with 0.3 ug/ul tetracycline (Sigma) overnight to induce OR expression. Cells were dye-loaded with 1.8uM Fluo-4 AM (Molecular Probes) for 45 minutes at 37C prior to each assay and Ca^{2+} mobilization was assayed in an FDSS6000 plate reader (Hammamatsu). Baseline readings were taken for 20s before automated addition of $2x10^{-3}$ M compound previously diluted in DMSO and assay buffer (20mM HEPES, 1x HBSS). Ratios were described as Maximum/Minimum response and each response was normalized to the maximum responder. Each odor was assayed in

triplicate per plate and 3 plates were run per cell line. Concentration response curves (CRCs) were run similarly.

Chemicals

All odorants were >99% pure or of the highest grade commercially available. Please see Supplemental Table 1 for a complete list of odorants used in this study including their corresponding CAS numbers.

Gene identification and sequence analyses

The primary amino-acid sequence of *D. melanogaster* Or43a protein was retrieved from GenBank (NP_523647). The *CqOr10b, CqOr2* and *CqOr9* genes were identified using the AaOR10 protein to tBLASTn query the *Culex quinquefasciatus* (Johannesburg strain) database located at the BROAD Institute Matches were manually annotated using ClustalW and refined using the Softberry Splice Site Prediction program. ClustalW was used to predict the exon/intron structures of each individual *Or* genes. Deduced amino-acid sequences of mosquito *Ors* were aligned using ClustalW and the resulting data matrix was submitted to the MEGA4 software (Tamura et al. 2007). A Neighbor-joining tree was constructed using a pair-wise distance method and gaps handled by pair-wise deletion. Inferred relationships were tested by bootstrapping based on 10,000 pseudoreplicates.

Results

OR2/OR10 proteins are highly conserved in mosquitoes

Approximately 95%, of *Ae*. *aegypti* ORs share less than 20% amino-acid sequence identity with the *An*. *gambiae* OR repertoire (Figure S1) with *Aedes* or *Anopheles* specific *Or* gene expansions accounting for most of this diversity (Bohbot et al., 2007). Notwithstanding the extraordinary conservation of *Ag/AaOr7* genes, a subset of five anopheline ORs stand out due to their unusually high sequence identity (above 50%) as compared to their homologs in *Ae. aegypti*. These OR homologs belong to the OR2/OR10, OR8 and OR11 protein groups, respectively. Both AaOR10/AgOR10 and AaOR2/AgOR2 share 71% amino-acid identity while all OR2s, AaOR9 and all OR10s share between 51% and 67% amino-acid sequence identity. Of these, only OR2s and OR10s display 70-79% amino-acid identity representing 0.02% of all 10,349 possible comparisons of the 131 AaORs with the 79 AgORs (Figure S1). It is noteworthy that AgOR9 (named numerically in order of discovery) is not part of this clade and the genome of *An. gambiae* appears to lack a homolog of AaOR9.

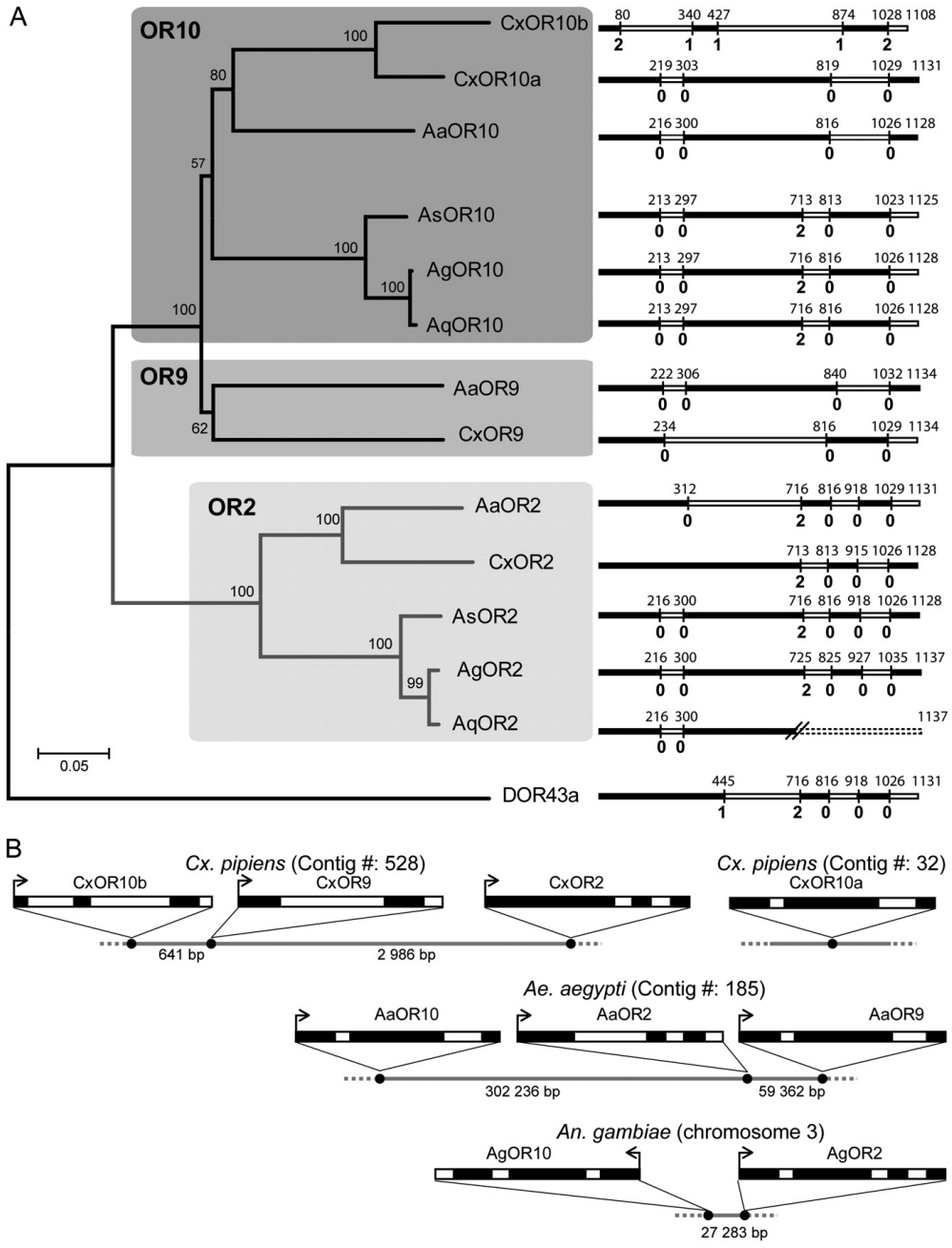

Figure 1. The Or2/9/10 clade predates the Anophelinae/Culicinae split. (A) Phylogenetic relationships of the mosquito OR2 (light grey shaded area), OR9 (medium grey shaded area) and OR2 (dark grey shaded area) clade of mosquitoes. Aa: *Aedes aegypti*; Cx: *Culex quinquefasciatus*; Ag: *An. gambiae*; Aq: *An. quadriannulatus*; As: *An. stephensi*. The P-distance tree was generated using MEGA 3.1 using a Neighbor-joining model. Branch lengths are proportional to the scale of sequence distance indicated by the bar below the tree. Bootstrap values (%) are based on 10000 replicates. Gene structures are indicated by black

and whites boxes. Intron positions and protein lengths are indicated above the gene structure. Intron phases are indicated in bold below the gene structure. Complete cDNA sequence was characterized for *AqOr2* whereas an incomplete genomic DNA sequence was obtained thus providing only the position of the first two introns. **(B)** Microsynteny and gene structure of *Ae. aegypti Or2/10, Cx. quinquefasciatus Or2/9/10* and *An. gambiae Or2/10* genes. Each filled black and white squares represents an exon. Distance between genes are indicated below individual contig

A survey of the Or2/Or10 genes was carried out in 3 additional species of the Anophelinae and the Culicinae lineages. Using bioinformatics and molecular approaches, *Or2*, *Or9* and *Or10* genes were identified from *Cx. pipiens quinquefasciatus*, *An. quadriannulatus* and *An. stephensi* (Figure 1A). *D. melanogaster* OR43a (DOR43a) was also included in this phylogenetic analysis as it represents the closest *Drosophila* homolog to the mosquito OR2/OR10 group. An alignment of the amino-acid sequences was carried out (data not shown) to build a sequence-based phylogenetic tree (Figure 1A). All 5 mosquito species studied herein contain one member of the *Or2* gene lineage and at least one member of the *Or10* lineage, which has apparently expanded in the Culicinae subfamily resulting in an additional *Or10* homolog (*CxOr10b*) in *Cx. quinquefasciatus*. However, *Or9* homologs were only identified in aedine mosquito species including *Ae. aegypti* and *Cx. quinquefasciatus*. Sequence identity (Figure S1), commonalities in gene structure (Figure 1A) and conserved syntenic relationships (Figure 1B), are consistent with the phylogenetic analysis. Overall, insofar as primary protein sequence is concerned, OR9 is more similar to OR10 than to any of the OR2 predicted proteins (Figure 1A). For example, *AaOr9* encodes a protein that is more similar to AaOR10 (69% amino-acid identity) than to AaOR2 (51% amino-acid identity).

Based on the unusual sequence similarity (Figure S1) and the phylogenetic relationships between OR2s, OR10s and AaOR9 (Bohbot et

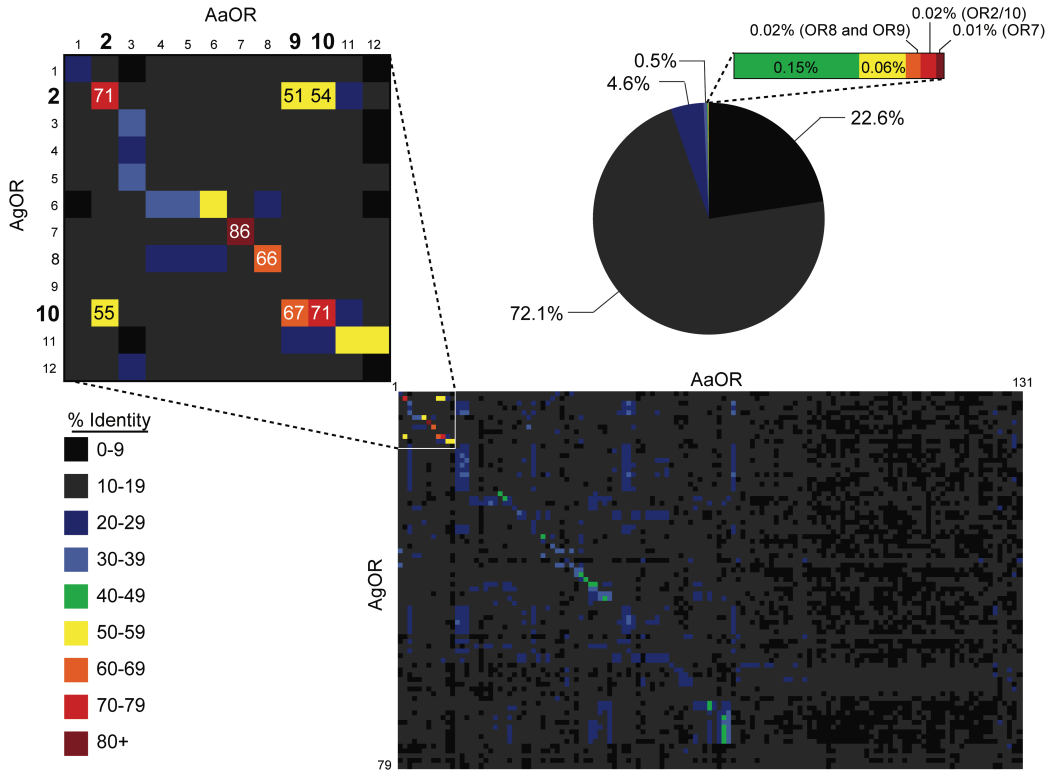

Figure S1. OR2/9/10 are the most conserved conventional receptors in the *Ae. aegypti* and *An. gambiae* repertoires. Protein sequence identity matrix between 131 *Ae. aegypti* and 79 *An. gambiae* ORs. The first twelve ORs from each species share the highest identity level including OR7 and OR2/9/10. The pie chart displays the percentage of 10,349 possible comparisons of the 131 AaORs with the 79 AgORs based on amino-acid sequence identity levels.

al. 2007), we hypothesized that the OR2/OR10 paralogs would manifest distinct odorant response profiles while the potential Aa/AgOR2 and Aa/AgOR10 pairs would share common odorant sensitivity profiles. To further examine these questions we carried out a detailed functional characterization within the OR2/OR10 clade to assess odorant sensitivities using two heterologous expression systems.

OR2/10 clade exhibits overlapping odor-response profiles

In order to establish the receptive range for divergent members of the OR2/OR10 clade, stable lines of HEK cells functionally expressing either AaOR2, AgOR2, AaOR9, AaOR10 or AgOR10 along with AgOR7 were established and challenged with a 30 odor panel (Figure 2). As expected, the tuning curves of orthologous pairs (Ag/AaOR10 and Ag/AaOR2) were strongly concordant in their ability to detect a subset of compounds in this panel (Figure 2). There were no instances in which an odor activated one ortholog and failed to activate its heterospecific counterpart, although some differences in absolute response levels were observed.

When paralogs were compared, the OR2 and OR10 clades showed considerable overlap in their ability to detect the panel, which is consistent with their overall relatedness. The tuning curve of AaOR9 closely resembled that of the OR10 clade's (Figure 2). There were a few odorants (Figure 2, arrows) for which one set of paralogs responded significantly more strongly than the other pair, and in these instances

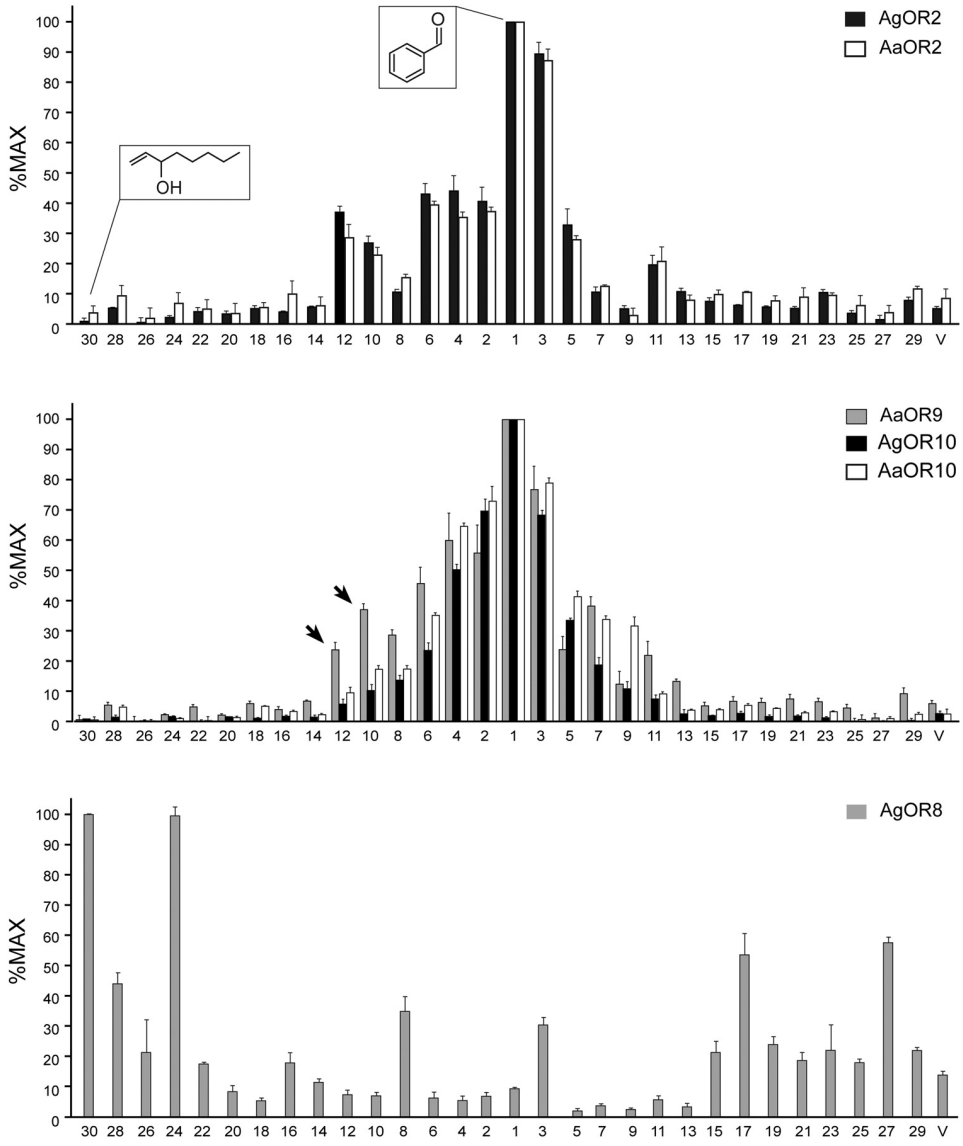

Figure 2. Members of the OR2/10 clade exhibit overlapping sensitivities. Tuning curves of AaOR2, AgOR2, AaOR9, AaOR10, AgOR10 and AgOR8. The 30 odorants are ordered along the x axis, with those eliciting the strongest responses for the OR2/10 clade near the center. Benzaldehyde and 1-octen-3-ol (chemical structures shown) elicited the highest response for the OR2/10 clade and OR8, respectively. Arrows indicate odorants for which AaOR9 responses are more similar to OR2s than to OR10s.

AaOR9 possessed an intermediate coding capacity in that it responded to virtually all activators of the 2/10 clade (Figure 2).

To further demonstrate that the specificity of the receptive capacity of these ORs, AgOr8, which has previously been shown to be an octenol receptor (Lu et al., 2007) with less than 20% amino-acid identity with OR2/10, was included in this survey. In HEK cells stably expressing AgOR7/AgOR8 proteins, odorant-induced responses were largely indifferent to the principal activators of the OR2/9/10 clade (Figure 2) and instead, closely mirrored the response profiles of AgOR8- expressing oocytes (Wang et al., 2010) and fly ORNs (Carey et al., 2010). All three expression systems manifested a significant proportion of the odorant responses directly recorded *in vivo* from AgOr8-expressing ORNs on the maxillary palp pegs of *An. gambiae* (Lu et al., 2007), which validates the use of cell-based OR expression. In all cases, control HEK-293 cells were indifferent to any odor tested (data not shown).

Indole is an important activating compound of the *Ae. aegypti* and *An. gambiae* OR2/OR10 clade

Our hypothesis was that sequence homology and divergence of the mosquito OR2/OR10 proteins would be reflected in their respective odorant sensitivities. Indeed, using the Xenopus oocyte expression system we observed significant sensitivity differences in response to indole between OR2/9/10 paralogs when expressed together with AgOR7 (Figure 3A). Several odorants including indole, 4-MP and benzaldehyde

have been identified as strong ligands for AgOR2 and AgOR10 in oocytes (Xia et al., 2008; Wang et al*.,* 2010**)** as well as in the *Drosophila* empty neuron expression system **(**Carey et al., 2010**)**. In the current study, AgOR2 and AaOR2 exhibited highest sensitivity to indole (Figure 3A and 4B; Supplemental Table 2) while AaOR9 and AaOR10 exhibited nearly identical responsiveness that were approximately 10-fold less sensitive than those observed for Aa/AgOR2 (Figure 3B). Of the paralogous ORs tested, AgOR10 was the least sensitive to indole (Figure 3A and 3B; Supplemental Table 2) while we observed uniform, albeit relatively low sensitivity in response to benzaldehyde and 4-MP, each of which elicited reduced responses at high concentrations from

Discussion

The increasing availability of whole insect genomes has provided novel opportunities for examining the evolutionary concepts of orthology and paralogy (Zdobnov and Bork, 2007). Current paradigms put forward the view that orthologous proteins retain the same function while paralogs tend to develop new ones (Koonin, 2005). In terms of insect olfaction, this concept is best illustrated by the highly conserved, non-conventional OR subclade that was first described in terms of its original member *Or83b* from *Drosophila* (Vosshall, 2000). Subsequent homologs were identified as *Or7* in mosquitoes (Hill et al*.,* 2002, Melo et al., 2004; Xia and Zwiebel 2006) or *Or2* in moths (Krieger et al., 2004; Nakagawa et al., 2005) and

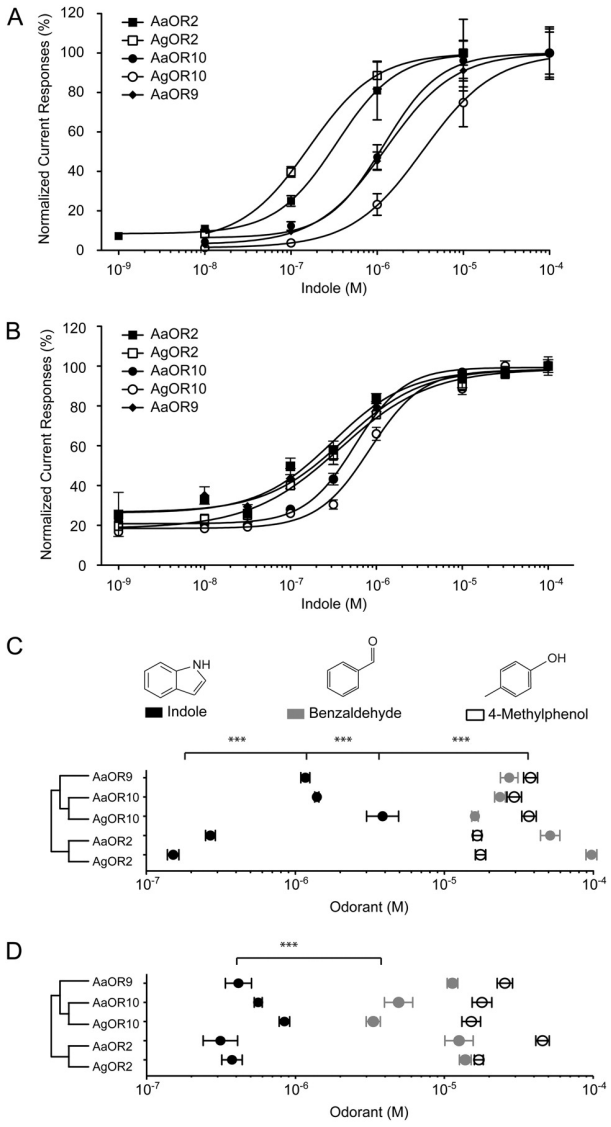

Figure 3. Indole activation correlate with the primary structure of the OR2/9/10 protein. Normalized concentration-response curves of OR2s, OR9 and OR10s expressed in Xenopus oocytes **(A)** and in HEK cells **(B)** in response to indole (n = 4-7). Odorant concentrations were plotted on a logarithmic scale. **(C)** Scatter chart displaying three functional OR groups: the OR2, AaOR9/AgOR10 and AaOR10 groups (n = 4-8) expressed in Xenopus oocytes. **(D)** Scatter chart displaying the sensitivity of the OR2/10 clade expressed in HEK cells in response to indole, 4-MP and benzaldehyde (n = 3-8). Three asterisks, $P < 0.001$ (ANOVA test with Tukey post test). The mean EC_{50} values and S.E.M of their scatter were determined using Prisall ORs tested. CRCs were also generated in HEK cells in order to examine whether sensitivity differences existed between AgOR10 and AaOR10 as well as to validate our oocyte-based assays. In

these studies, the OR2/10 clade was once again most sensitive to indole, followed by 4-MP and lastly benzaldehyde. Overall, the OR2/10 clade agonist rankings were comparable to those obtained using *Xenopus* oocytes (Figure 3C) further demonstrating the consistency of these analyses across multiple functional outputs.

hymenoptera (Robertson et al., 2010; Robertson and Wanner, 2006). Members of the *OR83b* family are expressed in a majority of insect ORNs (Vosshall, 2000; Pitts et al., 2004), functionally conserved (Jones et al*.,* 2005) and are required for general olfactory signaling (Larsson et al., 2004). Even so, these orthologous ORs are likely not to be directly involved in odorant recognition but rather are required for the proper translocation of the OR complex to the ORN dendrite membrane (Larsson et al. 2004) as well as functioning as a cation channel component of OR complexes (Sato et al. 2008; Wicher et al. 2008).

Despite an abundance of apparent OR ortho/paralogs in *Drosophila* (Clark et al., 2007; Guo and Kim, 2007; McBride, 2007; Nozawa and Nei, 2007; Gardiner et al., 2008) and mammalian systems (Branscomb et al*.* 2000; Ohara et al*.* 2009; Churcher and Taylor 2009; Dong et al*.* 2009) functional characterization of ortho/paralogs ORs are scarce in insects (Jones et al., 2005; Bohbot et al., 2007; Lu et al*.,* 2007; Pelletier et al., 2010b) as well as in mammals (Krautwurst et al. 1998; Schmiedeberg et al*.* 2007). In one example of such an analysis the I7 receptors of mouse and rat manifest differential odorant response profiles despite sharing 94% identity at the amino-acid level; the rat I7 receptor is more sensitive to octanal as compared to heptanal while mouse I7 displays the opposite sensitivities (Krautwurst et al. 1998). In addition, while the mouse Olfr43 and human OR1A1 orthologous pair selectively detect (*S*)-(−)-citronellol, a single amino-acid change between human OR1A1 and OR1A2 paralogs is

responsible for their differential response toward this compound (Schmiedeberg et al., 2007).

These few examples illustrate the caveats involved in predicting function solely from sequence alignments and phylogenetic analyses. In *Drosophila*, a recent study has examined the functional aspects of conserved classes of ORNs and associated *Or* genes across a range of species spanning ~40 million years of evolution (de Bruyne et al., 2010). With notable differences, *in vivo* ORN responses were found to be largely conserved over this evolutionary time span and attributed to *Or* gene loss or duplication and were generally correlated with primary sequence conservation of homologous ORN/*Or* pairs. Furthermore, by comparing the limited amount of primary sequence divergence between orthologous *Ors* with similar functional characteristics as well as paralogous *Ors* with differential odorant response profiles, the authors identified the amino acid residues associated with general *Or* functionality as well as those linked to determining odorant specificity (de Bruyne et al*.,* 2010). In mosquitoes OR2 (Pelletier et al., 2010a) and OR8 (Lu et al*.,* 2007; Bohbot and Dickens, 2009), are the only instances of demonstrated functional orthology. Overall, these examples suggest that functional conservation is characteristic of orthologous ORs while functional divergence is associated with, but not limited to paralogous ORs.

Insect ORs are characteristically divergent with relatively few examples of interspecific primary sequence homology. In order to

examine the evolutionary basis for the limited instances of OR conservation that are present and likely to reflect a biological imperative, we have carried out a molecular and functional survey within OR2/OR10 proteins which is the most conserved of the conventional mosquito *Or* subclades. The species utilized for this analysis belong to the two major subfamilies covering over 97% of all mosquitoes (Walter Reed Biosystematics Unit, http://www.mosquitocatalog.org/default.aspx?pgID=2). Among the OR2/OR10 clade, we have identified various degrees of sequence conservation likely reflecting both orthologous and paralogous relationships from which we infer the following evolutionary model: the Or2 and Or9/Or10 genes form two distinct monophyletic lineages, the likely product of a gene duplication event that occurred prior to the Anophelinae and Culicinae divergence. A second gene duplication event followed within the Culicinae lineage, giving rise to the *Or10* and *Or9* subgroups. Furthermore, the presence of an *Or9* lineage in both Aedes (*AaOr9*) and Culex (*CxOr9*) coincident with its absence from the *An. gambiae* genome suggest the second duplication occurred prior to the separation of the Culex and Aedes genera ~38 MYA (Besansky and Fahey, 1997; Foley et al., 1998). Alternatively, it is also possible that *Or9* was lost sometime in the anopheline lineage in which case it would be expected to be missing in some, but not necessary in all other anophelines besides *An. gambiae*. This hypothesis could be directly

Odorant Number	Odorant	CAS#	Chemical Class
1	benzaldehyde	100-52-7	aromatic
2	2-ethylphenol	90-00-6	aromatic
3	2-methylphenol	95-48-7	aromatic
4	acetophenone	98-86-2	aromatic
5	3-methylphenol	108-39-4	aromatic
6	2-acetylthiophene	88-15-13	heterocyclic
7	methyl benzoate	93-58-3	aromatic
8	2-ethyltoluene	611-14-3	aromatic
9	phenethyl acetate	103-45-7	aromatic
10	2-acetylpyridine	1122-62-9	heterocyclic
11	2-ethoxythiazole	15679-19-3	heterocyclic
12	4-methylthiazole	693-95-8	heterocyclic
13	2-acetylthiazole	24295-03-2	heterocyclic
14	4-methylcyclohexanol	589-91-3	alcohol
15	cyclohexanone	108-94-1	ketone
16	L(+) lactic acid	79-33-4	acid
17	ethyl formate	109-94-4	ester
18	hexanal	66-25-1	aldehyde
19	ethyl acetate	141-78-6	ester
20	2-nonanone	821-55-6	ketone
21	ammonium hydroxide	1336-21-6	base
22	octanoic acid	124-07-2	acid
23	thiazole	288-47-1	heterocyclic
24	3-octanone	106-68-3	ketone
25	hexanol	111-27-3	alcohol
26	hexanoic acid	142-62-1	acid
27	isovaleric acid	503-74-2	acid
28	ethyl butyrate	105-54-4	ester
29	isoamyl acetate	123-92-2	ester
30	1-octen-3-ol	3391-86-4	alcohol
V	Dimethyl Sulfoxide	67-68-5	solvent

Supplemental Table I. Characteristics of the panel of odorants used in this study. Odorant number, Common name, Chemical Abstracts Service (CAS) identification number, and chemical class are indicated.

assessed as additional genomic resources become available. We further posit that the *Or9* lineage represents a case of Culicinae-specific gene expansion that was likely selected by specific ecological requirements. It is possible the larval-specific expression of *AaOr9* (Bohbot et al*.,* 2007) is indicative of such a requirement.

To further examine these questions in vector mosquitoes, we have focused on the OR2/OR10 homologous group using independent heterologous expression systems to further demonstrate that sequence conservation correlates with shared odorant-induced activation patterns. When viewed within the context of the highly divergent mosquito *Or* gene families that are typical at both the intra- and inter-specific levels (Bohbot et al*.,* 2007; Bohbot and Dickens, 2009) and in light of considering the evolutionary distance between these species, the *Or2/Or10* gene lineage represents a striking case of structural and functional homology.

From a functional perspective, the aromatic heterocylic indole elicited the strongest responses from Aa/AgOR2 orthologs and to a lesser extent from OR9/10 paralogs. In contrast, other odorants in our panel such as 4-MP and benzaldehyde were observed to be significantly weaker agonists for the OR2/OR9/OR10 lineage with responses reduced between 5 and 1000-fold.

OR	Oocyte system			HEK cell system		
	Indole	4-MP	Benzaldehyde	Indole	4-MP	Benzaldehyde
AaOR2+AgOR7	-6.57 ± 0.03	-4.29 ± 0.06	-4.78 ± 0.03	-6.50 ± 0.11	-4.90 ± 0.09	-4.34 ± 0.04
AgOR2+AgOR7	-6.82 ± 0.04	-4.01 ± 0.03	-4.75 ± 0.03	-6.42 ± 0.07	-4.86 ± 0.04	-4.77 ± 0.03
AaOR9+AgOR7	-5.93 ± 0.03	-4.56 ± 0.06	-4.42 ± 0.05	-6.38 ± 0.08	-4.94 ± 0.03	-4.59 ± 0.05
AaOR10+AgOR7	-5.85 ± 0.01	-4.62 ± 0.03	-4.53 ± 0.05	-6.25 ± 0.03	-5.3 ± 0.09	-4.75 ± 0.06
AgOR10+AgOR7	-5.41 ± 0.11	-4.79 ± 0.02	-4.43 ± 0.05	-6.07 ± 0.03	-5.47 ± 0.05	-4.81 ± 0.06

Supplemental Table II. Relative activity of *Ae. aegypti* and *An. gambiae* OR2/OR10 towards indole as determined by two-electrode voltage-clamp on injected Xenopus oocytes. Mean $LogEC_{50}$ values ± s.e.m (n = 4-5 oocytes and n = 3 HEK cell plates) were extrapolated by fitting the data using non-linear regression curve fit function (see Materials and Methods).

Unlike other aromatic compounds that strongly activate a number of AgORs, sensitivity to indole appears to be narrowly restricted to members of the mosquito OR2/OR10 clade, AgOR11 and AgOR13 (Carey et al., 2010; Wang et al., 2010). However, the high responses of AgOR11 and AgOR13 to indole reported by Wang et al. (2010) do not necessarily imply high sensitivity to this odorant as CRCs and EC_{50} values were not reported for these receptors. Indeed, while benzaldehyde elicits high current responses in the OR2/OR10 clade, sensitivity to this compound is low compared to indole (Figure 4). The observation that other mosquito OR2 receptors exhibited similar response profiles supports the hypothesis that indole sensitivity is tightly conserved between, and indeed may be restricted to this narrow range of mosquito OR orthologs. This hypothesis is supported both by data reported here as well as the indole sensitivity recently reported for CxOR2 (Pelletier et al., 2010b), which overlaps with that of Aa/AgOR2. Aa/AgOR10 activation profiles while slightly different from Aa/AgOR2 maintained an ability to detect indole albeit with lower affinities. Finally, AaOR9 and AaOR10 paralogs responded similarly to indole suggesting that both ORs have redundant biochemical function, perhaps within different developmental contexts (Bohbot et al., 2007). Alternatively, we cannot rule out that the cognate ligands for these two receptors may be structurally similar to indole (Hughes et al., 2010). Lastly, we also acknowledge odorant binding proteins and other co-factors that are highly expressed in olfactory sensilla but are not present in

heterologous assay systems may be important modulators of chemosensory sensitivity *in vivo* (Biessmann et al. 2010; Pelletier et al. 2010b).

The functional conservation of indole sensitivity within the Aa/AgOR2/OR10 clade suggests that this response is an ancient trait that was present prior to the Anophelinae/Culicinae split (Krzywinski et al. 2001b). Moreover, the preservation of indole sensitivity within a narrow group of *Or* genes that make up the most highly conserved Aa/Ag/CxORs indicates this is important in the life cycles of mosquitoes. Indeed, indole is a ubiquitous volatile compound that has been linked to host seeking and oviposition in both aedine (Millar et al*.,* 1992; Du and Millar 1999; Syed and Leal 2009; Hill et al., 2009; Siju et al*.,* 2010) and anopheline mosquitoes (Blackwell and Johnson 2000; Meijerink et al., 2000; Takken et al., 2001; Meijerink et al., 2001; Qiu et al., 2006; Lindh et al*.,* 2008).

The original ecological context of this olfactory trait such as detection of oviposition sites, hosts, nectar sources or other elements of the mosquito life-cycle is unknown. Identification and functional characterization of OR2/OR10 homologs in non-blood feeding mosquitoes such as members of the Toxorhynchitinae subfamily that are attracted to water sites containing both phenols and indoles (Collins and Blackwell, 2002) may provide key evidence for the ancestral function of indole reception in adult mosquitoes. Such experiments would support the hypothesis that indole reception facilitates mosquito orientation towards

key ecological resources using an ancient olfactory mechanism. More studies will be needed to understand how indole detection intersects with other sensory modalities to inform mosquitoes about different environmental contexts.

CHAPTER III

FUNCTIONAL AGONISM OF INSECT ODORANT RECEPTOR ION CHANNELS

Preface

The following manuscript by Jones et al., has been accepted for publication in the *Proceedings of the National Academy of Sciences*. My contribution to this work included discovering and characterizing the described agonist VUAA1, performing Ca^{2+} mobilization studies and single sensillum recordings.

Abstract

In insects, odor cues are discriminated through a divergent family of odorant receptors (ORs). A functional OR complex consists of both a conventional odorant-binding OR and a non-conventional co-receptor (ORco) that is highly conserved across insect taxa. Recent reports have characterized insect ORs as ion channels, but the precise mechanism of signaling remains unclear. We report the identification and characterization of the first ORco family agonist, VUAA1, using the *Anopheles gambiae* co-receptor (AgORco) and other orthologs. These studies reveal that the ORco family can form functional, stand-alone ion channels, and in addition, provides a first in class agonist to further research in insect OR signaling. In light of the extraordinary conservation

and widespread expression of the ORco family, VUAA1 represents a powerful new family of compounds that can be used to disrupt the destructive behaviors of nuisance insects, agricultural pests, and disease vectors alike.

Introduction

In insects, olfactory cues are in part sensed through the activation of a family of cell-surface odorant receptors (ORs). *In vivo,* insect ORs form heteromeric complexes of unknown stoichiometry consisting of a conventional OR, and a universal co-receptor, now collectively referred to as OR co-receptor (ORco) (Benton et al., 2006). In this model, highly divergent conventional ORs provide coding specificity to the complex and have broad ligand specificities (Hallem and Carlson, 2004; Wang et al.,2010; Carey et al., 2010). In contrast, the functionally requisite ORco has not been shown to bind odorants and is extremely well conserved across taxa (Jones et al., 2005). ORco is required for neuronal cell-surface trafficking and proper signal transduction and it has been demonstrated that orthologs are functionally equivalent *in vivo* and *in vitro* (Larsson et al., 2004). While it is known that ORco is essential for OR-mediated chemoreception, the precise mechanism of signaling has remained unclear. Recent evidence supports two alternative, and not necessarily exclusive models for insect olfactory signal transduction. In both models, the OR complex signals ionotropically through odorant-gated

ion channels, however, one study demonstrates complex gating through cyclic nucleotides, while the other does not (Sato et al., 2008; Wicher et al., 2008).

ORs from the principal afro-tropical malaria vector, *Anopheles* gambiae (Ag), which partially dictate their host-seeking behavior, were used to examine the function of insect ORs. In *Anopheles gambiae,* 78 conventional *Or*s have been described and their coding specificities have been extensively characterized (Fox et al*.,* 2001,2002; Hill et al*.,* 2002; Lu et al*.,* 2007; Carey et al*.,* 2010). In *An. gambiae,* a single conventional *AgOr* is expressed in every olfactory receptor neuron (ORN) in conjunction with *AgOr7,* the ORco ortholog (Pitts, Fox and Zwiebel, 2004).

Materials and Methods

Cell Culture and Ca^{2+} imaging

Transient transfections of **pCI** (Promega)-containing OR constructs were performed with FuGENE 6 (Roche) into FLP-IN T-REX 293 (Invitrogen) cell lines. TRPV1 cells were a gift from Dr. D. Julius (Bohlen et al., 2010). Construction of the AgOR10 +AgORco cell line has been previously described(Bohbot et al., 2011).Fluo-4AM-dye-loaded cells were assayed for ligand response in an FDSS6000 (Hammamatsu) as previously described(Bohbot et al*.,* 2011).

Chemicals

Benzaldehyde (CAS 100-52-7) and Capsaicin (CAS 404-86-4) were purchased from Sigma-Aldrich. 8-Br-cAMP and 8-Br-cGMP were obtained from Enzo Life Sciences. VUAA1 (N-(4-Ethylphenyl)-2-((4-Et-5-(3-Pyridinyl)-4H-1,2,4-Triazol-3-yl)Thio)acetamide) was purchased from Sigma-Aldrich's Rare Chemical Library (CAS # 525582-84-7, product discontinued at time of print).. To ensure that observed activity was elicited from VUAA1, and not from a contaminant present in the mixture, we performed preparative High Performance Liquid Chromatography (HPLC). Briefly, 20mg VUAA1 was dissolved in a 50/50 mixture of methanol and DMSO, and HPLC was performed on a Phenomenex Luna 30x50-mm C18 prep column with 0.1% Trifluoracetic acid (TFA) in H_20 coupled to an acetonitrile gradient. Appropriate fractions were pooled and passed over a TFA scavenger column (Polymer labs, StratoSpheres SPE PL-HCO3 MP-resin). The solvent was removed by rotary evaporation with a Biotage V10 Roto-vap, yielding white powder. VUAA1 was subsequently re-dissolved in DMSO and assayed as described.

Characterization of chemical materials

^{1}H-NMR (400 MHz, DMSO-$_{d6}$) d 8.73 (d, *J* = 1.8 Hz, 1H), 8.65 (dd, *J* = 1.5, 4.8 Hz, 1H), 7.97 (dt, *J*= 1.9, 8.0 Hz, 1H), 7.49 (dd, *J* = 2.5, 8.3 Hz, 1H), 7.37 (d, *J* = 8.4 Hz, 2H), 7.04 (d, *J* = 8.4 HZ, 2H), 4.10 (s, 1H), 3.95 (q, *J* = 7.2 Hz, 2H), 2.43 (q, *J* = 7.6 Hz, 2H), 1.13 (t, *J* = 8.0 Hz, 3H), 1.04 (t, *J* =

8.0 Hz, 3H).^{13}C-NMR(400 MHz, DMSO-$_{d6}$) d 165.71, 152.92, 151.32, 150.95, 149.07, 139.35, 136.87, 136.33, 128.38, 124.34, 123.90, 119.58, 37.91, 27.97, 16.05, 15.42. HRMS (m/z) $[M]^+$ calculated for $C_{19}H_{22}N_5OS$, 368.1544 found 368.1545.

Patch-clamp recording in HEK cells

Currents from OR-expressing HEK293 cells were amplified using an Axopatch 200b Amplifier (Axon Instruments) and digitized through a Digidata 1322A (Axon Instruments). Electrophysiological data was recorded and analyzed using pCLAMP 10 (Axon Instruments). Electrodes were fabricated from quartz tubing (Sutter Instruments) and pulled to 4–6 MΩ for whole-cell recording. Electrodes were filled with internal solution [120mM KCl, 30mM D-glucose, 10mM HEPES, 2mM $MgCl_2$, 1.1mM EGTA, and 0.1 $CaCl_2$ (pH 7.35, 280mOsm)]. External (bath) solution contained 130mM NaCl, 34mM D-glucose, 10mM HEPES, 1.5mM $CaCl_2$, 1.3mM KH_2PO_4, and 0.5 $MgSO_4$ (pH 7.35, 300mOsm). Compounds were diluted in external solution and locally perfused to the recording cell using Perfusion Pencil (Automate Scientific) and controlled by a ValveLink 8.2 controller (Automate Scientific). Whole-cell recordings were sampled at 10kHz and filtered at 5kHz. Outside-out patches were obtained using 10- to 15-MΩ electrodes pulled from standard glass capillaries (World Precision Instruments) and fire-polished with an MF-830 micro forge (Narishige). Single-channel recordings were sampled at 20kHz.

Recordings were reduced to 1kHz and low-pass filtered at 500Hz for display and analysis using QuB (SUNY at Buffalo).

Single sensillum recordings:

Single sensillum recordings were performed on 4- to 7-day-old, non-blood-fed *Anopheles gambiae* females maintained on 10% sucrose and a 12 h/12 h light/dark cycle. Legs, wings and antennae were removed from cold-anesthetized females that were then restrained on double-stick tape with thread. A glass reference electrode filled with sensillar lymph Ringers (SLR) was placed in the eye, and the recording electrode filled with DMSO or VUAA1 diluted in SLR was used to puncture sensilla at their base (Xu et al*.,* 2005). Preparations were kept under a steady stream of humidified, synthetic air (21% O_2/ 79% N_2) to limit the basal activity of CpA. Sensilla that did not respond to CO_2 or 1-octen-3-ol were excluded from analysis. Responses were recorded and digitized using a Syntech IDAC-4 and analyzed with AutoSpike software (Syntech). A new glass recording pipette was used for every recording. Data was sampled at 12kHz.

Results

In the context of a larger effort to identify broadly effective insect repellents, we carried out high-throughput, calcium-imaging screens for novel modulators of the AgORco/AgOR10 complex expressed in human embryonic kidney (HEK293) cell lines. AgOR10 was chosen in particular

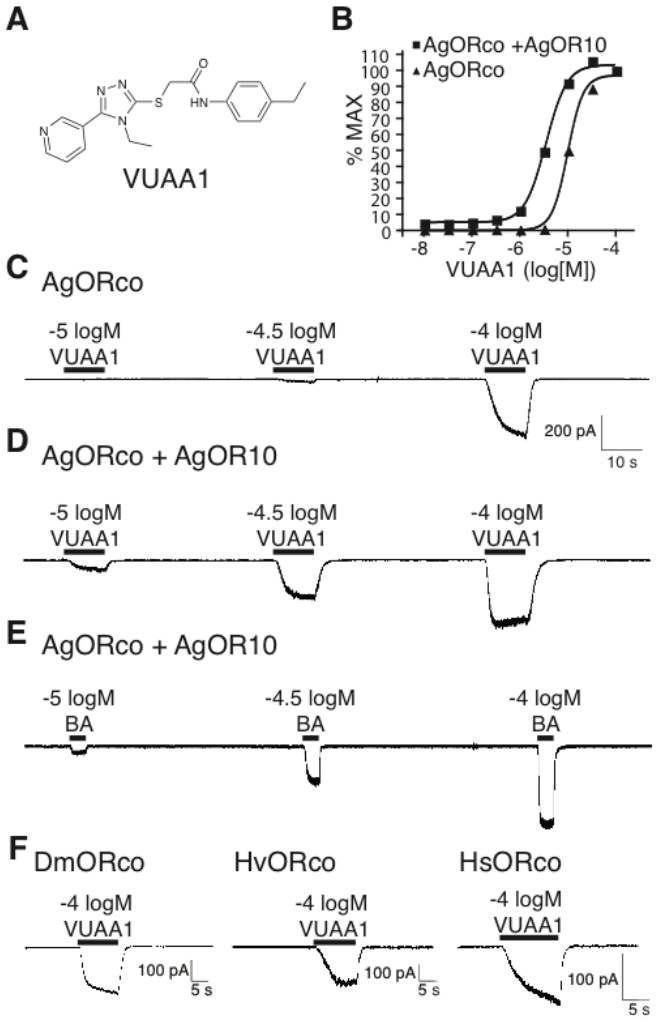

Figure 1. VUAA1 evokes macroscopic currents in HEK293 cells expressing AgORco and its orthologs.

(*A*) Structure of VUAA1**.** (*B*) Concentration–response curves (CRCs) generated from Fluo-4 acetoxymethyl ester-based Ca^{2+} imaging with AgORco and AgORco+AgOR10 cell lines in response to VUAA1. (*C*, *D*), Whole-cell patch clamp recordings of concentration-dependent responses to VUAA1 in cells stably expressing AgORco alone (*C*) and AgORco+AgOR10 (*D*). (*E*) Benzaldehyde (BA), an AgOR10 agonist, elicits concentration-dependent responses in AgORco+AgOR10 cells. (*F*) Whole-cell current responses to VUAA1 in HEK293 cells expressing DmORco, HvORco, and HsORco. Holding potentials of −60 mV were used in (*C*-*F*)**.**

on the basis of its molecular and functional conservation across multiple mosquito species (Bohbot et al*,* 2011).

Of 118,720 compounds screened against AgORco/OR10 cells, a single compound, denoted here as VUAA1, was identified which elicited activity consistent with allosteric agonism. Classification as an allosteric agonist was based on VUAA1's intrinsic efficacy and capacity to potentiate the response of the complex's response to a natural ligand, 2-ethylphenol.

The chemical identity of VUAA1 was verified using high-resolution mass spectrometry (HRMS) as well as ^{1}H and ^{13}C NMR [see methods]. VUAA1 was re-validated against AgORco+AgOR10 cells and elicited concentration-dependent responses that were not seen in control cells (Fig. 1b). In addition, VUAA1 activated several other AgORco+AgORx cell lines in the context of other, ongoing HTS screens. We pursued VUAA1 on the basis of its novelty, as a probe for AgOR pharmacology, and in light of its potential role as a modulator of olfactory driven behaviors in *An. gambiae*.

As AgORco was the common element among the functional responses of numerous AgORco+AgORx cell lines, we postulated that VUAA1 was a potential AgORco agonist. To test this hypothesis, whole-cell patch clamp responses were examined in AgORco+AgOR10-expressing cells and HEK293 cells stably expressing AgORco alone. In these experiments, VUAA1 elicited concentration-dependent inward currents in both AgORco- and AgORco+AgOR10-expressing cells (Fig.

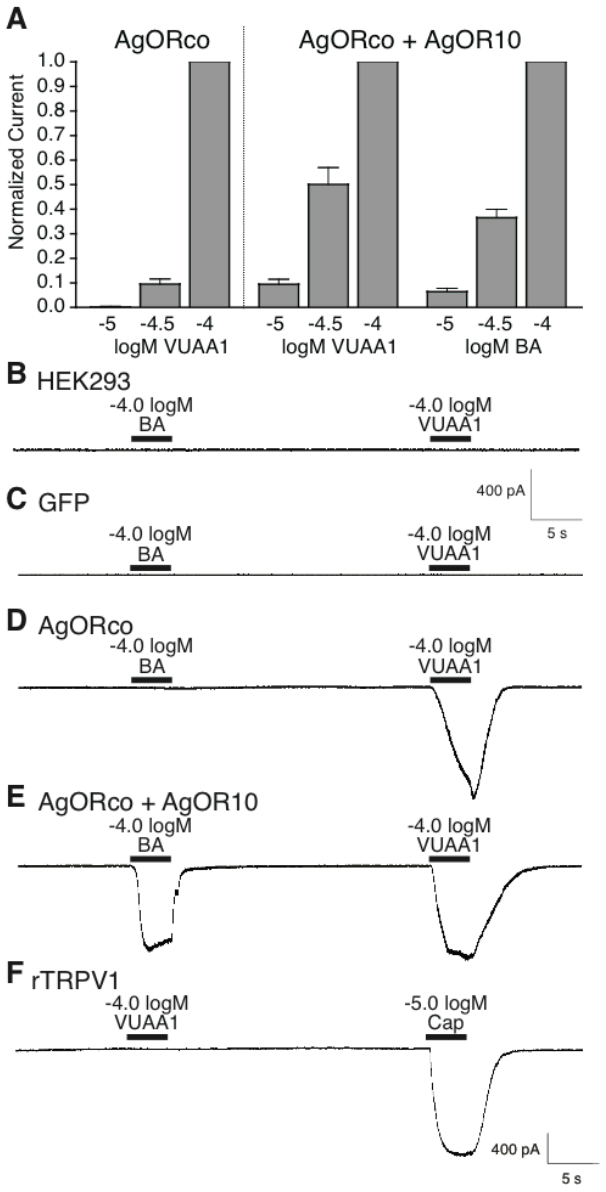

Supporting Figure 1. **VUAA1 and BA responses are AgOR specific.** (*A*) Histogram of normalized currents from concentration-dependent responses in Figure 1*C*-*E* (n=5). (*B*) Un-transfected HEK293 cells did not respond to either VUAA1 or BA (n=5). (*C*) GFP was co-transfected with ORco orthologs to identify cells expressing the OR. GFP-alone cells had no currents from VUAA1 or BA (n=4). (*D* and *E*) For comparison, both AgORco and AgORco+AgOR10 cells depolarized during VUAA1 application, while only AgORco+AgOR10 cells responded to BA. Holding potentials for all recordings were −60mV. (*F*) VUAA1 did not elicit currents in cells stably expressing another cation channel, rat transient receptor potential vanilloid 1 (rTRPV1), but did respond to the agonist capsaicin (n=4).

1c,d) demonstrating both that VUAA1 is an AgORco agonist and that currents were AgORco-dependent. The VUAA1-induced currents in AgORco+AgOR10 cells resembled those resulting from application of benzaldehyde, an AgOR10 agonist (Fig. 1e). AgORco+AgOR10 cells were more sensitive to VUAA1 than AgORco cells, producing inward currents at −5.0 logM, a concentration at which AgORco had no response. All currents induced by VUAA1 were AgORco dependent; no responses were observed in control cells (Fig. S1).

To further investigate the specificity of VUAA1 agonism, and to determine if it was capable of activating related orthologs, we tested ORco orthologs across Dipteran and Lepidopteran taxa. When we transiently transfected HEK cells with the ORco orthologs of *Drosophila melanogaster* and *Heliothis virescens*—DmORco and HvORco, respectively, VUAA1 elicited robust inward currents similar to AgORco-expressing cells (Fig.1f). These results demonstrate that VUAA1 is a broad-spectrum ORco family agonist capable of activating OR co-receptors within and across multiple insect orders. This is consistent with the high sequence identity that is characteristic of ORco family members (76% to DmORco and 67% to HvORco) as well as their previously demonstrated functional overlap (Jones et al*.,* 2005).

It has been previously demonstrated that the DmORco/ORx complex functions ionotropically, so we set out to characterize the conductive properties of the anopheline complex in response to VUAA1

(Wicher et al., 2008; Sato et al..2008). Using whole-cell patch clamp experiments, we determined the current–voltage relationships of AgORco on its own and in complex with AgOR10. Currents induced by VUAA1 in AgORco-expressing cells as well as those induced by VUAA1 or benzaldehyde in AgORco+AgOR10 cells were all nearly symmetrical (Fig. S2a-c). The reversal potential of AgORco alone in the presence of VUAA1 was −4.74 ± 3.17 mV, while AgORco+AgOR10 reversal potentials were +0.18 ± 0.02 mV with VUAA1 and −0.81 ± 2.12 mV with benzaldehyde (mean ± s.e.m., Fig. S2d). These current–voltage relationships do not indicate any voltage-dependent gating, and the near-zero reversal potentials are consistent with previous reports that described non-selective cation conductance (Sato et al., 2008; Wicher et al., 2008). We next examined whether VUAA1-induced responses could be attenuated by ruthenium red (RR), a general cation channel blocker previously found to inhibit insect OR currents (Sato et al., 2008). Application of RR reduced the VUAA1-elicited currents of AgORco cells by 79.4 ± 4.0%, while RR reduced VUAA1 and benzaldehyde responses of AgORco+AgOR10 cells by 68.3 ± 2.8% and 87.8 ± 1.8%, respectively (Fig. 2). Taken together, these data indicate that AgORco exhibits channel-like properties consistent with a non-selective cation channel.

In the next set of studies, outside-out membrane patches were excised from AgORco-expressing cells to examine single-channel currents evoked by VUAA1 (Fig. 3a). Here, spontaneous channel opening was

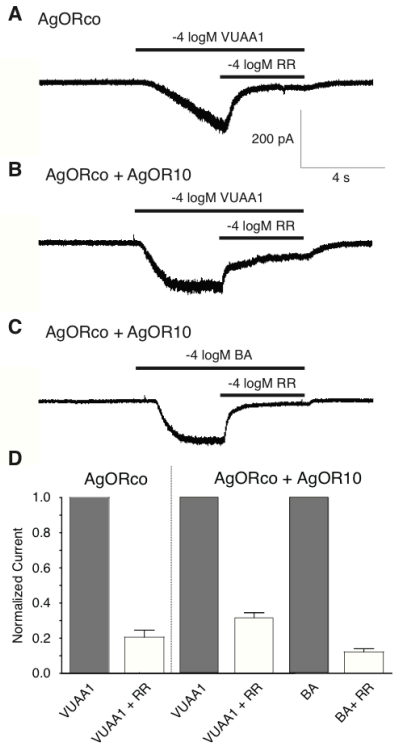

Figure 2. Ruthenium red blocks inward currents of AgORco alone and in complex.

(*A*-*C*) Representative traces of ruthenium-red-blocked inward currents in AgORco (*A*) and AgORco+AgOR10 (*B*, *C*) cells. Holding potential was −60 mV for (*A*-*C*). (*D*) Analysis of Ruthenium Red blockage of VUAA1 and BA-induced currents from *A* (n=5), *B* (n=5), *C* (n=4).

observed before VUAA1 stimulation, but with very low probability (P_o= 0.02) (Fig. 3b). During a 5-s application of VUAA1, channel opening probability increased to P_o= 0.38 (Fig. 3c). Subsequent to agonist washout, channel opening probability decreased to 0.00 (Fig. 3d). The average unitary current of AgORco was 1.3 ± 0.3 pA (mean ± st. dev) (Fig. 3c inset), which is comparable to previous single-channel studies of insect ORs (Sato et al..2008). Taken together, these data support the hypothesis that VUAA1 agonizes AgORco in the absence of other intracellular components and provide additional support for the ionotropic nature of this channel as well as the role of VUAA1 as a direct agonist of AgORco and other ORco family members.

We then investigated whether activation of AgORco involves second-messenger-based signaling, which has been reported to contribute to insect olfactory signaling (Wicher et al., 2008). In these studies, which are consistent with a previously published report, two cyclic nucleotide analogs (8-Br-cAMP and 8-Br-cGMP) were unable to evoke whole-cell currents in AgORco or AgORco+AgOR10 cells (Fig. 4a, b) (Sato et al., 2008). Importantly, *Rattus norvegicus* cyclic-nucleotide gated channel A2 (rCNGA2) demonstrated robust responses to 8-Br cGMP (Fig. 4c) (Dhallan et al., 1990). These data support a hypothesis in which an ionotropic mechanism is the principal, if not sole, signaling mechanism of functional AgOR complexes.

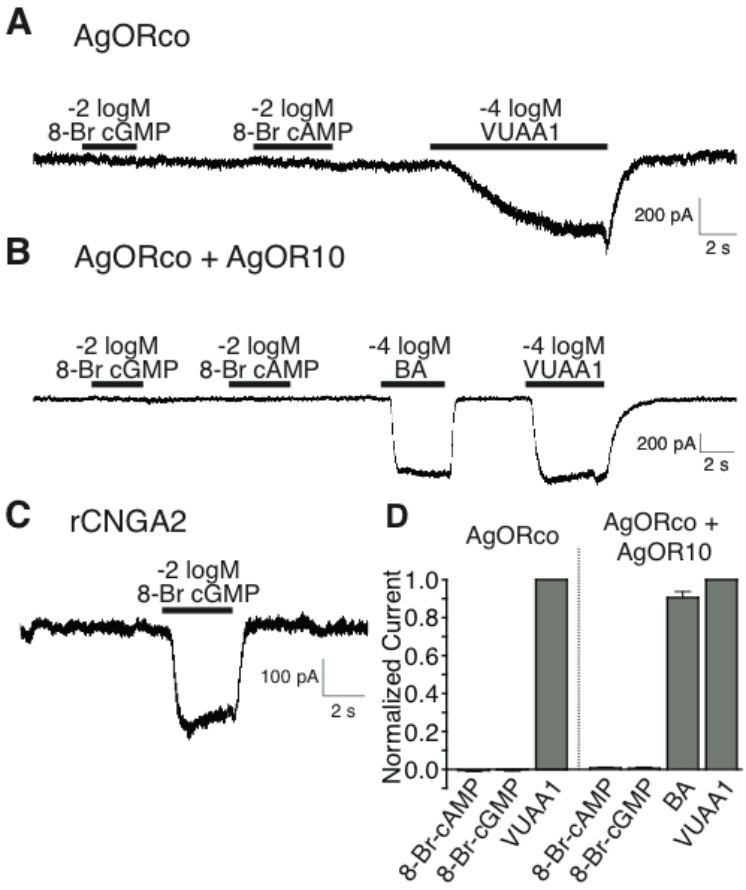

Figure 3. AgORco is a functional channel and responds to VUAA1 in outside-out membrane patches.

(*A*) Single-channel recording from an outside-out excised patch pulled from a cell-expressing AgORco. (*B*-*D*) Expansions of trace *A* before (*B*), during (*C*), and after (*D*) a 5-s application of −4.0 logM VUAA1. All-point current histograms of trace expansions are in the right panel of *B*-*D*. Excised membrane patch was held at −60 mV

In addition to demonstrating that AgORco alone and AgORco+AgOR10 complexes act as functional, ligand-gated ion channels, these studies have shown that VUAA1 elicits AgOR currents similar to those evoked by odorants. As an additional indicator of the specificity of VUAA1 for non-conventional ORco's, we tested VUAA1 on another non-selective cation channel, the transient receptor potential vanilloid receptor1 (TRPV1) (Caterina et al., 1997; Bohlen et al., 2010). In these controls, VUAA1 failed to evoke any response, while capsaicin elicited robust responses in TRPV1-expressing cells, thereby demonstrating that VUAA1 does not act as a general cation channel agonist (Fig. S2f).

We next performed single unit, extracellular electrophysiological recordings on the maxillary palp of adult female *An. gambiae* to determine whether VUAA1 could activate AgORco-expressing olfactory receptor neurons (ORNs) *in vivo.* We have previously demonstrated that the maxillary palp, an elongate olfactory appendage emanating from the head, contains only a single sensilla type, the capitate peg (Cp), and that all capitate pegs contain 3 chemosensory neurons (Lu et al., 2007). The highly stereotypic Cp sensilla, contain two AgORco/conventional OR-expressing ORNs (CpB and CpC), as well as a CO_2 sensitive neuron (CpA), which does not express AgORco. Single sensillum recordings (SSRs) involve puncturing the sensillum wall with a glass electrode, which enables the passive sampling of all sensillum neurons simultaneously. The activities of individual neurons are discriminated from each other

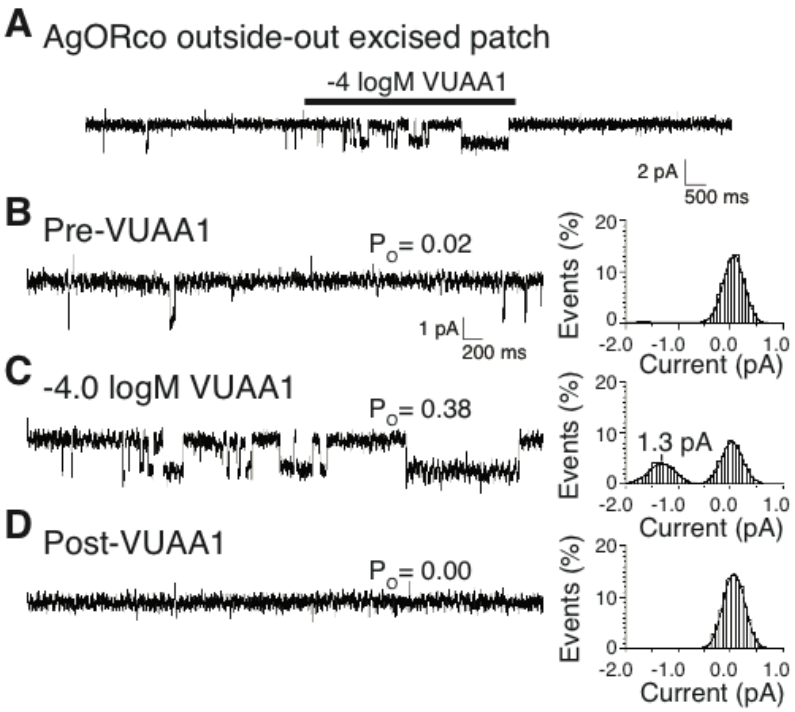

Figure 4. 8-Br-cAMP and 8-Br-cGMP did not elicit currents in AgORco or AgORco+AgOR10 cells.

(*A*) Representative trace from whole-cell recordings from cells expressing AgORco-expressing cells with application of 8-Br-cAMP, 8-Br-cGMP, and VUAA1. (*B*) Representative trace from cells expressing AgORco+AgOR10 with application of 8-Br-cAMP, 8-Br-cGMP, BA, and VUAA1. (*C*) Representative trace from cells expressing rCNGA2 with application of 8-Br-cGMP. Holding potentials for all recordings were −60mV. (*D*) Histogram of normalized currents from cyclic nucleotide and control responses (n=4). All currents normalized to VUAA1 responses.

based on compound response profiles and action potential amplitudes. In these preparations, CpA spike activity is clearly distinguished from those of CpB/C by its large action potential amplitude. CpB/C spikes were much smaller and in some preparations indistinguishable from each other. Consequently, the spike activities of CpB/C neurons were binned for data analysis. Accordingly, we reasoned that if VUAA1 acts as a specific AgORco agonist, we would expect it to selectively increase the spike frequency of the CpB/C neurons, but have no effect on CpA responses.

Because of its relatively high molecular weight, and despite multiple attempts, volatile delivery of VUAA1 was not feasible. As a result, VUAA1 was directly introduced to each sensillum via the glass-recording electrode, rather than through the more conventional method of volatile delivery. When VUAA1 was added to the electrode solution it increased the spike frequency of CpB/C neurons in a dose-dependent manner, while vehicle alone had no effect (Fig. 5a, b, d). Differential CpB/C spike activity was observed immediately after puncturing each sensillum, suggesting millisecond compound diffusion rates into the sensillum (Fig. 5a, b, d). At the completion of each assay, a CO_2 pulse was delivered to the sensillum to test whether VUAA1 affected the CpA neuron; in contrast to the responsiveness of the AgORco-expressing CpB/C neurons, CpA activity was unchanged in the presence of vehicle and/or VUAA1 (Fig. 5a, b, c). The ability of VUAA1 to activate AgORco-expressing ORNs *in vivo* further demonstrates that AgORco is an accessible biological target in *An.*

gambiae, which is not obscured by other proteins or cofactors involved in olfactory signal transduction.

Discussion

Here we report the identification and characterization of VUAA1, the first ORco family agonist that is capable of gating orthologs across multiple insect taxa. In contrast to previous models, these data support a hypothesis whereby AgORco and related ORco orthologs act as stand-alone ion channels, which can function independently of their heteromeric partners and are indifferent to cyclic nucleotide modulation. Additionally, because there are no known natural ligands for ORco family members, we suggest that AgORco and other ORco family members should, be recognized as allosterically-gated ion channel subunits rather than odorant receptors.

As ORco functionality is required for OR-mediated chemoreception across all insects, an ORco agonist would theoretically be capable of activating all OR-expressing ORNs. Accordingly, ORco agonism would be expected to severely impact the discrimination of odors across all insect taxa, affecting a broad range of chemosensory driven behaviors. In *An. gambiae* females universal ORN activation would likely disrupt a variety of olfactory-driven behaviors, most notably human host-seeking, which serves as the foundation for their ability to transmit malaria (Zwiebel and Takken, 2004). The discovery of a universal ORco agonist is also an

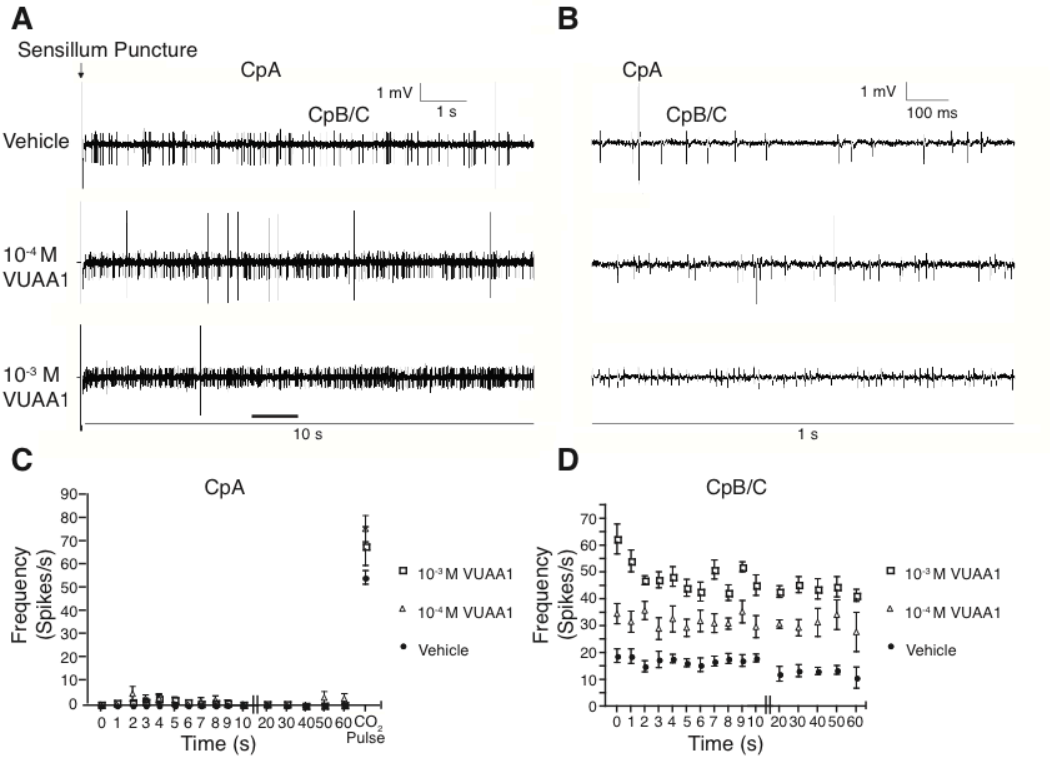

Figure 5. VUAA1 activates AgORco-expressing neurons in *Anopheles gambiae* females. (*A*) Representative traces of SSR recordings from capitate peg sensilla upon electrode puncture. VUAA1 or vehicle alone (DMSO) was delivered through the glass- recording electrode. CpA is discernible from the smaller CpB/C action potentials. (*B*) Expansions of traces in *A*. (*C*) Activity of CpA neuron in response to VUAA1. Spike frequency was calculated every second for the first 10 s after sensillum puncture and every 10 s thereafter. After 60 s, the preparation was pulsed for 2 s with atmospheric air to confirm a functional CpA neuron (n=6). (*D*) Activity of CpB/CpC neurons in response to VUAA1, as in *C*.

important step towards the development of a new generation of broad-spectrum agents for integrated management of nuisance insects and agricultural pests.

The *in vivo* VUAA1-mediated activation of AgORco-expressing cells serves as a proof-of-principle that targeting AgORco and other ORco orthologs is a viable approach for the development of behaviorally disruptive olfactory compounds (BDOCs) to control a wide range of insect pests and vectors. While it is premature to speculate as to the ultimate utility of VUAA1 as an anti-malarial BDOC or as a general modulator of insect chemosensory-driven behaviors, VUAA1 nevertheless represents an important tool for the direct study of AgORco and other ORco orthologs in insect chemosensory signal transduction.

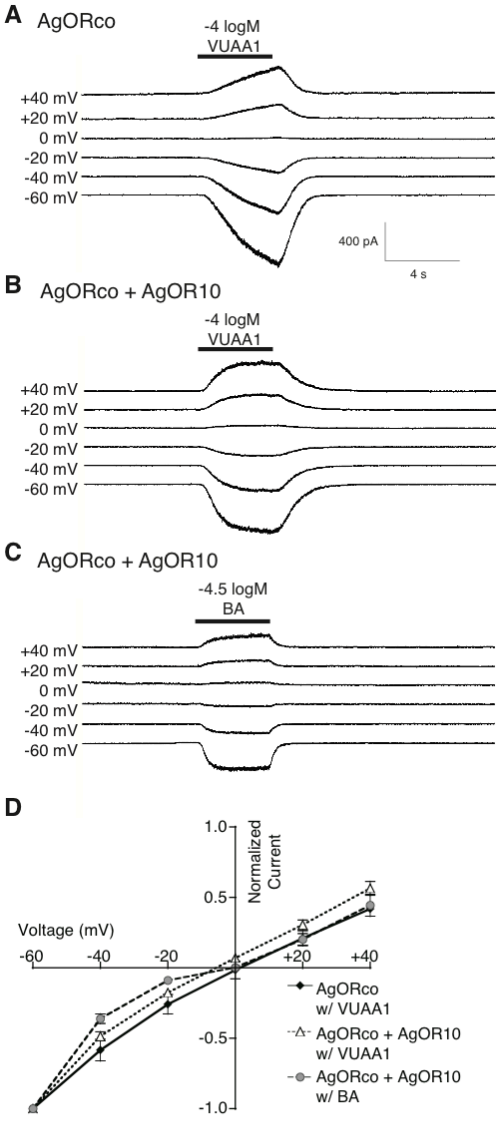

Supporting Figure 2. Channel-like currents elicited by application of VUAA1 to cells expressing AgORco alone or in complex. (*A*-*C*), Representative traces of voltage-dependent currents in AgORco (*A*) and AgORco+AgOR10 (*B* and *C*) cells. Holding potentials ranged from −60 mV to +40 mV in 20-mV increments. (*D*) Current–voltage relationships of *A* (n=3), *B* (n=7), and *C* (n=4) from normalized peak currents.

CHAPTER IV

TRANSCRIPTOME PROFILING OF CHEMOSENSORY APPENDAGES IN THE MALARIA VECTOR ANOPHELES GAMBIAE REVEALS TISSUE- AND SEX- SPECIFIC SIGNATURES OF ODOR CODING

Preface

The following manuscript, Jones et al., 2011 was submitted to PLoS Genetics on March 2, 2011. My contribution to this work included experimental design, dissections of mosquito tissues, data analysis and writing the manuscript.

Abstract

Chemosensory signal transduction guides the behavior of many insects including *Anopheles gambiae*, the major vector for human malaria in sub-Saharan Africa. To better understand the molecular basis of mosquito chemosensation, we used whole transcriptome RNA sequencing (RNA-seq) to compare transcript abundance profiles between the antennae and maxillary palps, the two major chemosensory tissues of adult female and male *An. gambiae*. This analysis revealed tissue-specific expression differences in gene families with known chemosensory function and in several other families heretofore unassociated with chemosensation. The antennae of both sexes expressed a greater diversity of known chemosensory genes than did the maxillary palps, but the repertoire of

these genes within each tissue was remarkably conserved between the sexes. These findings suggest that the chemoreceptive range, as defined by gene expression profiles, is similar in female and male *An. gambiae*. The crucial difference being that the higher absolute levels of chemosensory gene expression in females results in enhanced odor sensitivity.

Introduction

Insects rely heavily upon chemosensation, the ability to detect and react to environmental chemical cues, in virtually every aspect of their life cycle (Gillott, 2005). Chemosensation is critical to food source identification, predator avoidance, oviposition site selection, kin recognition, mate choice, and toxic compound avoidance. In insects, chemosensory neurons are contained within distinct tissues on many parts of the body, most conspicuously on the antennae and the maxillary palps located on the head. These appendages are decorated with sensory hairs, or sensilla, that house the neurons in which families of insect-specific receptors and other proteins transduce chemosensory signals (for reviews see McIver, 1982; Gilliott, 2005; de Bruyne and Baker, 2008; Sato and Touhara, 2009). Some insect sensory neurons have become highly specialized for the detection of single compounds, while others function more generally and are sensitive to multiple compounds (Hallem et al., 2006; Kaissling 2009; Touhara and Vosshall, 2009). While the

physiological and cellular basis of insect chemosensation have been studied for many years, its molecular underpinnings have only recently begun to be elucidated.

In mosquitoes, host-seeking behavior is driven largely by olfaction (Takken and Knols, 1999; Zwiebel and Takken, 2004). *An. gambiae* females display a strong preference for human hosts (anthropophily), which contributes substantially to their ability to transmit human diseases, including malaria (Costantini et al., 1999; Takken and Knols, 1999; Zwiebel and Takken, 2004). The identification of chemoreceptor gene families in the *An. gambiae* genome (Hill et al., 2002; Liu et al., 2010) has facilitated the correlation of behavioral observations and physiological sensitivities to receptor expression (Fox et al., 2001; Pitts et al., 2004; Kwon et al., 2006; Lu et al., 2007). Specific chemoreceptors expressed in antennal and palpal neurons of *An. gambiae* are sensitive to host odors, including volatile components produced from bacteria associated with human skin (Hallem et al., 2004; Carey et al., 2010; Verhulst et al., 2010; Wang et al., 2010). As a consequence, the function of select chemoreceptor genes in *An. gambiae* has been linked to semiochemicals that are integral to specific host seeking behaviors. Despite this progress, very little of the downstream signaling events and regulation of chemoreceptor function is known. Moreover, the potential chemosensory bases of sexually distinct behaviors in *An. gambiae* are poorly understood (Clements, 1999; Zwiebel and Takken, 2004; Howell and Knols 2009).

RNA-seq offers great potential to comprehensively study gene expression in head appendages of *An. gambiae* to provide insight into the molecular foundations of chemoreception. While several microarray-based studies have examined global transcript abundance in *An. gambiae* (Aguilar et al., 2005; Marinotti et al., 2005; Marinotti et al., 2006; Warr et al., 2007; Baton et al., 2009; Aguilar et al., 2010; Das et al., 2010; Cook and Sinkins, 2010), none has focused exclusively on chemoreceptive tissues. Moreover, unlike microarrays and older methods, RNA-seq provides transcriptome-wide sequence coverage with unbiased, highly quantitative results (Wang, Gerstein, Snyder, 2009) and greatly improved sensitivity (Mortazavi et al., 2008; 't Hoen et al., 2008). To date, RNA-seq has been used to address several functional and evolutionary questions pertaining to mosquito biology (Gibbons et al., 2009; Crawford et al., 2010; Hittinger et al., 2010; Neira-Oviedo, 2010; Bonizzoni et al., 2011).

Here we utilize RNA-seq to quantify global abundance levels of poly-adenylated transcripts of *An. gambiae* whole adults, antennae and maxillary palps across sexes. By mapping the generated short read sequences against the full set of annotated *An. gambiae* transcripts we have generated six tissue- and sex-specific transcriptome profiles. As expected, gene families with well-established chemosensory function displayed antenna- or palp-enhanced abundance, with antennae showing enhancement of a larger number of these genes. We also identified numerous members of other gene families enhanced in either antennae or

maxillary palps such as biotransformation enzymes, transcription factors, transmembrane receptors, ion channels, transporters and proteases which are likely to function in chemosensory pathways This broadens our understanding of the molecular biology in these peripheral sensory appendages and may lead to novel targets for insect control. Despite obvious morphological and molecular differences between the sexes, our data reveals an unanticipated level of sexual monomorphism with respect to the abundance of known chemoreceptive functional classes. Here we have utilized RNA-seq to quantify global abundance levels of poly-adenylated transcripts of *An. gambiae* whole adults, antennae and maxillary palps across sexes. By mapping the generated short read sequences against the full set of annotated *An. gambiae* transcripts we have generated six tissue- and sex-specific transcriptome profiles. As expected, gene families with well-established chemosensory function display antenna- or palp-enhanced abundance, with antennae showing enhancement of a larger number of these genes. We also have identified numerous members of other gene families that are enhanced in either antennae or maxillary palps, such as biotransformation enzymes, transcription factors, transmembrane receptors, ion channels, transporters and proteases which are likely to function in chemosensory pathways. Our data also revealed an unanticipated level of sexual monomorphism with respect to the abundance and distribution of known chemoreceptive functional classes in the antenna and the maxillary

palp. Taken as a whole, this study greatly broadens our understanding of the molecular processes involved in peripheral sensory appendages, raising new questions about basic dipteran biology and offering the potential for novel targets for insect control.

Materials and Methods

Mosquito rearing

An. gambiae sensu stricto, which originated from Suakoko, Liberia (della Torre et al., 1996), was reared as described (Qiu et al., 2004).

RNA isolation and sequencing

Tissues were hand dissected from 4-6 d.o. adult *An. gambiae* at ~ZT12 and immediately placed in RNA Later Ice (Ambion Corp.; Austin, TX) on ice. Total RNA was isolated from each sample using RNeasy columns (Qiagen Inc.; Carlsbad, CA) according to the manufacturer's protocol. mRNA isolation and cDNA library preparation were carried out using the Illumina mRNA sequencing kit (Illumina Inc.; San Diego, CA). Libraries were sequenced using an Illumina Genome Analyzer II.

AgOr and AgObp Reannotations

Novel *AgOrs* were identified by tBLASTn searches (www.ncbi.org; default parameters) using the previously identified AgOR peptides as queries.

Two new candidate *AgOrs* were identified and have been named *AgOrs 80* and *81*. Furthermore, *AgOrs 12*, *67*, *78* and *79* have been purged from the *AgOr* family as apparent duplication errors in the original assembly (Table 2). Three new candidate *AgObps* (*69*, *70* and *71*) were identified using similar tBLASTn searches and were added to the family based on two criteria: the candidate genes possessed motifs that exemplify the *Obp* family (Vogt, 1981; Hekmat-Scafe et al., 2002; Kruse, 2003; Xu et al., 2003) and each gene model encoded a unique transcript. Other genes resembling *Obps* were identified, but have not been included in the named members of the *AgObp* family. However we recognize the possibility that these genes may ultimately prove to be unique, or function as odor-carriers. These will be discussed in more detail below. Similarly, *AgObps 16*, *17*, *24, 58, 59, 61, 61,* and 65 were purged from the *AgObp* family as apparent duplication errors in assembly. All modifications to the *AgOr* and *AgObp* families have been submitted to VectorBase.

Data processing and abundance profiling

Individual *Illumina* read files were mapped to the recently updated (Dec. 2010) soft RepeatMasked version of the assembled *An. gambiae* genome, to the mitochondrial genome, and to the annotated *An. gambiae* transcripts (www.VectorBase.org). For purposes of mapping, all alternate transcript isoforms for a given gene were condensed under that gene's respective AGAP designation. Prior to mapping, individual reads were

quality checked and uniformly trimmed by 4 and 12 nucleotides on their 5- and 3-prime ends respectively to account for spurious adapter incorporation (5') and for sequencing reaction degeneration (3') Mapping was carried out using seqmap software, configured to allow for a maximum of three mismatches per read. Processed mapping data was then consolidated based upon AGAP number and the results summarized by rseq. Abundance level output by rseq is reported in terms of unique reads, total weighted reads, and transcript length. Total weighted reads and AGAP transcript length were used to calculate a normalized abundance level of Reads per Kilobase per Million reads mapped (RPKMs), for every AGAP in every tissue type (Mortazavi et al., 2008).

PfamA categorization

Peptide sequences from AgamP3.6 conceptual peptides (n=12,669) were compared to the PfamA dataset (The Pfam protein families database: Finn et al., 2010) using the default e-value threshold of 1.0.

Comparison of tissue abundance profiles

Statistical significance was assigned to each pairwise tissue comparison (antenna:body, palp:body, body:body) by setting up a Fisher's Exact test, evaluating gene-by-gene differences of weighted, mapped reads tot total mapped reads for a given sample. The Agam3.6 transcript annotation contains 13319 unique, annotated transcripts and the statistical

significance of the Fisher's Test was evaluated against a Bonferroni corrected p-value of 3.8x10-6.

Results and Discussion

RNA Sequencing and Gene Mapping

As a means of inferring gene expression in chemosensory appendages we employed single-end short read (43bp) RNA-seq technology to characterize the relative abundances of poly-adenylated RNAs in antennae, maxillary palps and whole bodies of female and male adult mosquitoes. We established tissue- specific gene expression profiles for each of our six samples by mapping the read sequence files against the annotated *An. gambiae* transcriptome, using an approach that quantitated transcript abundance per gene and which accounted for all annotated transcripts per gene (see Materials and Methods). As our reference transcriptome, we used the AgamP3.6 version of the *An. gambiae* gene annotation, which contains 12,669 protein-coding genes and 650 non-coding RNAs (www.VectorBase.org). For each of the tissue types assayed, we obtained an average 30.5 million sequence reads per tissue type and mapped them to the *An. gambiae* transcriptome, nuclear

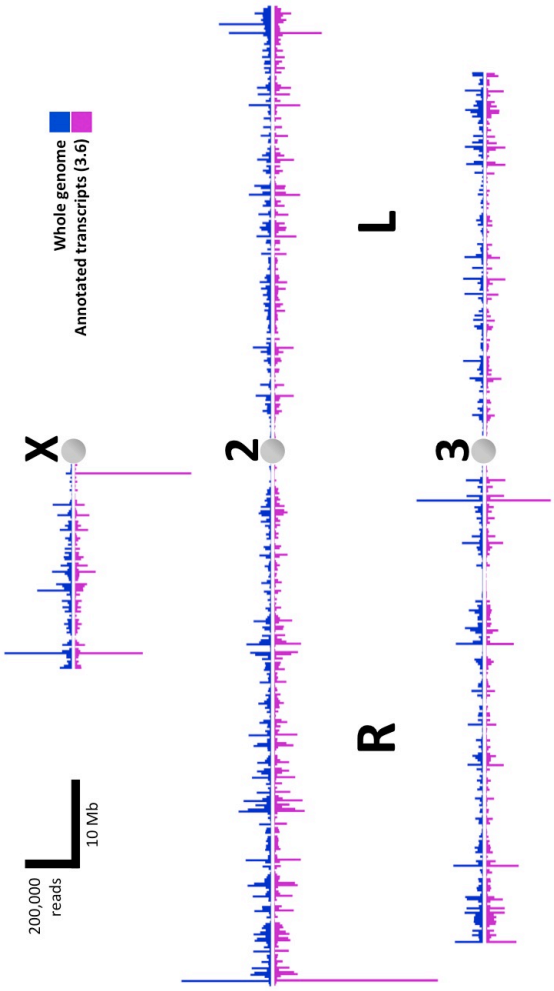

Figure 1. Read coverage of *An. gambiae* genome. Read count coverage of the nuclear genome (magenta) and of the transctiptome (blue). Vertical bars represent counts of sequence reads per 250kB interval along each of the three chromosomes.

and mitochondrial genomes (Table 1). On average, 57.4% of the reads per sample mapped to annotated genes, 91.5% to the nuclear genome (Table 1), and 2% to the mitochondrial genome (Table 1). Table S1 contains the complete RNA-seq data set described above, including the number of reads from each tissue sample that mapped to all 13,319 annotated *An. gambiae* genes.

On a whole-genome level, comparison of the density of reads sequenced from the female body along all chromosomes showed a high degree of correspondence between the number of reads mapped to the nuclear genome and the number of reads mapped to the transcriptome (Figure 1). That said, there are a few areas of asymmetry where a higher degree of mapping to either the transcriptome or to the genome was observed, most noticeably in the gene-rich autosomal telomeres and in several regions of the X chromosome (Figure 1). Greater mapping frequency to the transcriptome can generally be explained as reads that map to exon-exon junctions, which by their nature would not map to the genome. For example, the observed asymmetry in the 2R telomeric region is due to the high number of exon junction reads that mapped to two rhodopsin-family genes (Figure 1). Of the reads that mapped only to the genome, many of them are likely to represent unannotated 5'or 3' untranslated regions (UTRs). Moreover, there likely remain regions of the genome, most

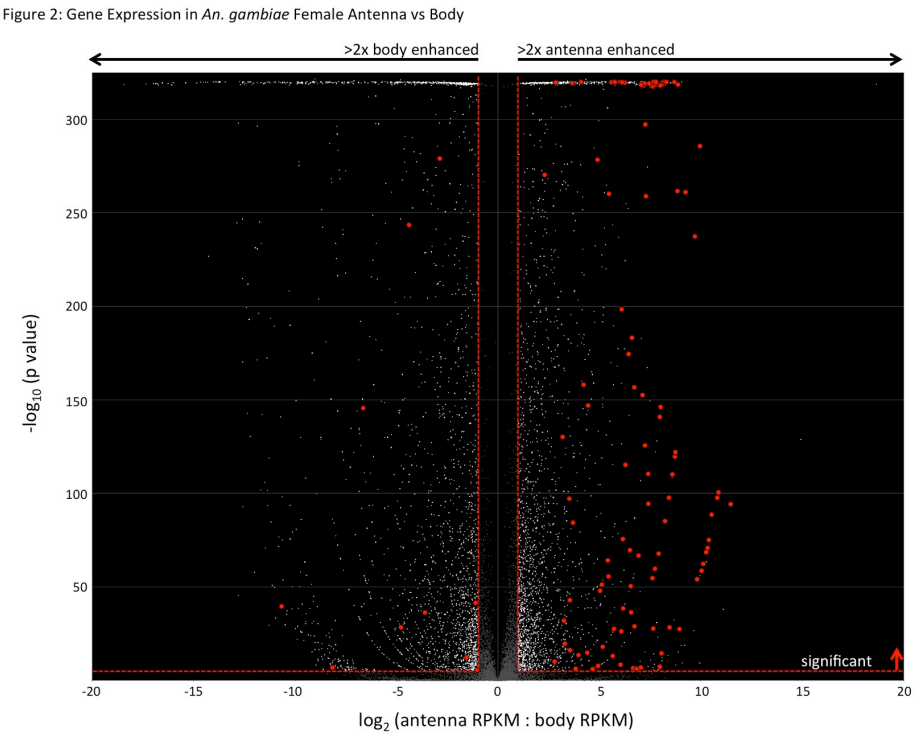

Figure 2. Gene Expression in *An. gambiae* Female Antenna vs Body
Volcano plot showing the relative abundance levels of genes in female whole body versus female antennae. The x-axis represents the $\log_2$ of the expression ratio (antenna RPKM: body RPKM) for each gene of the *An. gambiae* transcriptome. The y-axis represents the negative $\log_{10}$ of the p-value of Fisher's Exact test. White points (n=2201) represent genes that were both statistically significant (red horizontal line; p< 3.91e-06) and biologically significant (red vertical lines; greater than 2-fold difference in RPKMs). Gray points (n=10603) represent genes that either fell outside one or both of these significance criteria. Red points indicate the expression values of major chemosensory genes: *AgOrs*, *AgIrs*, *AgGrs*, and *AgObps*. RPKM values of 0.00 were transformed to 0.10 prior to calculating antenna:body ratios, such that those genes could also be represented on the plot.

notably the Y-chromosome, where novel exons and transcripts remain (Li et al., 2010).

To quantify relative differences in gene abundance levels, we calculated the **R**eads **P**er **K**ilobase per **M**illion (RPKM) reads value for each gene within a sample, a self-normalized value of absolute gene transcript abundance (Mortazavi et al., 2008). Mean and median RPKM values for each tissue type in this study were very similar across samples, as were the number of genes showing basal or greater levels of transcription (Table 1). RPKM values spanned more than 6 orders of magnitude for each of the tissue types examined (Table S1).

We assessed fold-differences in transcript abundance by independently comparing ratios of RPKM values between pairs of tissues within each sex: antennae to bodies and maxillary palps to bodies. For each of these pairwise comparisons we performed a Fisher's Exact Test on counts of mapped reads to determine statistical significance using a Bonferroni-corrected p-value ($p < 3.9x10^{-6}$; see Materials and Methods). Furthermore, we use the term "enhanced" to describe any gene that displayed at least 2-fold significant difference in abundance between samples (Figure 2). These conservative criteria were applied to avoid false positives stemming from variations within the sample

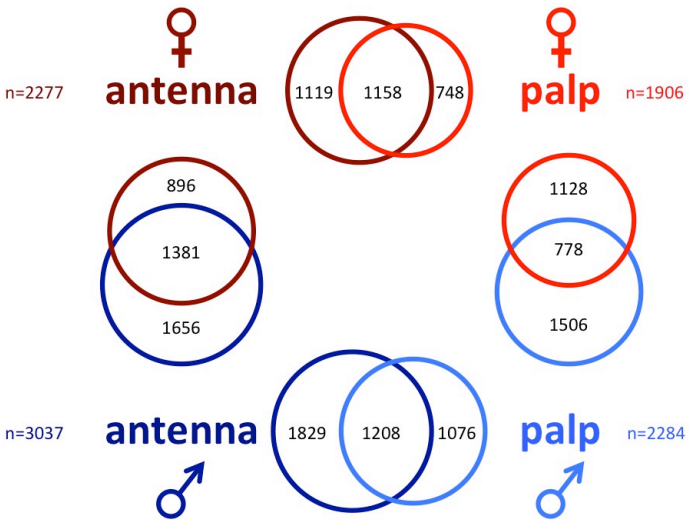

Figure 3: *An. gambiae* Enhanced Gene Pairwise Tissue Comparisons
Proportional Venn diagrams showing the various pairwise comparisons made in this study. Overlap represents the subset of genes that are significantly enhanced in both tissues.

themselves, as well as to reduce the number of genes that was used for subsequent analyses (Balweirz et al., 2009; Robinson et al., 2010).

Gene Expression Profiling in Chemosensory Tissues

To examine global gene expression patterns, we compared RPKM values pairwise for whole bodies versus either antennae or maxillary palps in both sexes; one such comparison is shown in Figure 2. Specifically, 4,587 genes displayed directional enhancement in the female antenna to body comparison (Figure 2, white dots). Of those, 2,277 were enhanced in the antenna (Figure 2, right half). Similarly, we found that 1,906 genes were enhanced in female palps, 3,037 genes were enhanced in male antennae, and 2,284 genes were enhanced in male palps. These 4 gene sets formed the basis of our subsequent analyses where we compared enhanced gene profiles between chemosensory tissues and across sexes (Figure 3).

Comparing the enhanced gene sets between the female antennae and palps revealed significant overlap, with 1,158 genes (61% of palp set) enhanced in both tissues (Figure 4). Similarly, male antennae and palps showed significant overlap with 1,208 genes enhanced in both tissues (53% of palp set; Figure 5). Interestingly, the most well-represented gene families in both of these overlapping sets were 7-transmembrance

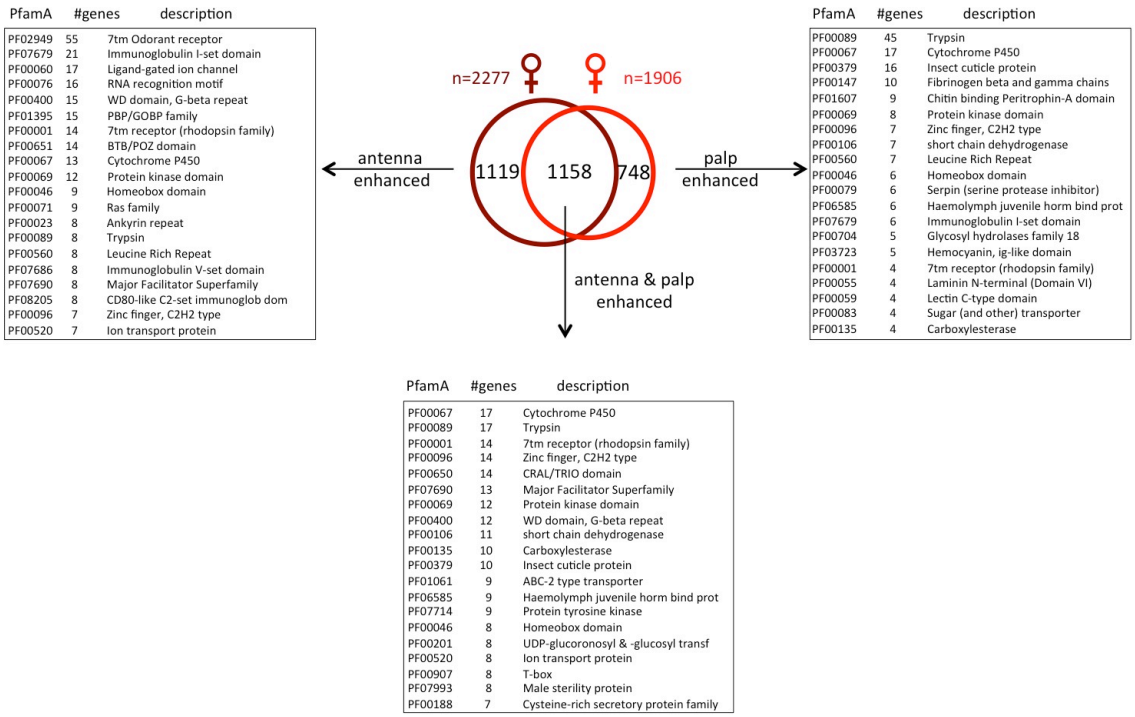

PfamA	#genes	description
PF02949	55	7tm Odorant receptor
PF07679	21	Immunoglobulin I-set domain
PF00060	17	Ligand-gated ion channel
PF00076	16	RNA recognition motif
PF00400	15	WD domain, G-beta repeat
PF01395	15	PBP/GOBP family
PF00001	14	7tm receptor (rhodopsin family)
PF00651	14	BTB/POZ domain
PF00067	13	Cytochrome P450
PF00069	12	Protein kinase domain
PF00046	9	Homeobox domain
PF00071	9	Ras family
PF00023	8	Ankyrin repeat
PF00089	8	Trypsin
PF00560	8	Leucine Rich Repeat
PF07686	8	Immunoglobulin V-set domain
PF07690	8	Major Facilitator Superfamily
PF08205	8	CD80-like C2-set immunoglob dom
PF00096	7	Zinc finger, C2H2 type
PF00520	7	Ion transport protein

PfamA	#genes	description
PF00089	45	Trypsin
PF00067	17	Cytochrome P450
PF00379	16	Insect cuticle protein
PF00147	10	Fibrinogen beta and gamma chains
PF01607	9	Chitin binding Peritrophin-A domain
PF00069	8	Protein kinase domain
PF00096	7	Zinc finger, C2H2 type
PF00106	7	short chain dehydrogenase
PF00560	7	Leucine Rich Repeat
PF00046	6	Homeobox domain
PF00079	6	Serpin (serine protease inhibitor)
PF06585	6	Haemolymph juvenile horm bind prot
PF07679	6	Immunoglobulin I-set domain
PF00704	5	Glycosyl hydrolases family 18
PF03723	5	Hemocyanin, ig-like domain
PF00001	4	7tm receptor (rhodopsin family)
PF00055	4	Laminin N-terminal (Domain VI)
PF00059	4	Lectin C-type domain
PF00083	4	Sugar (and other) transporter
PF00135	4	Carboxylesterase

PfamA	#genes	description
PF00067	17	Cytochrome P450
PF00089	17	Trypsin
PF00001	14	7tm receptor (rhodopsin family)
PF00096	14	Zinc finger, C2H2 type
PF00650	14	CRAL/TRIO domain
PF07690	13	Major Facilitator Superfamily
PF00069	12	Protein kinase domain
PF00400	12	WD domain, G-beta repeat
PF00106	11	short chain dehydrogenase
PF00135	10	Carboxylesterase
PF00379	10	Insect cuticle protein
PF01061	9	ABC-2 type transporter
PF06585	9	Haemolymph juvenile horm bind prot
PF07714	9	Protein tyrosine kinase
PF00046	8	Homeobox domain
PF00201	8	UDP-glucoronosyl & -glucosyl transf
PF00520	8	Ion transport protein
PF00907	8	T-box
PF07993	8	Male sterility protein
PF00188	7	Cysteine-rich secretory protein family

Figure 4. Female Antenna vs. Palp Enhanced Gene Sets
Proportional Venn diagram showing the numbers of genes that are significantly enhanced in female antenna and maxillary palps. Overlap represents the subset of genes that are significantly enhanced in both sexes. Boxes contain ranked lists of the most prevalent PfamA families in each data set.

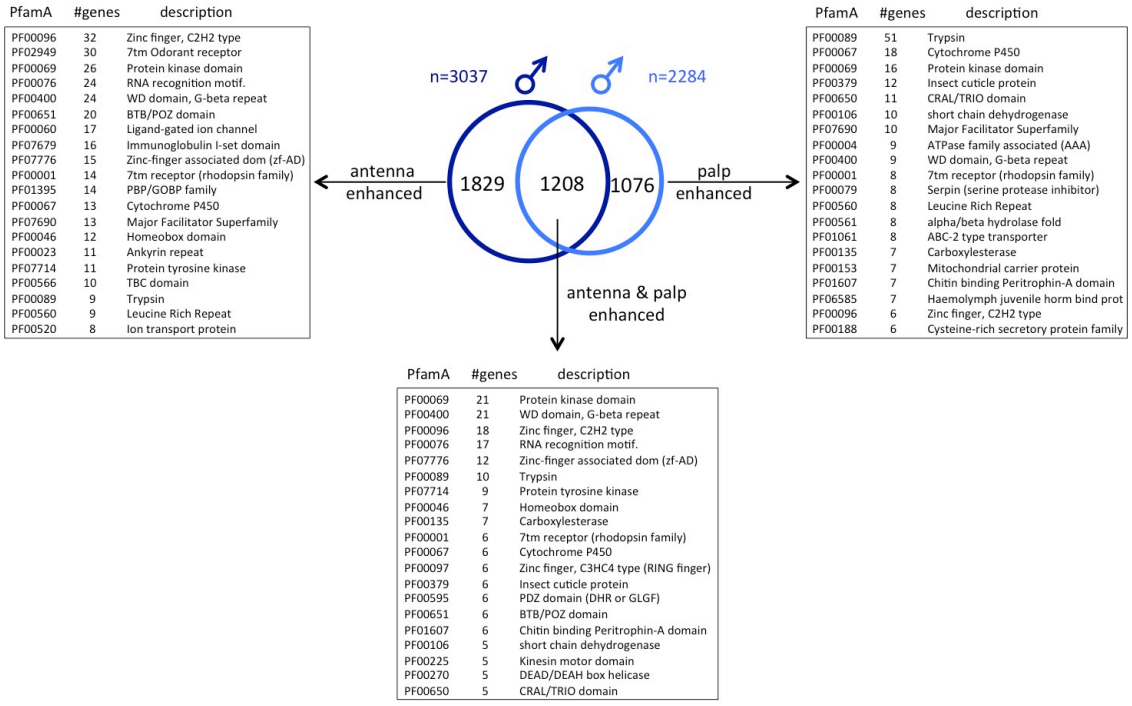

PfamA	#genes	description
PF00096	32	Zinc finger, C2H2 type
PF02949	30	7tm Odorant receptor
PF00069	26	Protein kinase domain
PF00076	24	RNA recognition motif.
PF00400	24	WD domain, G-beta repeat
PF00651	20	BTB/POZ domain
PF00060	17	Ligand-gated ion channel
PF07679	16	Immunoglobulin I-set domain
PF07776	15	Zinc-finger associated dom (zf-AD)
PF00001	14	7tm receptor (rhodopsin family)
PF01395	14	PBP/GOBP family
PF00067	13	Cytochrome P450
PF07690	13	Major Facilitator Superfamily
PF00046	12	Homeobox domain
PF00023	11	Ankyrin repeat
PF07714	11	Protein tyrosine kinase
PF00566	10	TBC domain
PF00089	9	Trypsin
PF00560	9	Leucine Rich Repeat
PF00520	8	Ion transport protein

PfamA	#genes	description
PF00089	51	Trypsin
PF00067	18	Cytochrome P450
PF00069	16	Protein kinase domain
PF00379	12	Insect cuticle protein
PF00650	11	CRAL/TRIO domain
PF00106	10	short chain dehydrogenase
PF07690	10	Major Facilitator Superfamily
PF00004	9	ATPase family associated (AAA)
PF00400	9	WD domain, G-beta repeat
PF00001	8	7tm receptor (rhodopsin family)
PF00079	8	Serpin (serine protease inhibitor)
PF00560	8	Leucine Rich Repeat
PF00561	8	alpha/beta hydrolase fold
PF01061	8	ABC-2 type transporter
PF00135	7	Carboxylesterase
PF00153	7	Mitochondrial carrier protein
PF01607	7	Chitin binding Peritrophin-A domain
PF06585	7	Haemolymph juvenile horm bind prot
PF00096	6	Zinc finger, C2H2 type
PF00188	6	Cysteine-rich secretory protein family

PfamA	#genes	description
PF00069	21	Protein kinase domain
PF00400	21	WD domain, G-beta repeat
PF00096	18	Zinc finger, C2H2 type
PF00076	17	RNA recognition motif.
PF07776	12	Zinc-finger associated dom (zf-AD)
PF00089	10	Trypsin
PF07714	9	Protein tyrosine kinase
PF00046	7	Homeobox domain
PF00135	7	Carboxylesterase
PF00001	6	7tm receptor (rhodopsin family)
PF00067	6	Cytochrome P450
PF00097	6	Zinc finger, C3HC4 type (RING finger)
PF00379	6	Insect cuticle protein
PF00595	6	PDZ domain (DHR or GLGF)
PF00651	6	BTB/POZ domain
PF01607	6	Chitin binding Peritrophin-A domain
PF00106	5	short chain dehydrogenase
PF00225	5	Kinesin motor domain
PF00270	5	DEAD/DEAH box helicase
PF00650	5	CRAL/TRIO domain

Figure 5: Male Antenna vs. Palp Enhanced Gene Sets. Proportional Venn diagram showing the numbers of genes that are significantly enhanced in male antenna and maxillary palps. Overlap represents the subset of genes that are significantly enhanced in both sexes. Boxes contain ranked lists of the most prevalent PfamA families in each data set.

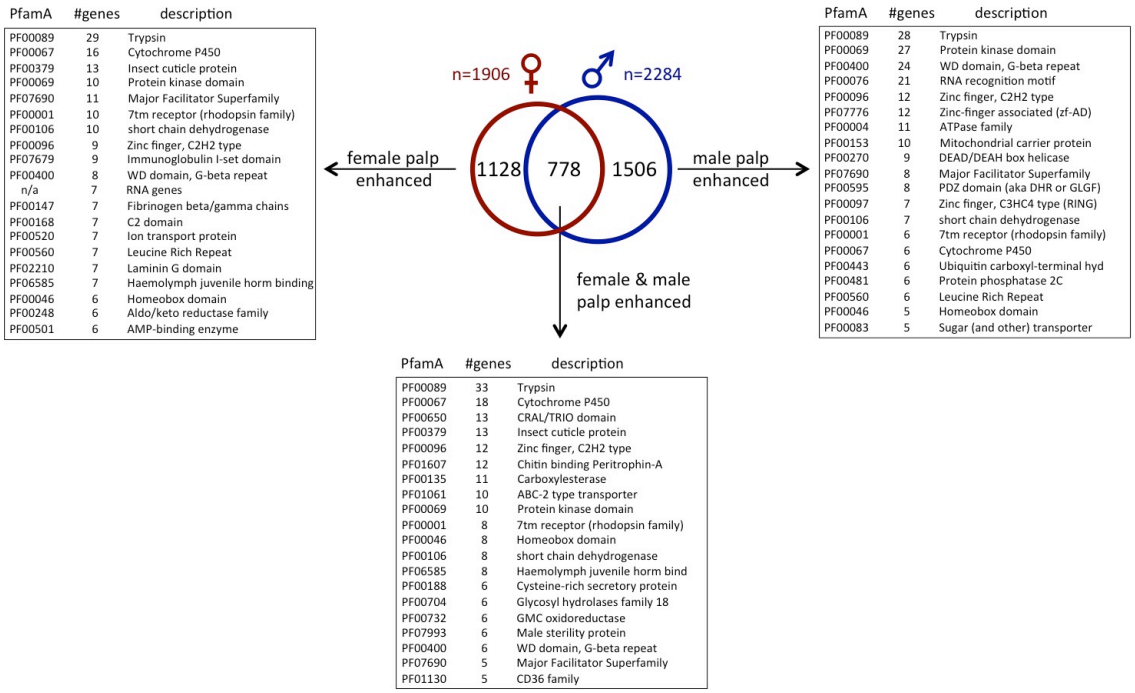

PfamA	#genes	description
PF00089	29	Trypsin
PF00067	16	Cytochrome P450
PF00379	13	Insect cuticle protein
PF00069	10	Protein kinase domain
PF07690	11	Major Facilitator Superfamily
PF00001	10	7tm receptor (rhodopsin family)
PF00106	10	short chain dehydrogenase
PF00096	9	Zinc finger, C2H2 type
PF07679	9	Immunoglobulin I-set domain
PF00400	8	WD domain, G-beta repeat
n/a	7	RNA genes
PF00147	7	Fibrinogen beta/gamma chains
PF00168	7	C2 domain
PF00520	7	Ion transport protein
PF00560	7	Leucine Rich Repeat
PF02210	7	Laminin G domain
PF06585	7	Haemolymph juvenile horm binding
PF00046	6	Homeobox domain
PF00248	6	Aldo/keto reductase family
PF00501	6	AMP-binding enzyme

PfamA	#genes	description
PF00089	28	Trypsin
PF00069	27	Protein kinase domain
PF00400	24	WD domain, G-beta repeat
PF00076	21	RNA recognition motif
PF00096	12	Zinc finger, C2H2 type
PF07776	12	Zinc-finger associated (zf-AD)
PF00004	11	ATPase family
PF00153	10	Mitochondrial carrier protein
PF00270	9	DEAD/DEAH box helicase
PF07690	8	Major Facilitator Superfamily
PF00595	8	PDZ domain (aka DHR or GLGF)
PF00097	7	Zinc finger, C3HC4 type (RING)
PF00106	7	short chain dehydrogenase
PF00001	6	7tm receptor (rhodopsin family)
PF00067	6	Cytochrome P450
PF00443	6	Ubiquitin carboxyl-terminal hyd
PF00481	6	Protein phosphatase 2C
PF00560	6	Leucine Rich Repeat
PF00046	5	Homeobox domain
PF00083	5	Sugar (and other) transporter

PfamA	#genes	description
PF00089	33	Trypsin
PF00067	18	Cytochrome P450
PF00650	13	CRAL/TRIO domain
PF00379	13	Insect cuticle protein
PF00096	12	Zinc finger, C2H2 type
PF01607	12	Chitin binding Peritrophin-A
PF00135	11	Carboxylesterase
PF01061	10	ABC-2 type transporter
PF00069	10	Protein kinase domain
PF00001	8	7tm receptor (rhodopsin family)
PF00046	8	Homeobox domain
PF00106	8	short chain dehydrogenase
PF06585	8	Haemolymph juvenile horm bind
PF00188	6	Cysteine-rich secretory protein
PF00704	6	Glycosyl hydrolases family 18
PF00732	6	GMC oxidoreductase
PF07993	6	Male sterility protein
PF00400	6	WD domain, G-beta repeat
PF07690	5	Major Facilitator Superfamily
PF01130	5	CD36 family

Figure 6. Female vs. Male Antenna Enhanced Gene Sets
Proportional Venn diagram showing the numbers of genes that are significantly enhanced in female and male antenna. Overlap represents the subset of genes that are significantly enhanced in both sexes. Boxes contain ranked lists of the most prevalent PfamA families in each data set.

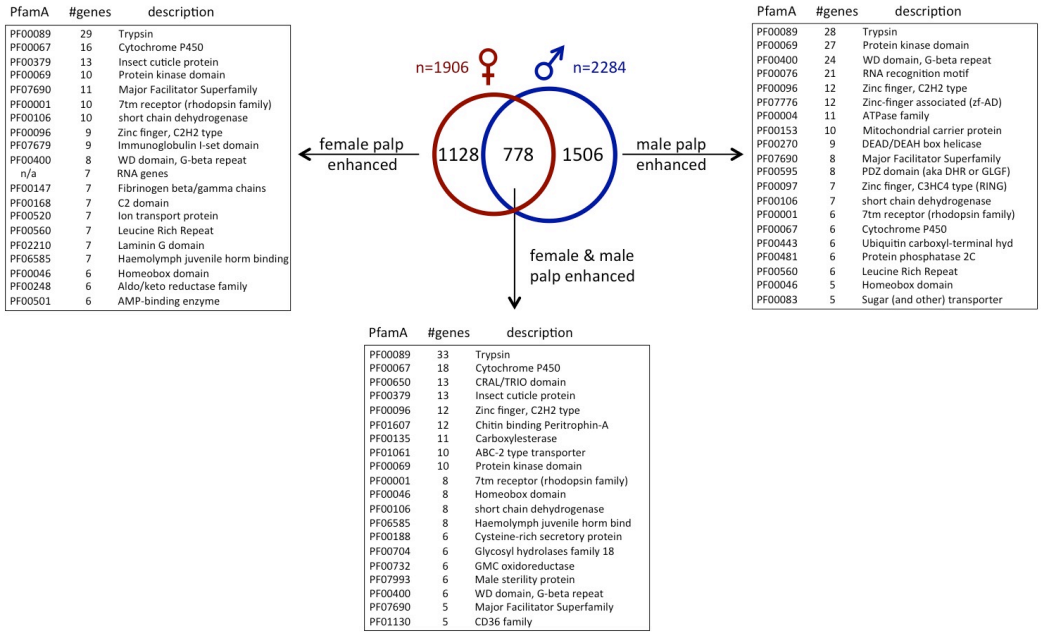

PfamA	#genes	description
PF00089	29	Trypsin
PF00067	16	Cytochrome P450
PF00379	13	Insect cuticle protein
PF00069	10	Protein kinase domain
PF07690	11	Major Facilitator Superfamily
PF00001	10	7tm receptor (rhodopsin family)
PF00106	10	short chain dehydrogenase
PF00096	9	Zinc finger, C2H2 type
PF07679	9	Immunoglobulin I-set domain
PF00400	8	WD domain, G-beta repeat
n/a	7	RNA genes
PF00147	7	Fibrinogen beta/gamma chains
PF00168	7	C2 domain
PF00520	7	Ion transport protein
PF00560	7	Leucine Rich Repeat
PF02210	7	Laminin G domain
PF06585	7	Haemolymph juvenile horm binding
PF00046	6	Homeobox domain
PF00248	6	Aldo/keto reductase family
PF00501	6	AMP-binding enzyme

PfamA	#genes	description
PF00089	28	Trypsin
PF00069	27	Protein kinase domain
PF00400	24	WD domain, G-beta repeat
PF00076	21	RNA recognition motif
PF00096	12	Zinc finger, C2H2 type
PF07776	12	Zinc-finger associated (zf-AD)
PF00004	11	ATPase family
PF00153	10	Mitochondrial carrier protein
PF00270	9	DEAD/DEAH box helicase
PF07690	8	Major Facilitator Superfamily
PF00595	8	PDZ domain (aka DHR or GLGF)
PF00097	7	Zinc finger, C3HC4 type (RING)
PF00106	7	short chain dehydrogenase
PF00001	6	7tm receptor (rhodopsin family)
PF00067	6	Cytochrome P450
PF00443	6	Ubiquitin carboxyl-terminal hyd
PF00481	6	Protein phosphatase 2C
PF00560	6	Leucine Rich Repeat
PF00046	5	Homeobox domain
PF00083	5	Sugar (and other) transporter

PfamA	#genes	description
PF00089	33	Trypsin
PF00067	18	Cytochrome P450
PF00650	13	CRAL/TRIO domain
PF00379	13	Insect cuticle protein
PF00096	12	Zinc finger, C2H2 type
PF01607	12	Chitin binding Peritrophin-A
PF00135	11	Carboxylesterase
PF01061	10	ABC-2 type transporter
PF00069	10	Protein kinase domain
PF00001	8	7tm receptor (rhodopsin family)
PF00046	8	Homeobox domain
PF00106	8	short chain dehydrogenase
PF06585	8	Haemolymph juvenile horm bind
PF00188	6	Cysteine-rich secretory protein
PF00704	6	Glycosyl hydrolases family 18
PF00732	6	GMC oxidoreductase
PF07993	6	Male sterility protein
PF00400	6	WD domain, G-beta repeat
PF07690	5	Major Facilitator Superfamily
PF01130	5	CD36 family

Figure 7. Female vs. Male Palp Enhanced Gene Sets
Proportional Venn diagram showing the numbers of genes that are significantly enhanced in female and male maxillary palps. Overlap represents the subset of genes that are significantly enhanced in both sexes. Boxes contain ranked lists of the most prevalent PfamA families in each data set.

receptors (PF00001), protein kinases (PF00069), cytochrome P450s (PF00067), trypsins (PF00089), carboxylesterases (PF00135), and potential transcription factors (PFs 00046 and 00096; Figures 4 and 5, bottom tables). However, we also observed several differentially enhanced gene sets between the antennae and palps (Figures 4 and 5). The *An. gambiae Ors* (*AgOrs;* Hill et al., 2002; PfamA family PF02949) were the most prevelant class in female antennae (Figure 4, left table) and second-most in the male antennae (Figure 5, left table). Other chemosensory gene families, such as ligand-gated ion channels, which include the recently identified ionotropic receptors (*AgIrs;* Liu et al., 2010; PF00060), and odorant binding proteins (*AgObps*; Xu et al., 2004; PF01395) were highly represented in the antennae (Figures 4 and 5) . It is clear from these antennae-to-palp analyses that both extensive overlap and significant distinctions in gene expression profiles exist. The consistent identification of the same Pfam familes in all enhanced gene sets implicates functional groups that can be studied in greater detail to elucidate their potential roles in mosquito chemosensation.

To attempt to distinguish similarities and differences in gene expression patterns between sexes, we compared the 2,277 female, and the 3,037 male antennal-enhanced genes and identified a common set of 1381 genes (Figures 3 and 6). Once again, this set included *AgOrs*, *AgIrs*, and *AgObps* (Figure 6, bottom table). Despite many commonalities in gene expression, there were also 896 female antennae-specific enhanced

genes and, surprisingly, nearly 1700 male antennae-specific enhanced genes (Figures 3 and 6).

Given the obvious sexual dimorphism of *An. gambiae* antennae (Figure 7), the comparison of female to male antennae is not straightforward. Chemosensory sensilla, and *AgOr*-containing neurons in particular, are found over the full length of the female antenna, whereas male antennae house ~3-fold fewer chemosensilla that are restricted the two most distal segments (Ismail, 1964; McIver, 1982; Sutcliff, 1993; Schymura et al., 2010). Furthermore, while female antennae are predominantly chemosensory, male antennae are also highly specialized for hearing (Pennetier et al., 2010; Gibson et al., 2010). . Accordingly, the *An. gambiae* orthologs of the *D. melanogaster* trpV channels *Nanchung* and *inactive*, which are required for hearing in the fruitfly, were enhanced in antennae of both *An. gambiae* sexes (AGAPs 012241 and 000413, respectively; Table 2), but their absolute abundances were much higher in male antennae (RPKMs of 183.92 and 104.49 in males and 20.54 and 7.66 respectively, in females). This elevated abundance of auditory-associated genes in the male antenna is consistent with male *An. gambiae* mating behavior where an acute sense of hearing facilitates the recognition of female wing beats (Charlwood and Jones, 1979; Gibson et al., 2010; Pennetier et al., 2010). Given that wild female mosquitoes are likely to mate just once, while males swarm daily in search of a mate (Goma 1963; Charlwood and Jones 1979; Howell and Knols 2009), the

specialization shift away from olfaction and toward audition in the principle male sensory organ is reasonsable presumably as a mechanism to increase male mating success.

In the maxillary palps, as in the antennae, considerable overlap was found in gene expression profile between the sexes. In the palp, 778 genes were common between the 1,906 female palp-enhanced gene set and the 2,284 male palp-enhanced gene set (Figure 3 and Figure 8). Interestingly, the fraction of enhanced gene overlap was much lower in the palps than in the antennae (Figures 6 and 8); only 41% of the total female palp-enhanced set was shared with males, compared to 61% of the total female antennal-enhanced set that was shared with males. In light of the antennal sexual dimorphism the even greater divergence in overlapping gene sets between female and male palp may indicate the presence of cryptic sex-specific specializations.

These comparisons also revealed multiple classes of genes outside the expected chemosensory gene families that displayed enhanced tissue abundance. A detailed examination of the abundance patterns of a subset of other gene families is provided in Table 2, many of which are represented in Figures 3 and 4. Nearly half of the members of the large superfamily of 7-transmembrane (7tm) receptors (114 of the 241 recognized by PfamA), exclusive of the *AgOrs*, were enhanced in at least one of the chemosensory tissues examined (Table 2). This may indicate unrecognized roles in sensory reception or regulation of chemoreceptor

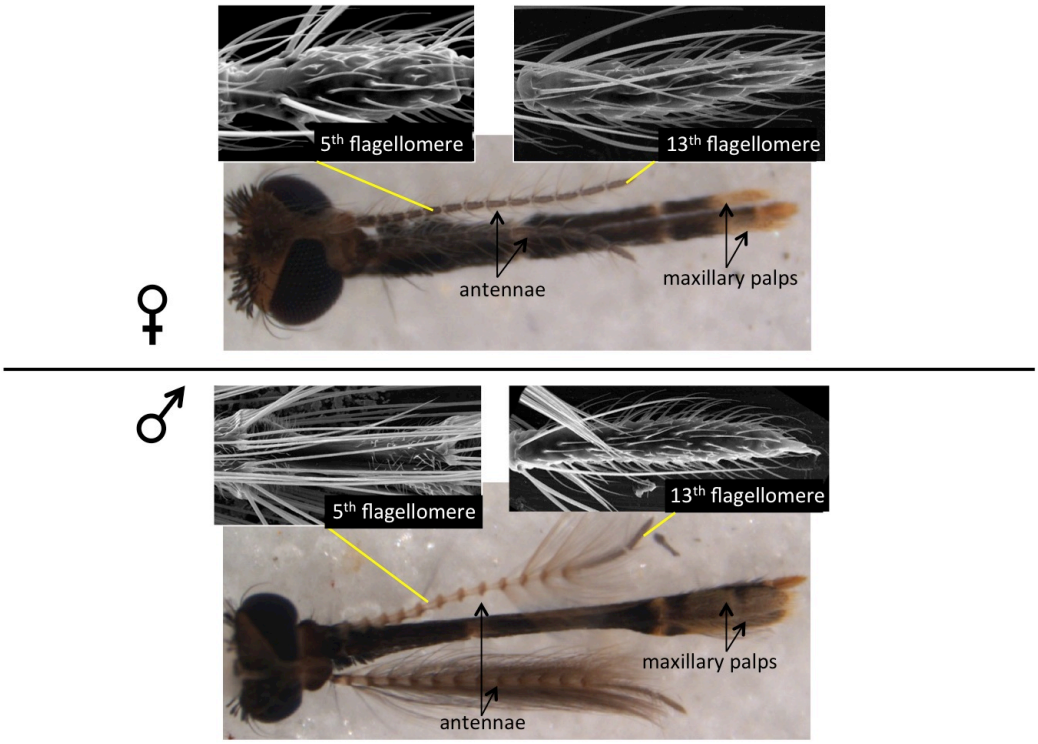

Figure 8. Sexual Dimorphism in *An. gambiae* Chemosensory Tissues
Brightfield images of *An. gambiae* female and male heads. Antennae and maxillary palps are indicated. Scanning electron micrographs show details of the fifth and thirteenth flagellomeres (segments) of female and male antennae, respectively.

neuron or accessory cell function. Importantly, efferent projections from serotonergic, or tachykinin neuroendocrine cells have been identified in mosquito chemosensory appendages (Meola et al., 2000, 2002; Siju et al., 2008;). Thus the expression of serotonin (AGAPs 002232, 002679, 004222, 004223, 007136, and 011481), and tachykinin (AGAPs 001592 and 012824) receptor homologs in *An. gambiae* antennae and maxillary palps (Table S1) is consistent with a neuromodulatory role for these compounds.

Other gene families with multiple members that displayed chemosensory enhancement include the CD36 family, some members of which function in insect olfaction (Rogers et al., 1999; Benton et al., 2009); ion channels and transporters, which include the recently identified chemosensory ionotropic receptors (Liu et al., 2010; Croset et al., 2010; Abuin et al., 2011). In addition biotransformation enzymes, such as carboxyesterases and cytochrome P450s that are potential odor degrading/biotransformation enzymes (Maibeche-Coisne et al., 2002; Durand et al., 2010a, 2010b;); carbonic anhydrases involved in carbon dioxide detection in mammals (Chandrashekar et al., 2009) and transcription factors, including the *An. gambiae* homologs of *acj6* and *pdm3*, *D. melanogaster* pou-type transcription factors involved in *DmOr* gene regulation and ORN axon targeting (Ayer and Carlson, 1991,1992; Clyne et al., 1999; Lee and Salvaterra, 2002; Tichy et al., 2008; Bai et al., 2009; Bai and Carlson, 2010) were observed.

We also identified a number of small, soluble proteins with enhanced chemosensory tissue abundance in both sexes (Table 3), such as the CRAL-TRIO (PF00650) and cysteine-rich secretory (PF00188), and hemolymph juvenile hormone binding proteins (JHBP, PF06585). To our knowledge, the first two gene families have not been linked to chemosensation, but the members of the JHBP family have been identified in screens of high abundance genes in mosquito antennae (Justice et al., 2003; Bohbot and Vogt, 2005). Moreover the JHBP gene, *takeout*, links the circadian clock and feeding behavior in *D. melanogaster* (Sarvo-Blot et al., 2000) and modulates aggregation behavior in *Locusta migratoria* (Guo et al., 2011). The extremely high abundance levels of some members of these 3 gene families suggest potential chemosensory functions analogous to other soluble lipophilic carriers such as the *Obps.*

Chemosensory Gene Families

In light of the existing literature on the molecular mechanisms underlying the processes of peripheral chemosensation in vector mosquitoes, we examined in detail the abundance patterns *AgOrs*, *AgIrs*, *AgObps* and gustatory receptors (*AgGrs*). As expected, the vast majority of *AgOrs* were highly enhanced in antennae. Of the 76 *AgOrs, 58* showed significantly higher expression in female antennae as compared to only 36 in male antennae (Figure 8). The entire set of male-enhanced *AgOr*s was contained within the female enhanced set. None of the larval-specific

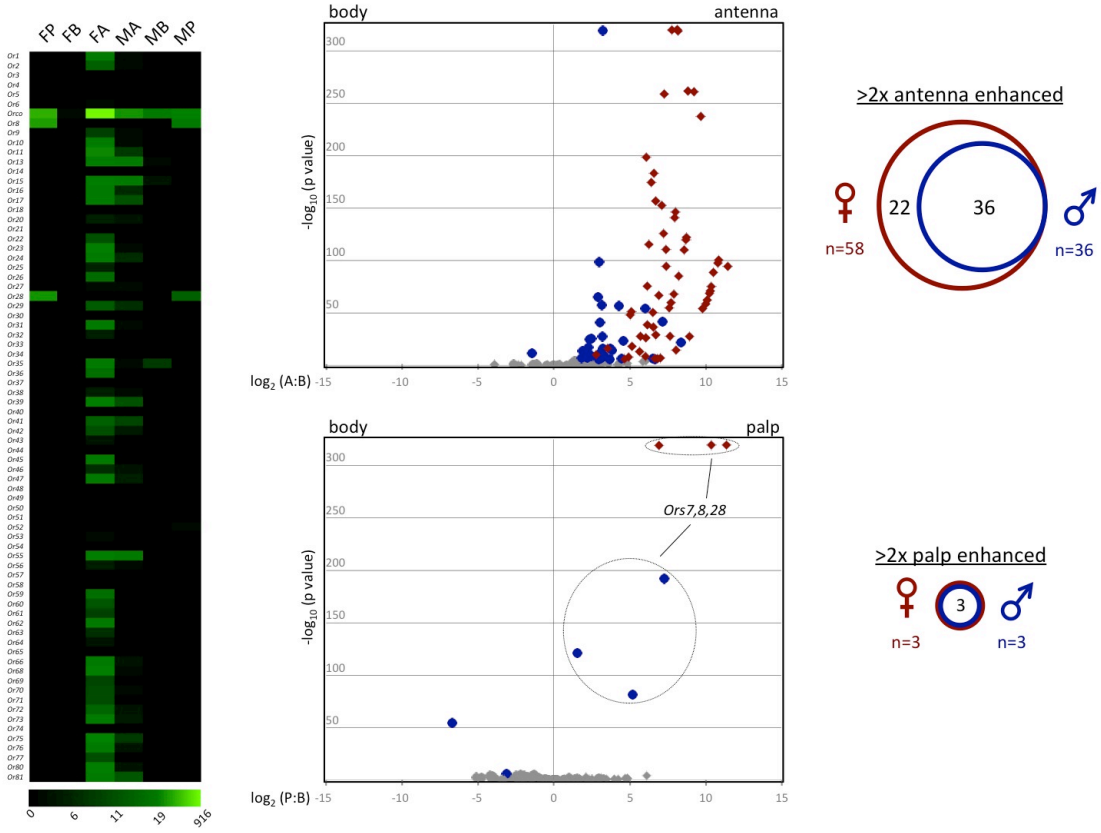

Figure 9. *AgOr* Expression Profile

Left panel is an expression profile map. Green color intensity scale (below map) indicates increasing RPKM values from left to right. (FP – female palp; FB – female body; FA – female antenna; MA – male antenna; MB – male body; MP – male palp). **Middle panels** – volcano plots showing the relative abundance of *AgOrs* in body versus antennae. Individual data points were plotted at the intersection of the $\log_{10}$ of Fisher's exact test (y-axis) and the $\log_2$ of the ratio of antenna (or palp) RPKM: body RPKM (x-axis) for each gene. Red diamonds or blue circles represent significantly enhanced *AgOrs* in antenna (top panel) or maxillary palps (bottom panel) of females and males, respectively. Gray points represent *AgOrs* that fell below the significance threshold of 3.91e-06 or the 2-fold differential expression cutoff. RPKM values of 0.00 were transformed to 0.10 prior to calculating RPKM ratios, such that those genes could also be represented on the plot. **Right panels** – Proportional Venn diagrams showing the number of *AgOrs* that are significantly enhanced in female and male antenna (top) and maxillary palp (bottom).

AgOrs: 37, 40, 52, or *58,* was enhanced in adult antennae or palps, supporting previous observations (Xia et al., 2008). In the palps, only *AgOrs8* and *28* and *AgOrco* (recently renamed from *AgOr7* to reflect its capacity as an obligate **co**-receptor in *Or* signaling) were enhanced in female maxillary palps (Figure 9), a result consistent with our previous study on odor coding in the *An. gambiae* maxillary palps (Lu et al., 2007). The same 3 *AgOrs* were enhanced in male palps (Figure 9). Several members of the recently described *AgIr* gene family (Croset et al., 2010; Liu et al., 2010) displayed significant enhancement in antennae of both sexes (Figure 10), further supporting their potential roles as chemosensory receptors in *An. gambiae*. A high degree of overlap was observed between the sexes, where 21 *AgIrs* were enhanced in both. Similar to the *AgOrs*, there were many fewer *AgIrs* enhanced in the palps compared to the antennae, with 7 and 6 enhanced in female and male palps, respectively. Furthermore, the degree of overlap (3 genes) between the sexes was much less pronounced in the palp (Figure 10).

The *AgGrs* were the only class that did not overlap in the antennae between the sexes, with very few showing enhancement in either females or males (Figure 11). Only *AgGr1* was enhanced in female antennae, while *AgGrs, 33, 48, 49,* and *50* were enhanced in male antennae. Notably, one member of this large gene family, *AgGr33* was strongly enhanced in the male antenna (Figure 11), perhaps indicating a specialized function in male antennae. In contrast to the acute sexual

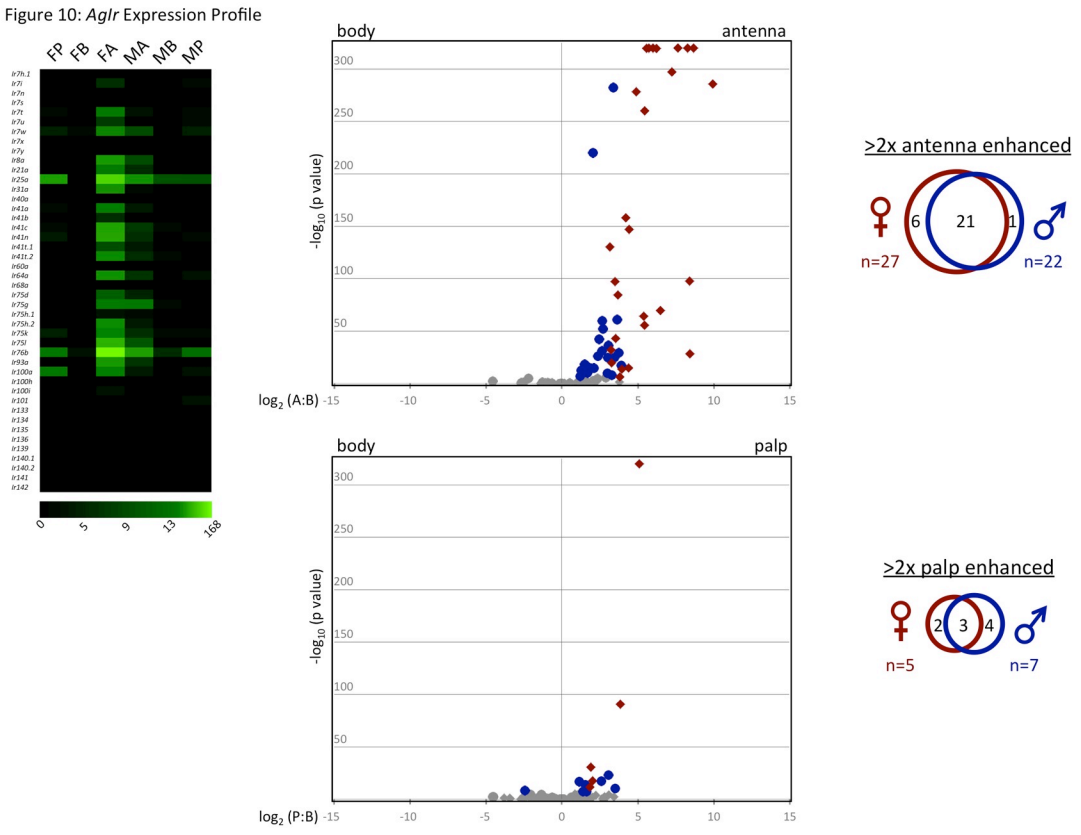

Figure 10. *Aglr* Expression Profile

Left panel is an expression profile map. Green color intensity scale (below map) indicates increasing RPKM values from left to right. Column labels same as Figure 9. **Middle panels** – volcano plots showing the relative abundance of *Aglrs* in body versus antennae. Individual data points were plotted at the intersection of the $\log_{10}$ of Fisher's Exact test (y-axis) with the $\log_2$ of the ratio of antenna (or palp) RPKM: body RPKM (x-axis) for each gene. Red diamonds or blue circles represent significantly enhanced *Aglrs* in antenna (top panel) or maxillary palps (bottom panel) of females and males, respectively. Gray points represent *Aglrs* that fell below the significance threshold of 3.91e-06 or the 2-fold differential expression cutoff. RPKM values of 0.00 were transformed to 0.10 prior to calculating abundance ratios, such that those genes could also be represented on the plot. **Right panels** – Proportional Venn diagrams showing the number of *Aglrs* that are significantly enhanced in female and male antenna (top) or palp (bottom).

dimorphism displayed in the antennae, both sexes showed high abundance of *AgGrs 22*, *23*, and *24*, in their maxillary palps (Figure 10).

These three *AgGrs* are homologs of the *D. melanogaster* carbon dioxide receptors (Kwon et al., 2007; Cayirlioglu et al., 2008; Robertson and Kent 2009) and are expressed in capitate peg sensilla on the maxillary palps where they have been directly implicated in *An. gambiae* CO_2 sensing (Lu et al., 2007).

Enhanced chemosensory abundance of members of the large *AgObp* family was evident across all tissues and sexes (Table S1). Sixteen classical and three C-plus *AgObp*s were significantly enhanced in the female antennae (Figure 12). Of these, 17 (Table S1) were also significantly enhanced in the male antennae (Figure 12) including the LUSH homolog, *AgObp4* (Kim et al., 1998). *AgObp19* was the only one to demonstrate significantly enhanced abundance in the female antennae and in no other tissue. In the maxillary palp, enhancement of *AgObp* transcripts also displayed substantial overlap between sexes, where the 4 male enhanced *AgObps* were all enhanced in females. Overall, *AgObp* abundance was nearly identical between male and female chemosensory tissues (Figure 12).

In contrast, atypical *AgObp*s were not enhanced in any of the tissues examined, which is consistent with previous results suggesting that expression of this subfamily is limited to pre-adult stages (Xu et al.,

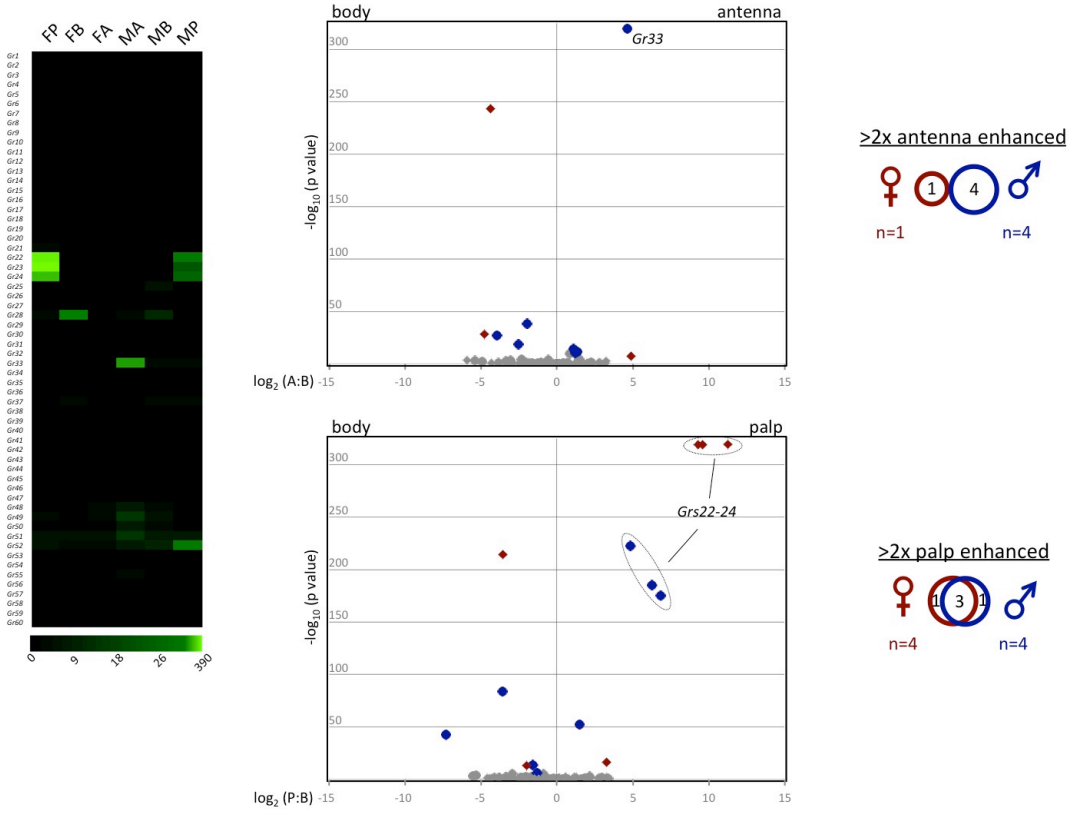

Figure 11. *AgGr* Expression Profile

Left panel is an expression profile map. Green color intensity scale (below map) indicates increasing RPKM values from left to right. Column labels same as Figure 9. **Middle panels** – volcano plots showing the relative abundance of *AgGrs* in body versus antennae. Individual data points were plotted at the intersection of the $\log_{10}$ of Fisher's exact test (y-axis) with the $\log_2$ of the ratio of antenna (or palp) RPKM: body RPKM (x-axis) for each gene. Red diamonds or blue circles represent significantly enhanced *AgGrs* in antenna (top panel) or maxillary palp (bottom panel) of females and males, respectively. Gray points represent *AgGrs* that fell below the significance threshold of 3.91e-06 or the 2-fold differential expression cutoff. RPKM values of 0.00 were transformed to 0.10 prior to calculating expression ratios, such that those genes could also be represented on the plot. **Right panels** – Venn diagrams showing the number of *AgGrs* that are significantly enhanced in female and male antenna (top) or palp (bottom).

2005). With the exception of *AgObps 47*, *48*, *57*, which had RPKMs of >1000, abundance of the members of the Plus-C *AgObp* subfamily was very low. Of these, it is noteworthy that *AgObp48* was one of the most highly expressed genes (RPKM=32311) in any tissue, with significant abundance in both the male and female olfactory tissues (Table S1). While *AgObps*, and insect *Obps* in general are among the most highly expressed gene families in chemosensory tissues their role in non-pheromone chemosensation remains largely undefined.

It has been hypothesized that *Obps* act as molecular shuttles/chaperones, which deliver to receptors and/or transiently protect specific odorants from biotransformation enzymes (Vogt, 1987; Lerner et al.,1990). If individual *Obps* bind a subset of odorants, it is reasonable to hypothesize that in tissues with high *Or* and therefore odor-coding complexity such as the antennae, the *Obp* landscape would need to be similarly complex in order to bind the required range of odorants. The converse would also be expected for tissues with reduced odor coding complexity such as the maxillary palp.

The female antenna expresses transcripts for 58 conventional *AgOrs* whose levels are significantly enhanced over the body, while the female palp expresses only 3. Furthermore, the odorant response profiles of the palp- expressed *AgOrs*8 and *28* are also vastly different from the de-orphanized antennal *AgOrs* (Lu et al., 2007; Carrey et al., 2010; Wang et al., 2010). These differences in *AgOr* coding capacity and their

expression profiles strongly suggest that the ability of the female antennae to sense odors is much greater than the maxillary palp.

In *An. gambiae* females both the antennae and maxillary palps expressed 21 *AgObp* family members with an RPKM >10, of which 19 were found in both (Table S1). While not all of these *AgObps'* abundance levels meet our significance criteria for enhancement, these genes are nevertheless expressed in these tissues. Thus although the *AgObp* complexity is almost identical, these two appendages,display a vastly different *AgOr* complexity and odor coding capacity (odor space). This analysis confounds standing theories about *Obp* function; if all antennal *Obps* are required for signaling, then their presence in the palp, with its much more limited odor space, would appear superfluous. Given this broad expression, and a demonstrated lack of functional overlap, this analysis instead suggests that in at least some instances, *Obps* act as low-pass filters for environmental odorants rather than as specific odorant-carrier agents. Therefore, *Obps* may act to solubilize odors in some cases, but as molecular sinks in others, adding yet another dimension to peripheral odor coding.

Diverse Roles for Chemosensory Tissues

To explore the effect of morphology on observed *AgOr* expression, we attempted to normalize sex-specific differences in transcript abundance by scaling up male *AgOrs* in proportion to the number of female

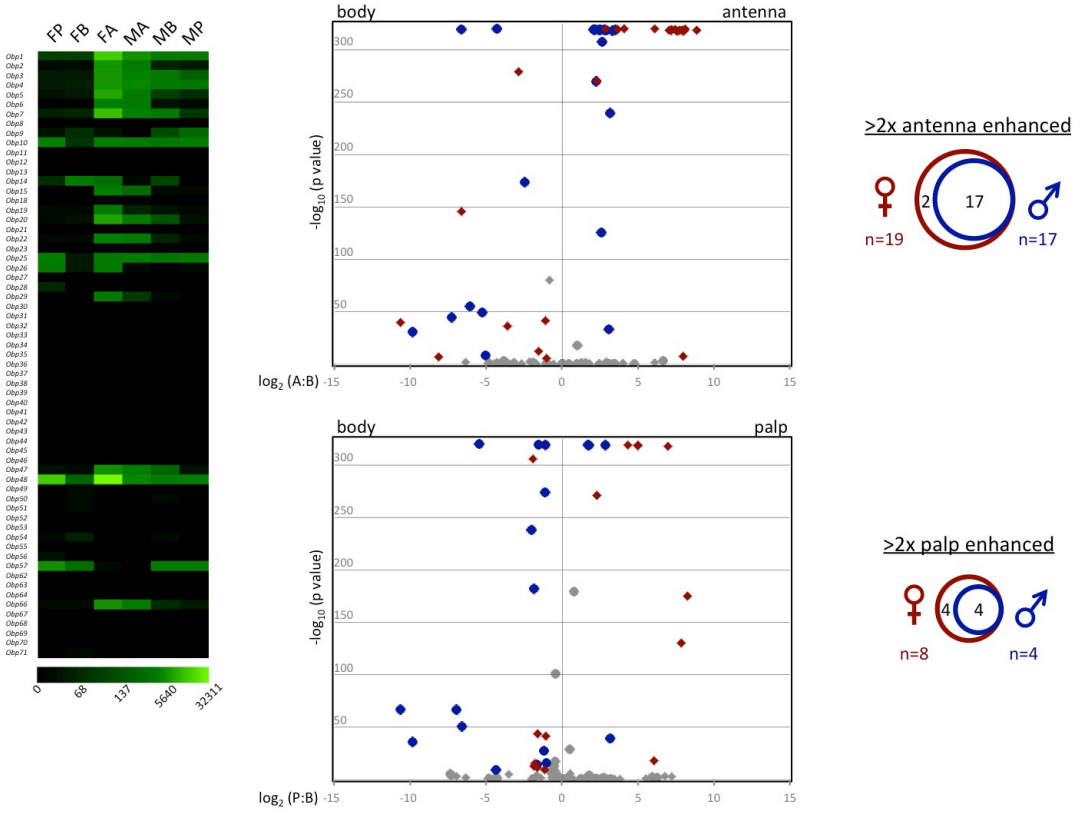

Figure 12. *AgObp* Expression Profile

Left panel is an expression profile map. Green color intensity scale (below map) indicates increasing RPKM values from left to right. Column labels same as Figure 9. **Middle panels** – volcano plots showing the relative abundance of *AgObps* in body versus antennae. Individual data points were plotted at the intersection of the $\log_{10}$ of Fisher's exact test (y-axis) with the $\log_2$ of the ratio of antenna (or palp) RPKM: body RPKM (x-axis) for each gene. Red diamonds or blue circles represent significantly enhanced *AgObps* in antenna (top panel) or maxillary palps (bottom panel) of females and males, respectively. Gray points represent *AgObps* that fell below the significance threshold of 3.91e-06 or the 2-fold differential expression cutoff. RPKM values of 0.00 were transformed to 0.10 prior to calculating expression ratios, such that those genes could also be represented on the plot. **Right panels** – Venn diagrams showing the number of *AgObps* that are significantly enhanced in female and male antenna (top) or palp (bottom).

chemosensilla. *AgOrs* are known to be expressed in the trichoid sensilla, the predominant sensillar type and not in grooved peg sensilla (Pitts et al., 2004). Sensilla counts indicate that female antennae house an average of 630 trichoid sensilla while male antennae house an average of 225 trichoid sensilla (Ismail, 1964; McIver et al., 1982; Pitts and Zwiebel 2006). We therefore multiplied the male *AgOr* RPKMs by a factor of 630/225 or 2.8. After normalizing, *AgOr* expression profiles were qualitatively very similar in females and males (Figure 13), although the male *AgOr* RPKM values remained lower than those in females. Based on the same logic, we also normalized *AgIr* expression in male antennae (Figure 13). Because we postulated that *AgIrs* are localized in neurons housed in grooved peg sensilla (GP) as they are in *D. melanogaster* (Benton et al., 2009; Liu et al., 2010), we used a GP normalization factor of 4.2, which is the fold difference in GP numbers between female and male *An. gambiae* antennae (McIver, 1982). As with *AgOrs*, the *AgIr* gene expression patterns were qualitatively similar in both sexes after normalization (Figure 13). These results suggest that male antennae express similar *AgOr* and *AgIr* chemoreceptor repertoires as the female antennae, although, importantly, at reduced absolute levels.

The *AgOr* and *AgGr* abundance profiles in the maxillary palps support a similar conclusion. Although *AgOrs 7, 8,* and *28* and *AgGrs22-24* were enhanced in both sexes, their abundance levels were lower in

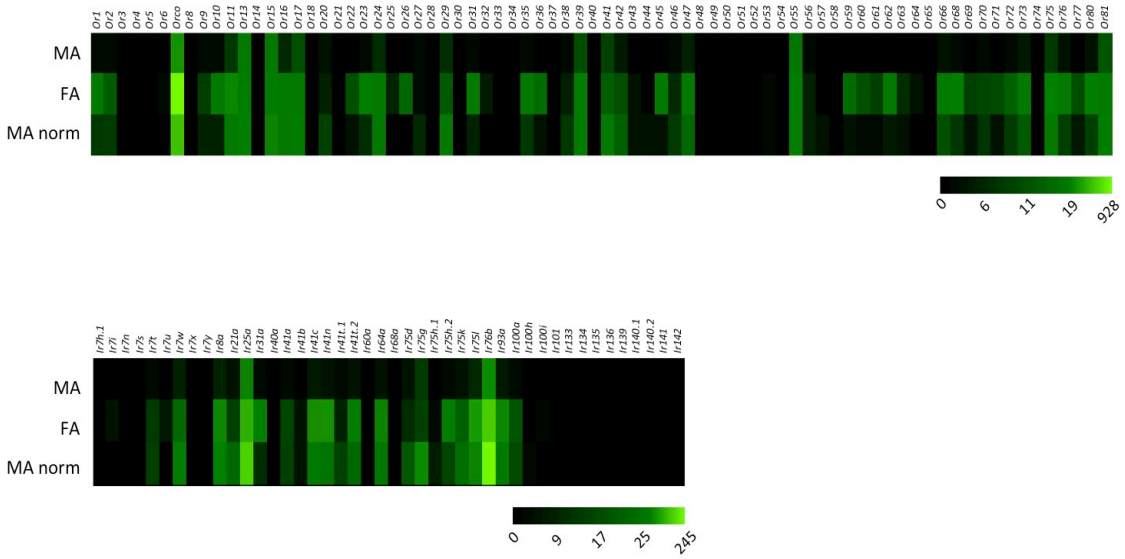

Figure 13. Sensilla-normalized *AgOr* and *AgIr* Expression Profiles
Expression profile maps using a green color scale to represent RPKM values for *AgOr* (top panel) and *AgIr* (bottom panel) families. MA – male antenna RPKMs. FA – female antennae RPKMs. MA norm – male antenna normalized RPKMs. Male antennae *AgOrs* were scaled up by a factor of 2.8. Male antennae *AgIrs* were scaled up by a factor of 4.2. Scales shown below expression maps. Color scales shown below maps indicate increasing RPKM values from right to left

males than in females (Figures 9 and 11). As is the case for *An. gambiae* antennae, the maxillary palps are sexually dimorphic and in males they house about 4-fold fewer chemosensilla (McIver 1982; Lu et al., 2007).

This could account for the apparent lower chemosensory gene transcript abundances in males. Normalizing male palp *AgOrs* and *AgGrs* by this factor brings their absolute RPKM values closer to those of females, but does not affect the qualitative observation that the identical chemoreceptors are enhanced there (data not shown). The same can be said for *AgObps* in the antennae and maxillary palps (Figures 10 and 12), where this gene family is generally more enhanced in females than in males. Assuming that the transcript abundance profiles seen here are meaningful at the functional level, both sexes would potentially be receptive to a qualitatively similar odor space, with females perhaps having a lower threshold response to odors and thus greater chemoreceptive power. In either case, the aforementioned differences in gene abundance profiles could also be functionally relevant and serve as the basis for distinguishing qualitatively and quantitatively female and male chemosensory abilities. These competing hypotheses are directly testable using a combination of electrophysiological recording and behavioral response assays. Moreover, the requirement in chemoreception for any of the differentially expressed genes could potentially be explored by gene silencing.

Conclusion

We are interested in understanding the molecular components of the chemosensory pathways that moderate the physiological and behavioral alterations that distinguish blood-feeding, female mosquitoes that carry out disease-transmission and males that do neither. Considerable effort has been devoted to catalog the semiochemicals released by potential blood-meal hosts that act as attractive signals for female mosquitoes (Takken and Knols, 1999; Zwiebel and Takken, 2004) as well understand the odorant response profiles of AgOrs (Lu et al., 2007; Carey et al., 2010; Wang et al., 2010). At the same time, there is a paucity of data that addresses whether male *An. gambiae* are sensitive to the same semiochemicals or simply do not respond to them in the same way. Inasmuch as differential gene expression between the sexes may serve as a potential mechanism for modulating peripheral sensitivity, we have carried out a comprehensive comparative analysis of the chemosensory transcriptomes of adult male and female *An. gambiae*. In addition to identifying genes that may function in sexually differential responses, this analysis has revealed many genes that are enhanced in the antennae and maxillary palps of both sexes and are therefore likely to play essential roles in maintaining neuronal and or chemosensory functionality.

RNA sequencing has provided unparalleled resolution for the examination of global gene expression profiles in chemosensory tissues and bodies of an organism of great medical importance. By their very

nature, this data are not only broad, covering nearly the entire transcriptome of the organism, but deep, allowing one to observe not only gene expression patterns, but address questions regarding gene structure, alternative splicing, and polymorphisms to name just a few possibilities. This study has begun to explore the potential of this data set and establishes an important precedent in the use of RNA-seq for the study of chemosensation in a disease vector.

Tables and Table Legends

Table 1. *An. gambiae* RNA-seq Mapping and Abundance Data

	Overall Totals		Weighted Mapped Read Counts			Gene Expression			
tissue type	**reads**	**mapped reads (%)**	**transcriptome v3.6**	**nuclear gnm.**	**mito. gnm.**	**Gene Coun**	**median**	**mean RPK**	**std.dev.**
female body *(fb)*	27877821	25358733 (90.96)	16606092 (59.57)	14680019	263602	12145	8.87	59.74	543.15
female antenna	25980364	24123025 (92.85)	14617276 (56.26)	15280026	80727	11722	9.38	59.22	732.65
female palp *(fp)*	27449612	25984839 (94.66)	15293125 (55.71)	16700334	420897	12297	10.37	56.44	496.05
male body *(mb)*	31876060	30226447 (94.82)	17603111 (55.22)	16016349	2408310	12253	8.34	54.01	424.05
male antenna	33950770	32144101 (94.68)	18231088 (53.70)	21427148	241273	11986	10.34	46.01	229.14
male palp *(mp)*	35705184	33339629 (93.37)	22596709 (63.29)	17625684	536952	12146	8.40	49.14	286.49

Table 1. Legend

Cells in each row contain information corresponding to the **tissue type** listed. **Overall Totals: Reads**: total number of short reads generated from each sample. Mapped reads: the number (and percentage) of total reads that were mapped to the transcriptome, nuclear genome, and/or the mitochondrial genome. **Weighted Mapped Read Counts: Transcriptome v3.6**: the number (and percentage) of reads mapped to version 3.6 of the *An. gambiae* transcriptome. **Nuclear gnm.**: the number the number of reads mapped to the assembled *An. gambiae* genome. **Mito. gnm**: the number reads mapped to the *An. gambiae* mitochondrial genome. **Gene Expression Summary: Gene count**: the total number of annotated genes in each tissue type having an **RPKM** (**R**eads **P**er **K**ilobase per **M**illion) greater than zero. **Mean, median** and **std. deviation** of the RPKM values for each tissue type.

Table 2. Enhanced Gene Classes in *An. gambiae* Chemosensory Tissues

				Enhanced >2x ----------			
gene class	**PfamA**	**PfamA description**	***#An.gambiae***	**FA**	**MA**	**FP**	**MP**
7tm Receptor	PF00001	7tm receptor (rhodopsin family)	84	28	20	18	14
7tm Receptor	PF02949	7tm Odorant receptor (Or)	78	56	31	3	3
7tm Receptor	PF08395	7tm Chemosensory receptor (Gr)	52	1	4	3	4
7tm Receptor	PF00002	7tm receptor (Secretin family)	11	2	1	0	2
7tm Receptor	PF00003	7tm sweet-taste receptor of 3 GCPR	7	4	5	2	1
lipophilic carrier	PF01395	PBP/GOBP family	62	18	17	6	4
lipophilic carrier	PF00650	CRAL/TRIO domain	43	17	9	17	16
lipophilic carrier	PF06585	Haemolymph juvenile hormone binding	24	10	5	15	9
lipophilic carrier	PF00188	Cysteine-rich secretory protein family	20	7	2	9	7
lipophilic carrier	PF03392	Insect pheromone-bind. family, A10/OS-D	7	2	2	4	1
CD36/SNMP	PF01130	CD36 family	14	5	1	7	5
channel/transporter	PF07690	Major Facilitator Superfamily	65	21	16	16	13
channel/transporter	PF00083	Sugar (and other) transporter	49	7	4	7	8
channel/transporter	PF00060	Ligand-gated ion channel	29	22	20	5	3
channel/transporter	PF00520	Ion transport protein	27	15	10	9	3
channel/transporter	PF02931	Neurotrans.-gated ion-channel ligand bind.	24	10	6	4	0
channel/transporter	PF00858	Amiloride-sensitive sodium channel	23	5	2	1	1
channel/transporter	PF01061	ABC-2 type transporter	19	10	4	12	11
channel/transporter	PF00005	ABC transporter	18	4	3	5	2
channel/transporter	PF00664	ABC transporter transmemb.	15	4	2	2	4
channel/transporter	PF07885	Ion channel	9	3	3	1	1
biotransformation	PF00067	Cytochrome P450	113	30	19	34	24
biotransformation	PF00135	Carboxylesterase	50	15	13	14	14
biotransformation	PF00043	Glutathione S-transferase, C-term.	18	6	1	4	1
biotransformation	PF02798	Glutathione S-transferase, N-term.	17	5	3	4	3
transcription factor	PF00096	Zinc finger, C2H2 type	114	21	50	21	24
transcription factor	PF00046	Homeobox domain	76	17	19	14	13
transcription factor	PF00651	BTB/POZ domain	54	17	26	5	7
transcription factor	PF00010	Helix-loop-helix DNA-binding	41	6	6	5	6
transcription factor	PF00250	Fork head domain	19	6	8	3	4
transcription factor	PF07716	Basic region leucine zipper	14	3	4	1	3
transcription factor	PF00292	Paired box domain	10	3	5	3	3
transcription factor	PF00907	T-box	11	8	6	8	5
transcription factor	PF00170	bZIP transcription factor	8	3	3	2	2
transcription factor	PF00157	Pou domain - N-terminal to homeobox	4	2	3	3	1

Table 2. Legend

Cells in each row contain information corresponding to the **gene class** listed. **PfamA**: PfamA family number. **PfamA description**: PfamA family description. **# in *An. gambiae***: number of genes identified in PfamA searches of *An. gambiae* transcriptome. **enhanced >2x**: number of genes in each PfamA family that were enhanced relative to bodies in the specified tissues, relative to bodies. FA – female antenna, MA – male antenna, FP – female palp, MP – male palp

Table S1. Complete *An. gambiae* Transcriptome Expression Data

VectorBase ID: Unique VectorBase (www.vectorbase.org) identification number for each *An. gambiae* gene. **transcript length**: length in base pairs of the longest annotated transcript for each gene. **chromosomal location**: chromosome arm, location of the first base pair of the initiator codon, location of the last base pair of the stop codon, reading frame (1 for plus strand or -1 for minus strand), gene name (if any). **best match to NR database (-*An. gambiae*)**: best match to non-redundant protein database (http://www.ncbi.nlm.nih.gov/BLAST/blastcgihelp.shtml#protein_databases) with *An. gambiae* proteins removed. **%ID**: percent amino acid identity between *An. gambiae* and best match peptides. **PfamA best hit**: best match to protein family identified in PfamA searches (http://pfam.janelia.org/). **e-value**: relevance value as returned in PfamA searches. **PfamA description**: protein family description. **gene**: *AgOr*, *AgIr*, *AgGr*, and *AgObp* gene families identified for easy reference. **RPKM**: normalized abundance values for each gene in the indicated tissues. **unique hits**: number of RNA-seq reads that map uniquely to each gene. **total hits**: weighted number of RNA-seq reads (unique plus fraction of non-unique) that map to a given gene. RPKM values in bold type indicate significantly enhanced abundance (>2-fold) in the antenna or palp relative to body for a given gene.

CHAPTER V

PHARMACOLOGICAL CHARACTERIZATION OF AGORS

Preface

The following chapter describes the methodology and results of a high-throughput screen to identify modulators of the AgOR10+AgORco complex. This is a manuscript in preparation. The final contents are still being determined owing to concerns of protecting the intellectual property of the assay and resulting hits, which may be licensed in the future. There is also an additional results and discussion section which describes the development of structure-activity relationships for VUAA1 and related analogs. This work is a follow-up to 61/406,786 US PROVISIONAL PATENT “Compositions for Inhibition of Insect Host Seeking” (Zwiebel, Jones, Pask and Rinker). We do not anticipate these results to be published because of intellectual property concerns. My contribution involves generation of the AgOR10+AgORco cell line, data analysis, SAR follow-up and writing of the manuscript.

Introduction

Mosquitoes and other hematophagous arthropod vectors locate their human hosts through a variety of sensory cues. Chief among these are odorants emitted from the skin and breath of an individual. The economic

and medical consequences of the diseases these insects transmit are immense, and developing nations lack the resources to develop new chemical control methods (Snow, 2005). Moreover, numerous off-target effects surrounding existing insecticides such as dichlorodiphenyltrichloethane (DDT) and related compounds make the development of new agents important (van den Berg, 2009). The development of repellent agents, which are potentially less toxic than insecticides, is an attractive option to reduce disease burdens (van der Goes van Naters and Carlson, 2006).

To date, the methodological approaches to mosquito control strategies have relied on assessing new attractants and repellants in the context of whole-organism behavior. Such approaches are resource-intensive, require large amounts of compound, and are not amenable to high-throughput (Paluch, Bartholomay, and Coats, 2010). In an effort to circumvent this bottleneck, we have investigated the feasibility of employing high throughput screening (HTS) technologies that heretofore have principally been the preview of pharmacologic drug discovery.

The molecular basis of host seeking relies heavily on a family of 76 odorant receptors (*AgORs* in *An. gambiae,* Hill et al., 2002). Seventy-five of these AgORs are conventional ORs that directly interact with odorants (Sato et al., 2008; Jones et al., 2011), and form a heteromeric complex of unknown stoichiometry with the OR co-receptor (ORco, Neuhaus et al., 2004, Benton et al., 2006). The ORx-ORco complex forms a functional ion

channel, which is ionotropically gated upon odorant binding (Sato et al., 2008; Wicher et al., 2008; Jones et al., 2011). The ORco is well conserved across insect taxa both genetically and functionally (Jones et al., 2005; Pitts et al., 2004; Larrson et al., 2004; Jones et al., 2011). The functional coding space varies for each of the conventional ORs, wherein some ORs are specialists and respond to a very small subset of compounds, and others are generalists and are sensitive to many compounds (Carey et al., 2010; Wang et al., 2010).

Greater than 50% of conventional ORs have been functionally characterized through various heterologous expression methods (Lu et al., 2007; Xia et al., 2008; Carey et al., 2010; Wang et al., 2010). In these systems a conventional OR is expressed along with ORco; signal is not observed in the absence of ORco. Although these heterologous systems are not as sensitive as the native neurons in their ability to detect nanomolar odorant concentrations, they recapitulate the agonist rankings of OR-expressing neurons (Lu et al., 2007; Carey et al., 2010). This serves as a proof-of-concept that these expression systems are excellent substitutes for the native system, and allow for extensive throughput outside of the constraints of the mosquito.

Of the nearly sixty ORs expressed in the antennal tissues of adult *Anopheles gambiae*, AgOR10 is one of only two conventional odorant receptors that is more than 69% conserved between the blood-feeding mosquito subfamilies of *Anophelinae* and *Culicinae* (Bohbot et al., 2011;

LJZ unpublished data). This conservation, along with a robust responsiveness to a known, attractive, semiochemical implicate AgOR10 in an active role in olfactory-mediated behaviors of hematophagous mosquitoes (Bohbot et al., 2011). Consequently, we have developed a high-throughput screening protocol to examine the modulatory capacity of 150,000 small molecules against AgOR10+AgORco expressed in HEK293 cells.

Materials and Methods

Cell Line Generation

To create a cell culture expression vector capable of co-expressing AgORco in conjunction with a conventional AgOR10, pcDNA5/FRT/TO (Invitrogen) was modified to create two individual expression cassettes each under the control of separate CMV/TetO2 promoters and BGH poly-adenylation signals. Flp-In™ T-REx™ 293 cell lines (Invitrogen) were transfected with the modified pcDNA5 plasmid along with POG44 (a plasmid encoding FLP recombinase) to facilitate site-specific recombination. Stable cell lines were selected using Hygromycin B (150 ug/ml, Invitrogen). Cells were maintained in DMEM (Invitrogen) supplemented with 10% tetracycline-free FBS (HyClone) and blasticidin 15 ug/ml (Invitrogen). Monoclonal populations were grown to confluence

and assayed for response to a panel of odorants previously described (Bohbot et al., 2011).

Calcium Fluorometry

24h prior to each assay, cells were plated at a concentration of 25,000 cells/well in a black-walled, clear-bottomed 384-well plate (Greiner Bio-One, Longwood, FL). Plated cells were treated with 0.3 ug/ul tetracycline (Sigma) overnight to induce incubated at 37°C, 5% CO_2 overnight. The following day, cells were incubated for 45 min at 37°C with 20 µl of 3 µM Fluo-4/acetoxymethyl ester (Fluo-4AM), prepared as a 2.3 mM stock in DMSO, mixed in a 1:1 ratio with 10% (w/v) Pluronic acid F-127 (Invitrogen), and diluted in calcium assay buffer (Hanks' balanced salt solution, 20 mM HEPES, and 2.5 mM probenecid). Dye-buffer was then replaced with 20 µl of calcium assay buffer.

Vanderbilt Molecular Screening Library test compounds were prepared from 10 mM DMSO stocks, and diluted to 10uM in individual, 384-well, 15mm poly-propylene (PP) plates using an Echo 555 acoustic liquid handler (Bucher biotec, Basel, Switzerland). Test compounds were diluted in assay buffer to 20uM. Control compounds were prepared in a separate 384-well, deep well (22mm) PP plate (Greiner Bio-One, Longwood, FL) and diluted in assay buffer to 50um.

Fluorescence readings were conducted in a Hamamatsu imaging-based plate reader (excitation, 470 ± 20 nm; emission, 540 ± 30 nm;

FDSS6000; Hamamatsu Corporation, Bridgewater, NJ). We assayed each cell plate over the course of a five-minute protocol, which consisted of three separate compound additions interspersed with latency periods to allow baseline return. Compound additions were performed at assay timepoints 5, 120, and 220 seconds. The volumes of each compound addition were 20ul, 10ul, and 12ul, at concentrations of 2x, 5x and 5x respectively. Fluorescent readings were taken at 1s intervals over the course of the entire assay. Additional, half-second fluorescent readings were taken during the 30 seconds subsequent to each addition to better quantify response kinetics.

Raw data were exported to Excel (Microsoft, Redmond, CA), and the maximum fluorescence reading for each trace was measured. Concentration-response curves were integrated and fitted using a four-parameter logistic equation in Prism (GraphPad Software, Inc., San Diego, CA).

Hit Identification

The following algorithm was used to determine hit criteria for Agonists:Agonist IF: [A1+x]>(1.05*[avgEC_0+x]) AND [A3+x]<[EC_{80}+x]. Where x= the baseline RFU (Relative Fluorescent Unit) assessed at the beginning of the run; A1= The peak RFU after addition of library compound 1; EC_0=RFU response of control well to addition of DMSO only; A3= the peak RFU response of the experimental well after EC_{80}

concentration of 2-EP was added; EC_{80}= peak RFU of control well which received only EC_{80} concentration of 2-EP.The following algorithm was used to determine hit criteria for Potentiators: Potentiator IF: [A2+x]-[A2-A3]>(1.2*[avgEC_{20}+x]-[avgEC_{20}-A3]). Where x= as above; A2= The peak RFU after addition of EC20 concentration of 2-EP to the experimental well; A3= as above; EC_{20}= peak RFU of control well which received only EC_{20} concentration of 2-EP; EC0=RFU response of control well to addition of DMSO only; A3= the peak RFU response of the experimental well after EC_{80} concentration of 2-EP was added. The following algorithm was used to determine hit criteria for Antagonists : Antagonist IF: [A3+x]<(0.7*[EC_{80}+x])Where x= as above; A3= as above; EC80= as above.

Results and Discussion

Screen Design

The format of the screen was a “triple-add” assay, which is an efficient way to examine a test compound’s intrinsic agonism and its ability to potentiate or antagonize the response of the positive control (Figure 1). In the first add, library compound is added to the experimental well and the library compound’s agonist capacity is examined. Subsequently, in the second add, an [EC_{20}] of 2-EP was added to each well to determine the compounds’ ability to potentiate the ORs response to cognate ligand.

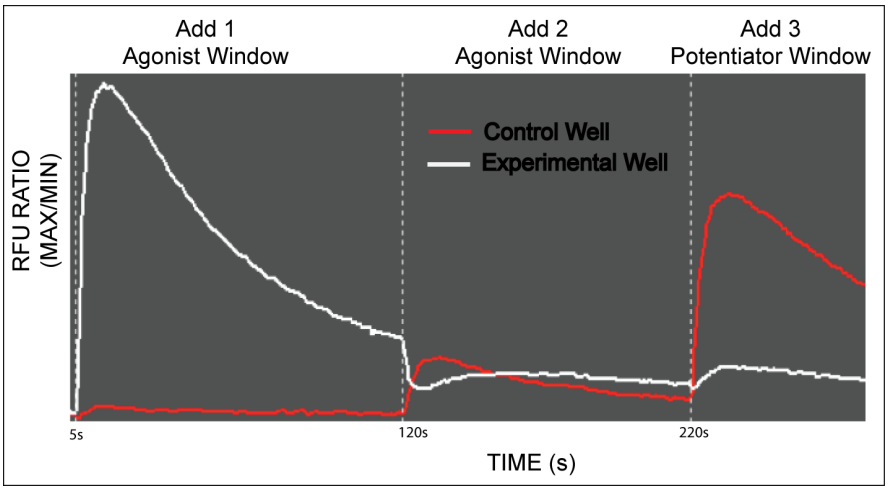

Figure 1. Representative example of Raw Fluorescence Readout for a novel AgOR10 agonist. Control well trace demonstrating no response to DMSO in addition 1, and increasing responses to 2-EP EC_{20} and EC_{80} (Red Trace). Experimental well trace demonstrating strong response to library compound in addition 1, and FLUO-4AM dye exhaustion for Add 2 and Add 3. Dashed lines indicate additions.

Lastly, in the third add, an [EC_{80}] of 2-EP was added to each test well to test for antagonism. These three windows allowed for an efficient and cost-effective measure of a test compound's modulatory effects on AgORs.

We tested the assay for robustness by determining the z-factor of control wells within pilot experiments (Figure 2). A Z-factor of 0.79 was found, which provided a large signal to noise ratio and powerful hit discrimination capabilities. The tuning curves of AgOR10 demonstrate that an AgOR that is more broadly tuned than a majority of the de-orphanized AgORs (Wang et al., 2010; Carey et al., 2010; Bohbot et al., 2011). Likely as a result of this demonstrated functional broadness, the agonist hit rate for AgOR10 agonists was 1% (1520 hits / 150,000 compounds tested). Agonists were determined by an algorithm (defined in methods), which identified compounds with a response that was significantly greater than the baseline control and that removed auto-fluorescent compounds. To validate the results, all hits were retested in duplicate against AgOR10+AgOR7 cells as well as un-induced cells which did not express AgOR10+AgORco to test for responses specific to the OR complex (Figure 3). We found that 266 agonists of AgOR10 were revalidated that did not activate un-induced cells. Thus, the confirmed hit rate dropped to 0.17%.

Agonist Hit Analysis

AgOR10 tuning curves demonstrate that AgOR10 is strongly activated by a series of substituted aromatics (Bohbot et al., 2011). The agonist hit results were no different, and AgOR10 demonstrated strong responses to a number of complex aromatic compounds. One such hit series, focused on an imine moiety (Figure 4). We detected 77 validated hits in this series. Interestingly, imines are generally unstable in solution, where acid hydrolysis generally leads to the production of aldehyde and aniline degradation products. These potential degradation products will have to be investigated using mass spectrometry analysis to confirm hit identity. At present it is impossible to determine whether AgOR10 is in fact responding to the starting compound or its derivatives. In addition to the imine series, we identified other series including a sulfonamide series, a Diels-Alder adduct series, and a piperazine amide series.

VUAA1 Structure/Activity Analysis

This AgOR10 screen led to the discovery of VUAA1 (discussed previously). In order to follow up on this validated lead, we have begun to develop structure/activity relationships around VUAA1 to identify potentially more efficacious molecules. To identify the bio-active moieties of VUAA1, we have used *in silico* screening to search for VUAA1-like compounds within the Vanderbilt molecular screening library. Through the testing of these compounds, which diverge from the VUAA1 “core”, we will

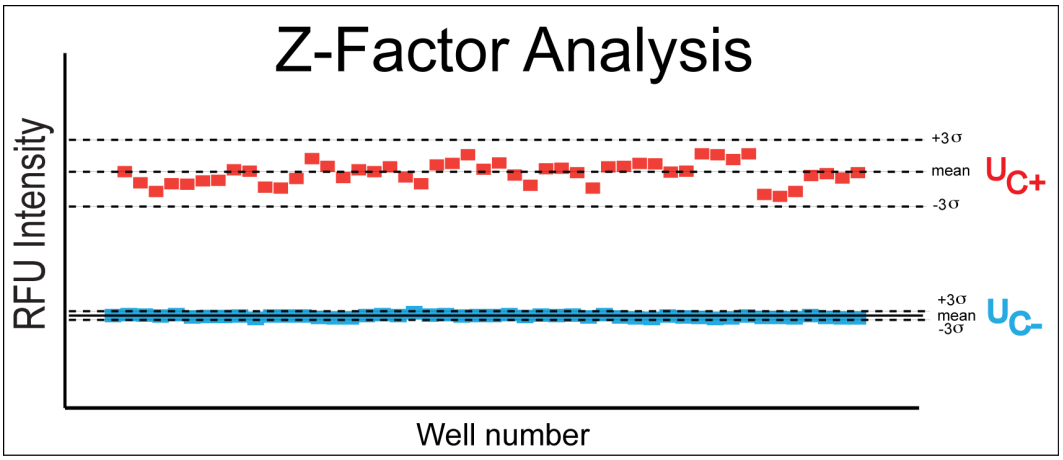

Figure 2. Z Factor analysis of pilot experiments for EC80 concentrations of 2-ethyphenol and DMSO only control. Each data point represents the response to 2-EP (U_{c+}) or DMSO only (U_{c-}). Central dashed line for each group represents the mean, while upper and lower dashed lines represent (+/-) 3 standard deviations from the mean, respectively.

examine those regions important for VUAA1 activity. With stringent search criteria, we have located approximately 416 compounds that share common moieties with VUAA1. When these 416 compounds were tested in a single-add experiment against AgOR10+AgORco and AgOR28+AgORco cells, none demonstrated agonism. Akin to the discovery of Serotonin receptor antagonists, we postulated that VUAA1-related molecules that we examined possessed similar affinity to the ORco, but lacked efficacy (Leff et al., 1986). We re-tested these 416 compounds in a double-add experiment to identify antagonism and found that 10 compounds had the capacity to agonize both the AgOR10+AgORco complex and the AgOR28 +AgORco complex. These compounds are currently being tested for follow up to define a new class of AgORco antagonists, a first-in-class demonstration of AgORco antagonism.

Of the compounds tested from this 416 compound set, it was surprising that we did not identify other agonists with activity similar to VUAA1. One possible interpretation of these results is that VUAA1 agonism is dependent on the anilide moiety, which was not preserved in this particular 416 compound set.

In addition to the *in silico* search for VUAA1-related molecules, we also began a directed *de novo* synthesis of VUAA1 analogs, which allowed us to tailor molecules closer to VUAA1 than those in the VICB library. To date, 7 compounds have been generated and examined (Figure

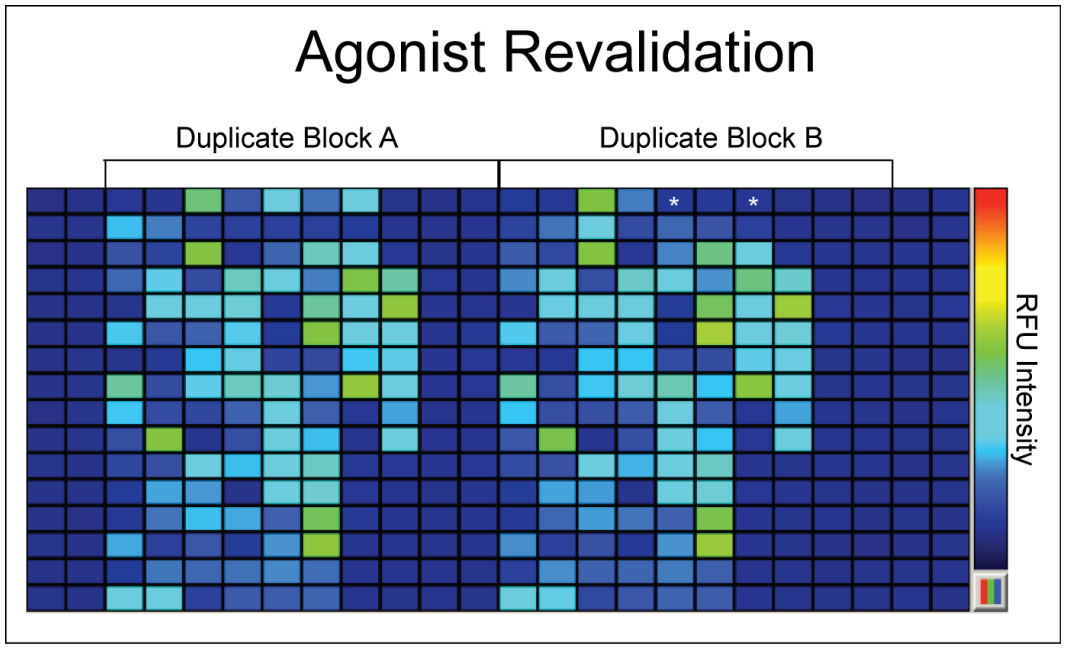

Figure 3. The plate schematic and response intensity for a representative agonist hit revalidation. Candidate hits were revalidated in duplicate blocks on the same plate to control for regional differences in RFU intensity. (*) indicates example where a hit revalidated in one block, but failed to revalidate in another block.

5). Only two of these compounds elicited a response from AgOR28+AgORco cells. The response, however, from both molecules was almost double that of an equimolar response of the parent molecule.

Conclusions

In this study, we report a calcium mobility assay for mosquito olfactory receptors and the application of a high-throughput screen to identify novel OR modulators. We were limited to screening against a library of molecules exhibiting known drug-like properties. These compounds tended to have a higher molecular weight than odorants known to elicit responses from ORs (Wang et al., 2010, Carey et al., 2010). Indeed this high molecular weight is likely indicative of low volatility, and thus unlikely to be considered an "odorant". Lead characterization will likely involve deconstructing these hits into lower molecular weight structures to increase volatility.

The Structure/Activity Relationships for VUAA1 have proven to be exceptionally narrow. This is consistent with our hypothesis the ORco is not in fact a receptor, but rather a channel, which lacks a conventional ligand binding site. ORco activation is thus dependent on allosteric activation by the conventional ORx. As ORco lacks a classical orthosteric binding site, VUAA1, in a yet unknown manner increases the open probability of ORco, or reduces the probability of closing once in the open state. Future VUAA1 analogs will be generated in an attempt to decrease

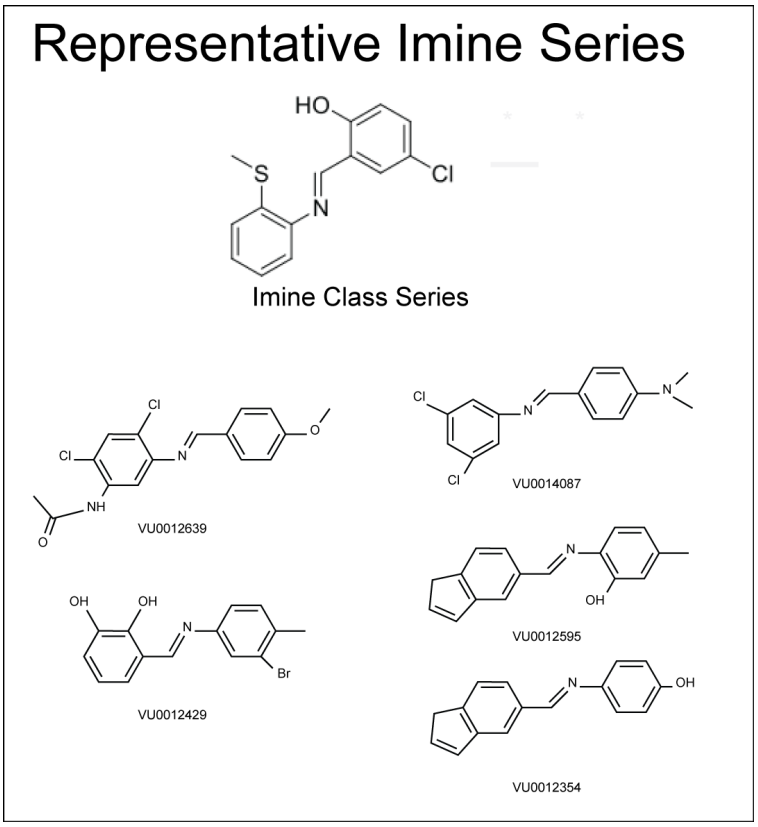

Figure 4. Representative imine series of revalidated hits from primary screen of AgOR10+AgORco.

the molecular weight to increase volatility for field trials, and increase VUAA1 efficacy.

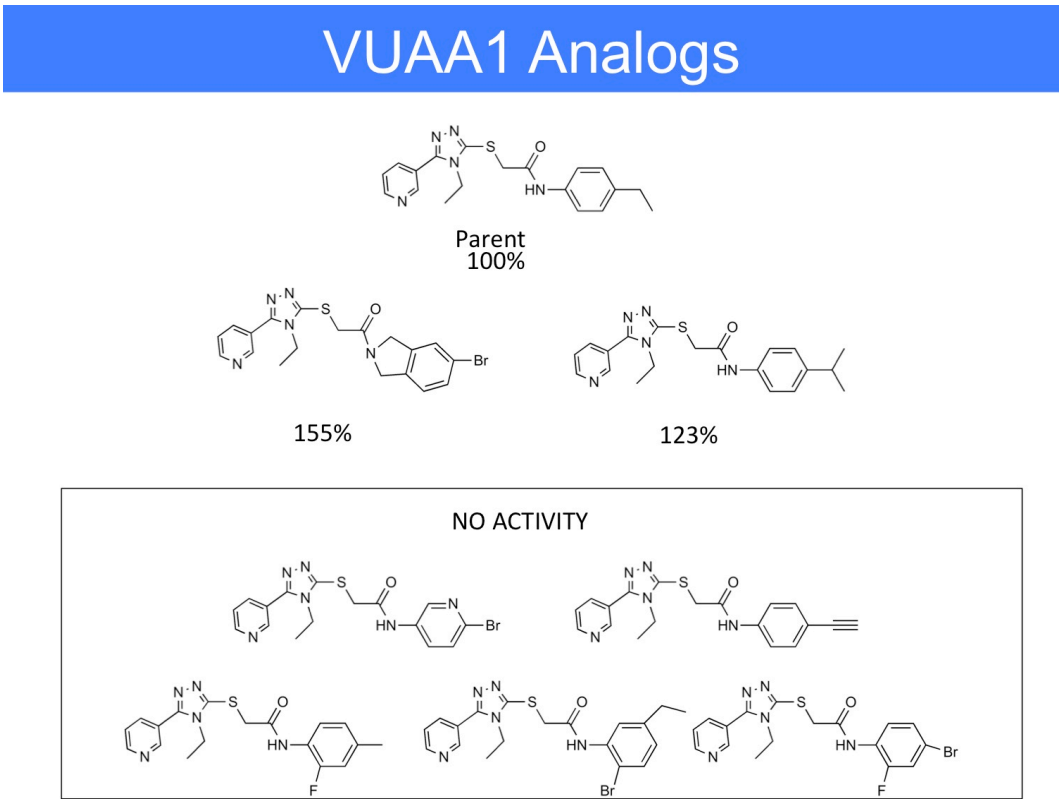

FIGURE 5. VUAA1 Analogs with demonstrated activity. %'s indicate the percent of activity of each compound compared to an equimolar concentration of the parent molecule, VUAA1.

CHAPTER VI

CONCLUSIONS AND FUTURE DIRECTIONS

In an attempt to characterize the full suite of chemosensory genes expressed on the principal olfactory organs, the antennae and maxillary palp, we utilized high-throughput RNA sequencing (RNAseq). RNAseq is superior to other gene expression profiling methods in that it is highly quantitative and is non-biased, in that it does not require *a priori* gene model knowledge (Mortazavi, 2008). Gene expression in the antennae and maxillary palps was compared to the bodies of each sex to identify genes that were significantly enhanced in chemosensory tissues. As expected, classes of genes with known chemosensory function were highly enhanced in the antennae and palps, but we also identified a number of other gene families with enhanced chemosensory expression suggesting previously unknown roles in olfactory processes. There was a surprsing amount of sexual monomorphism in terms of chemosensory gene complexity. This suggests that males and females can sense the same sets of odorants, but that the enhanced expression of these genes increases female sensitivity to odors.

In addition to identifying the suite of chemosensory receptors present on the antennae and maxillary palps, these studies have established functional relationships between ORs of multiple vector

mosquito species. We have shown that genetically conserved mosquito ORs are functionally conserved across more than 150 million years of evolutionary time. Functional conservation of the OR2/9/10 clade was demonstrated for 30 plant and human volatiles important to the life history of many mosquitoes. These studies have laid the groundwork for the development of agents that can target mosquito ORs across species, which could ultimately reduce transmission of important disease agents.

In the search for agents that could modify conventional ORs across mosquito species, we discovered the first ORco agonist, VUAA1. This ORco agonist was initially designated as an allosteric agonist of AgOR10 (Vanderbilt University allosteric agonist #1). More than 150,000 compounds were screened against AgOR10+AgORco from the Vanderbilt Small Molecule Library, and VUAA1 was the only compound that demonstrated allosteric agonism. However, in subsequent analyses the demonstrated activity was not consistent with allosteric agonism. Follow-up testing demonstrated that VUAA1 had the capacity to activate multiple AgOR expressing cell lines, including AgOR8, AgOR10, and AgOR65. As all of these cell lines also expressed AgORco, I postulated that VUAA1 was an AgORco agonist. To test this hypothesis, we then treated cells expressing AgOR7 alone with VUAA1 and discovered the first ligand capable of gating AgOR7. In addition, these experiments also demonstrated that ORco can form stand-alone ion channels which are themselves capable of functional agonism. It is currently unclear whether

ORco forms stand-alone channels *in vivo*, or what the functional implications of this would be. This work refutes a previous study, which suggested that ORco is also a cyclic nucleotide gated (GNG) channel (Wicher et al., 2008). We observed no evidence for cyclic nucleotide gating of ORco. This analysis redefines the model for insect odorant receptor signal transduction. VUAA1 is a first in class agonist, which serves as proof of concept that ORco can be chemically modulated and subsequently gated. We have begun to develop structure activity relationships around VUAA1.

It would seem unlikely for a plant or animal species to evolve an ORco family ligand apart from use as a defensive allomone. To date, there are no known natural ligands for ORco family members. Accordingly, we would posit that AgORco and other ORco family members should no longer be considered receptors, but rather be recognized as allosterically gated ion channels. While there is no evidence to suggest that the ORco channel has a natural orthosteric binding site, modulation of ion channels demonstrating intrinsic spontaneous openings, but which lack orthosteric sites is not without precedent. Indeed, synthetic small molecules have been shown to open other cation channels without classical orthosteric binding sites. These examples include the large conductance calcium-activated K+ channels, which are activated by benzimidazolone derivatives or voltage-gated sodium channels activated by lipid-soluble neurotoxins (Olesen et al., 1993; Wang and Wang, 2004).

The ultimate aim of this work is to develop a sufficient understanding of mosquito olfaction systems to generate a new class of next generation insect repellents. Unfortunately, the field lacks a comprehensive study that examines the feasibility of a repellent-based disease reduction program. There is however, strong evidence that because repellents have demonstrated remarkable protection against mosquito bites (approximately 96% in numerous field trials), an efficacious repellent would reduce disease burdens (Lindsay & Janneh, 1989; Frances et al., 1998,1999,2001; Trigg 1996; Govere et al., 2000; Moore et al., 2002; Costantini et al., 2004). The few studies that have been performed suggest that with high compliance and repellent efficacy, malaria levels would drop below those achieved with insecticide treated nets (Moore, et al., 2007; Kiszewski & Darling, 2010). However, such studies have drawn on the benchmark mosquito repellent DEET, which has a number of limitations. DEET provides limited protection over time, requires frequent re-application, and dissolves plastics, which together makes application compliance difficult (reviewed in Paluch et al., 2010). In addition, in areas of high compliance, those users who do not apply repellent are put at greater risk because mosquitoes are diverted to non-compliant individuals; this raises a number of ethical problems (Moore et al., 2007). We aim to develop agents superior to this DEET standard, without many of the drawbacks and complications.

The utility of an ORco agonist would be to activate all OR-expressing ORNs for a given insect. In *Anopheles gambiae* females, this would represent greater than 80% of all olfactory sensilla on the antennae, and all olfactory sensilla on the maxillary palp (McIver, 1982). As these are the principal olfactory organs of the mosquito, blanket activation of all ORNs would severely limit their ability to discriminate odors in theenvironment. The mosquito would simply be unable to interpret the flood of afferent electrical activity. Universal ORN activation would thus disrupt a variety of olfactory-driven behaviors, specifically human host-seeking, which serves as the foundation for their ability to transmit disease.

ORco is present in insects as early as the aphids and conserved into the Lepidopterans. The hemimetabolous *An. gambiae* Orco is 55% identical to the holometabolous aphid *Acyrthosiphon pisum,* demonstrating incredible conservation virtually across all insect taxa (Dipterans and aphids diverged very early in insect taxonomy). We have demonstrated VUAA1 agonism of Orco as distant as hymonoperta (60% identical), suggesting that VUAA1 agonism has the potential to agonize ORco's across all insect taxa. Insects, or the diseases they transmit, are largely responsible for the 35% of all agricultural crops that are lost annually (Pimentel, 1991). Crop loss of this magnitude has immense economic and health consequences, and as a result finding new ways of decreasing such loss is important. One such method will be to interfere with the

olfactory systems of agricultural pest insects. A large number of plant volatiles have been demonstrated to attract important crop pests, such as the onion fly *Delia antiqua,* and the apple pests *Rhagletis* flies (Reviewed in van der Goes van Naters and Carlson, 2006).

Unfortunately, non-specific ORco activation is a double-edged sword, and would affect beneficial insects such as the honeybee *Apis mellifera*. Thus, an Orco agonist would have to be used responsibly in areas of greatest risk. Nevertheless these studies represent a large step forward for the field in terms of defining the model of signal transduction and introducing a new tool for its study. We hope, that through further development of VUAA1, the utility of an ORco agonist would range from keeping nuisance insects from residential neighborhoods to repelling destructive agricultural pests from critical production areas, and reduce disease burdens worldwide.

REFERENCES

Aguilar, R., Jedlicka, A. E., Mintz, M., Mahairaki, V., Scott, A. L., and Dimopoulos, G. (2005). Global gene expression analysis of Anopheles gambiae responses to microbial challenge. *Insect Biochem Mol Biol* **35**, 709-719.

Aguilar, R., Simard, F., Kamdem, C., Shields, T., Glass, G. E., Garver, L. S., and Dimopoulos, G. (2010). Genome-wide analysis of transcriptomic divergence between laboratory colony and field Anopheles gambiae mosquitoes of the M and S molecular forms. *Insect Mol Biol* **19**, 695-705.

Allan, S. A., and Kline, D. L. (1998). Larval rearing water and preexisting eggs influence oviposition by Aedes aegypti and Ae. albopictus (Diptera: Culicidae). *J Med Entomol* **35**, 943-947.

Anton, S., and Hansson, B. S. (1995). Sex pheromone and plant-associated odour processing in antennal lobe interneurons of male *Spodoptera littoralis* (Lepidoptera: Noctuidae). *Journal of Comparative Physiology, A* **176**, 773-789.

Arensburger, P., Megy, K., Waterhouse, R. M., Abrudan, J., Amedeo, P., Antelo, B., Bartholomay, L., Bidwell, S., Caler, E., Camara, F., Campbell, C. L., Campbell, K. S., Casola, C., Castro, M. T., Chandramouliswaran, I., Chapman, S. B., Christley, S., Costas, J., Eisenstadt, E., Feschotte, C., et al. (2010). Sequencing of Culex quinquefasciatus establishes a platform for mosquito comparative genomics. *Science* **330**, 86-88.

Ayer, R. K., Jr., and Carlson, J. (1991). acj6: a gene affecting olfactory physiology and behavior in Drosophila. *Proc Natl Acad Sci U S A* **88**, 5467-5471.

Ayer, R. K., Jr., and Carlson, J. (1992). Olfactory physiology in the Drosophila antenna and maxillary palp: acj6 distinguishes two classes of odorant pathways. *J Neurobiol* **23**, 965-982.

Bai, L., and Carlson, J. R. (2010). Distinct functions of acj6 splice forms in odor receptor gene choice. *J Neurosci* **30**, 5028-5036.

Bai, L., Goldman, A. L., and Carlson, J. R. (2009). Positive and negative regulation of odor receptor gene choice in Drosophila by acj6. *J Neurosci* **29**, 12940-12947.

Balwierz, P. J., Carninci, P., Daub, C. O., Kawai, J., Hayashizaki, Y., Van

Belle, W., Beisel, C., and van Nimwegen, E. (2009). Methods for analyzing deep sequencing expression data: constructing the human and mouse promoterome with deepCAGE data. *Genome Biol* **10**, R79.

Baton, L. A., Robertson, A., Warr, E., Strand, M. R., and Dimopoulos, G. (2009). Genome-wide transcriptomic profiling of Anopheles gambiae hemocytes reveals pathogen-specific signatures upon bacterial challenge and Plasmodium berghei infection. *BMC Genomics* **10**, 257.

Beehler, J. W., Millar, J. G., and Mulla, M. S. (1994). Protein hydrolysates and associated bacterial contaminants as oviposition attractants for the mosquito *culex quinquefasciatus*. *Medical and Veterinary Entomology* **8**, 381-385.

Bentley, M. D., and Day, J. F. (1989). Chemical ecology and behavioral aspects of mosquito oviposition. *Annu Rev Entomol* **34**, 401-421.

Bentley, M. D., McDaniel, I. N., Yatagai, M., Lee, H.-P., and Maynard, R. (1979). *p*-Cresol: an oviposition attractant of *aedes triseriatus*. *Environmental Entomology* **8**, 206-209.

Benton, R., Sachse, S., Michnick, S. W., and Vosshall, L. B. (2006). Atypical membrane topology and heteromeric function of Drosophila odorant receptors in vivo. *PLoS Biol* **4**, e20.

Benton, R., Vannice, K. S., Gomez-Diaz, C., and Vosshall, L. B. (2009). Variant ionotropic glutamate receptors as chemosensory receptors in Drosophila. *Cell* **136**, 149-162.

Bernier, U. R., Kline, D. L., Barnard, D. R., Schreck, C. E., and Yost, R. A. (2000). Analysis of human skin emanations by gas chromatography/mass spectrometry. 2. Identification of volatile compounds that are candidate attractants for the yellow fever mosquito (Aedes aegypti). *Anal Chem* **72**, 747-756.

Besansky, N. J., and Fahey, G. T. (1997). Utility of the white gene in estimating phylogenetic relationships among mosquitoes (Diptera: Culicidae). *Mol Biol Evol* **14**, 442-454.

Biessmann, H., Andronopoulou, E., Biessmann, M. R., Douris, V., Dimitratos, S. D., Eliopoulos, E., Guerin, P. M., Iatrou, K., Justice, R. W., Krober, T., Marinotti, O., Tsitoura, P., Woods, D. F., and Walter, M. F. (2010). The Anopheles gambiae odorant binding protein 1 (AgamOBP1) mediates indole recognition in the antennae of female mosquitoes. *PLoS One* **5**, e9471.

Blackwell, A., and Johnson, S. N. (2000). Electrophysiological investigation of larval water and potential oviposition chemo-attractants for Anopheles gambiae s.s. *Ann Trop Med Parasitol* **94**, 389-398.

Bohbot, J., Pitts, R. J., Kwon, H. W., Rutzler, M., Robertson, H. M., and Zwiebel, L. J. (2007). Molecular characterization of the Aedes aegypti odorant receptor gene family. *Insect Mol Biol* **16**, 525-537.

Bohbot, J., and Vogt, R. G. (2005). Antennal expressed genes of the yellow fever mosquito (Aedes aegypti L.); characterization of odorant-binding protein 10 and takeout. *Insect Biochem Mol Biol* **35**, 961-979.

Bohbot, J. D., and Dickens, J. C. (2009). Characterization of an enantioselective odorant receptor in the yellow fever mosquito Aedes aegypti. *PLoS One* **4**, e7032.

Bohbot, J. D., Jones, P. L., Wang, G., Pitts, R. J., Pask, G. M., and Zwiebel, L. J. (2011). Conservation of indole responsive odorant receptors in mosquitoes reveals an ancient olfactory trait. *Chem Senses* **36**, 149-160.

Bohlen, C. J., Priel, A., Zhou, S., King, D., Siemens, J., and Julius, D. (2010). A bivalent tarantula toxin activates the capsaicin receptor, TRPV1, by targeting the outer pore domain. *Cell* **141**, 834-845.

Bonizzoni, M., Dunn, W. A., Campbell, C. L., Olson, K. E., Dimon, M. T., Marinotti, O., and James, A. A. (2011). RNA-seq analyses of blood-induced changes in gene expression in the mosquito vector species, Aedes aegypti. *BMC Genomics* **12**, 82.

Bowen, M. F. (1991). The sensory physiology of host-seeking behavior in mosquitoes. *Annu Rev Entomol* **36**, 139-158.

Branscomb, A., Seger, J., and White, R. L. (2000). Evolution of odorant receptors expressed in mammalian testes. *Genetics* **156**, 785-797.

Cabrera, M., and Jaffe, K. (2007). An aggregation pheromone modulates lekking behavior in the vector mosquito Aedes aegypti (Diptera: Culicidae). *J Am Mosq Control Assoc* **23**, 1-10.

Carey, A. F., Wang, G., Su, C. Y., Zwiebel, L. J., and Carlson, J. R. (2010). Odorant reception in the malaria mosquito Anopheles gambiae. *Nature* **464**, 66-71.

Caterina, M. J., Schumacher, M. A., Tominaga, M., Rosen, T. A., Levine, J. D., and Julius, D. (1997). The capsaicin receptor: a heat-activated ion

channel in the pain pathway. *Nature* **389**, 816-824.

Cayirlioglu, P., Kadow, I. G., Zhan, X., Okamura, K., Suh, G. S., Gunning, D., Lai, E. C., and Zipursky, S. L. (2008). Hybrid neurons in a microRNA mutant are putative evolutionary intermediates in insect CO2 sensory systems. *Science* **319**, 1256-1260.

Chandrashekar, J., Yarmolinsky, D., von Buchholtz, L., Oka, Y., Sly, W., Ryba, N. J., and Zuker, C. S. (2009). The taste of carbonation. *Science* **326**, 443-445.

Charlwood, J. D., and Jones, M. D. R. (1979). Mating behaviour in the mosquito, *Anopheles gambiae s.l.* Close range and contact behaviour. *Physiological Entomology* **4**, 111-120.

Churcher, A. M., and Taylor, J. S. (2009). Amphioxus (Branchiostoma floridae) has orthologs of vertebrate odorant receptors. *BMC Evol Biol* **9**, 242.

Clark, A. G., Eisen, M. B., Smith, D. R., Bergman, C. M., Oliver, B., Markow, T. A., Kaufman, T. C., Kellis, M., Gelbart, W., Iyer, V. N., Pollard, D. A., Sackton, T. B., Larracuente, A. M., Singh, N. D., Abad, J. P., Abt, D. N., Adryan, B., Aguade, M., Akashi, H., Anderson, W. W., et al. (2007). Evolution of genes and genomes on the Drosophila phylogeny. *Nature* **450**, 203-218.

Clements, A. N. (1992) *The Biology of Mosquitoes*, Chapman & Hall, London, Glasgow, New York, Tokyo, Melbourne, Madras

Clyne, P. J., Certel, S. J., de Bruyne, M., Zaslavsky, L., Johnson, W. A., and Carlson, J. R. (1999). The odor specificities of a subset of olfactory receptor neurons are governed by Acj6, a POU-domain transcription factor. *Neuron* **22**, 339-347.

Clyne, P. J., Warr, C. G., Freeman, M. R., Lessing, D., Kim, J., and Carlson, J. R. (1999). A novel family of divergent seven-transmembrane proteins: candidate odorant receptors in Drosophila. *Neuron* **22**, 327-338.

Collins, L. E., and Blackwell, A. (2002). Olfactory cues for oviposition behavior in Toxorhynchites moctezuma and Toxorhynchites amboinensis (Diptera: Culicidae). *J Med Entomol* **39**, 121-126.

Cook, P. E., and Sinkins, S. P. (2010). Transcriptional profiling of Anopheles gambiae mosquitoes for adult age estimation. *Insect Mol Biol* **19**, 745-751.

Cork, A., and Park, K. C. (1996). Identification of electrophysiologically-active compounds for the malaria mosquito, Anopheles gambiae, in human sweat extracts. *Med Vet Entomol* **10**, 269-276.

Costantini, C., Badolo, A., and Ilboudo-Sanogo, E. (2004). Field evaluation of the efficacy and persistence of insect repellents DEET, IR3535, and KBR 3023 against Anopheles gambiae complex and other Afrotropical vector mosquitoes. *Trans R Soc Trop Med Hyg* **98**, 644-652.

Costantini, C., Sagnon, N., della Torre, A., and Coluzzi, M. (1999). Mosquito Behavioral Aspects of Vector-Human Interactions in the *Anopheles gambiae* complex. *Parassitologia* **41**, 209-217.

Couto, A., Alenius, M., and Dickson, B. J. (2005). Molecular, anatomical, and functional organization of the Drosophila olfactory system. *Curr Biol* **15**, 1535-1547.

Crawford, J. E., Guelbeogo, W. M., Sanou, A., Traore, A., Vernick, K. D., Sagnon, N., and Lazzaro, B. P. (2010). De novo transcriptome sequencing in Anopheles funestus using Illumina RNA-seq technology. *PLoS One* **5**, e14202.

Croset, V., Rytz, R., Cummins, S. F., Budd, A., Brawand, D., Kaessmann, H., Gibson, T. J., and Benton, R. (2010). Ancient protostome origin of chemosensory ionotropic glutamate receptors and the evolution of insect taste and olfaction. *PLoS Genet* **6**, e1001064.

Curtius, H. C., Mettler, M., and Ettlinger, L. (1976). Study of the intestinal tyrosine metabolism using stable isotopes and gas chromatography-mass spectrometry. *J Chromatogr* **126**, 569-580.

Dahanukar, A., Lei, Y. T., Kwon, J. Y., and Carlson, J. R. (2007). Two Gr genes underlie sugar reception in Drosophila. *Neuron* **56**, 503-516.

Das, S., Radtke, A., Choi, Y. J., Mendes, A. M., Valenzuela, J. G., and Dimopoulos, G. (2010). Transcriptomic and functional analysis of the Anopheles gambiae salivary gland in relation to blood feeding. *BMC Genomics* **11**, 566.

Datta, S. R., Vasconcelos, M. L., Ruta, V., Luo, S., Wong, A., Demir, E., Flores, J., Balonze, K., Dickson, B. J., and Axel, R. (2008). The Drosophila pheromone cVA activates a sexually dimorphic neural circuit. *Nature* **452**, 473-477.

Davis, E. E. (1977). Response of the antennal receptors of the male *Aedes aegypti* mosquito. *Journal of Insect Physiology* **23**, 613-617.

de Bruyne, M., and Baker, T. C. (2008). Odor detection in insects: volatile codes. *J Chem Ecol* **34**, 882-897.

de Bruyne, M., Smart, R., Zammit, E., and Warr, C. G. (2010). Functional and molecular evolution of olfactory neurons and receptors for aliphatic esters across the Drosophila genus. *J Comp Physiol A Neuroethol Sens Neural Behav Physiol* **196**, 97-109.

della Torre, A., Favia, G., Mariotti, G., Coluzzi, M., and Mathiopoulos, K. D. (1996). Physical map of the malaria vector Anopheles gambiae. *Genetics* **143**, 1307-1311.

Dhallan, R. S., Yau, K. W., Schrader, K. A., and Reed, R. R. (1990). Primary structure and functional expression of a cyclic nucleotide-activated channel from olfactory neurons. *Nature* **347**, 184-187.

Ditzen, M., Pellegrino, M., and Vosshall, L. B. (2008). Insect odorant receptors are molecular targets of the insect repellent DEET. *Science* **319**, 1838-1842.

Dobritsa, A. A., van der Goes van Naters, W., Warr, C. G., Steinbrecht, R. A., and Carlson, J. R. (2003). Integrating the Molecular and Cellular Basis of Odor Coding in the Drosophila Antenna. *Neuron* **37**, 827-841.

Dong, D., He, G., Zhang, S., and Zhang, Z. (2009). Evolution of olfactory receptor genes in primates dominated by birth-and-death process. *Genome Biol Evol* **1**, 258-264.

Du, Y. J., and Millar, J. G. (1999). Electroantennogram and oviposition bioassay responses of Culex quinquefasciatus and Culex tarsalis (Diptera: Culicidae) to chemicals in odors from Bermuda grass infusions. *J Med Entomol* **36**, 158-166.

Durand, N., Carot-Sans, G., Chertemps, T., Bozzolan, F., Party, V., Renou, M., Debernard, S., Rosell, G., and Maibeche-Coisne, M. (2010). Characterization of an antennal carboxylesterase from the pest moth Spodoptera littoralis degrading a host plant odorant. *PLoS One* **5**, e15026.

Durand, N., Carot-Sans, G., Chertemps, T., Montagne, N., Jacquin-Joly, E., Debernard, S., and Maibeche-Coisne, M. (2010). A diversity of putative carboxylesterases are expressed in the antennae of the noctuid moth Spodoptera littoralis. *Insect Mol Biol* **19**, 87-97.

Elgaali, H., Hamilton-Kemp, T. R., Newman, M. C., Collins, R. W., Yu, K., and Archbold, D. D. (2002). Comparison of long-chain alcohols and other

volatile compounds emitted from food-borne and related Gram positive and Gram negative bacteria. *J Basic Microbiol* **42**, 373-380.

Finn, R. D., Mistry, J., Tate, J., Coggill, P., Heger, A., Pollington, J. E., Gavin, O. L., Gunasekaran, P., Ceric, G., Forslund, K., Holm, L., Sonnhammer, E. L., Eddy, S. R., and Bateman, A. (2010). The Pfam protein families database. *Nucleic Acids Res* **38**, D211-222.

Fishilevich, E., and Vosshall, L. B. (2005). Genetic and functional subdivision of the Drosophila antennal lobe. *Curr Biol* **15**, 1548-1553.

Foley, D. H., Bryan, J. H., Yeates, D., and Saul, A. (1998). Evolution and systematics of Anopheles: insights from a molecular phylogeny of Australasian mosquitoes. *Mol Phylogenet Evol* **9**, 262-275.

Foster, W. A., and Hancock, R. G. (1994). Nectar-related olfactory and visual attractants for mosquitoes. *J Am Mosq Control Assoc* **10**, 288-296.

Fox, A. N., Pitts, R. J., Robertson, H. M., Carlson, J. R., and Zwiebel, L. J. (2001). Candidate odorant receptors from the malaria vector mosquito Anopheles gambiae and evidence of down-regulation in response to blood feeding. *Proc Natl Acad Sci U S A* **98**, 14693-14697.

Fox, A. N., Pitts, R. J., and Zwiebel, L. J. (2002). A Cluster of Candidate Odorant Receptors from the Malaria Vector Mosquito, *Anopheles gambia*e. *Chem Senses* **27**, 453-459.

Frances, S. P., Cooper, R. D., Popat, S., and Beebe, N. W. (2001). Field evaluation of repellents containing deet and AI3-37220 against Anopheles koliensis in Papua New Guinea. *J Am Mosq Control Assoc* **17**, 42-44.

Frances, S. P., Cooper, R. D., Popat, S., and Sweeney, A. W. (1999). Field evaluation of the repellents deet, CIC-4, and AI3-37220 against Anopheles in Lae, Papua New Guinea. *J Am Mosq Control Assoc* **15**, 339-341.

Frances, S. P., Cooper, R. D., and Sweeney, A. W. (1998). Laboratory and field evaluation of the repellents deet, CIC-4, and AI3-37220 against Anopheles farauti (Diptera: Culicidae) in Australia. *J Med Entomol* **35**, 690-693.

Frey, M., Stettner, C., Pare, P. W., Schmelz, E. A., Tumlinson, J. H., and Gierl, A. (2000). An herbivore elicitor activates the gene for indole emission in maize. *Proc Natl Acad Sci U S A* **97**, 14801-14806.

Galindo, K., and Smith, D. P. (2001). A large family of divergent

Drosophila odorant-binding proteins expressed in gustatory and olfactory sensilla. *Genetics* **159**, 1059-1072.

Gardiner, A., Barker, D., Butlin, R. K., Jordan, W. C., and Ritchie, M. G. (2008). Drosophila chemoreceptor gene evolution: selection, specialization and genome size. *Mol Ecol* **17**, 1648-1657.

Gardner, C. L., and Ryman, K. D. (2010). Yellow fever: a reemerging threat. *Clin Lab Med* **30**, 237-260.

Gibbons, J. G., Janson, E. M., Hittinger, C. T., Johnston, M., Abbot, P., and Rokas, A. (2009). Benchmarking next-generation transcriptome sequencing for functional and evolutionary genomics. *Mol Biol Evol* **26**, 2731-2744.

Gibson, G., Warren, B., and Russell, I. J. (2010). Humming in tune: sex and species recognition by mosquitoes on the wing. *J Assoc Res Otolaryngol* **11**, 527-540.

Gillot, C. (2005) *Entomology*, 3rd ed., Springer

Global Malaria Program, W. (2010) *World Malaria Report 2010*, WHO Press, Geneva, Switzerland

Gong, Z., Son, W., Chung, Y. D., Kim, J., Shin, D. W., McClung, C. A., Lee, Y., Lee, H. W., Chang, D. J., Kaang, B. K., Cho, H., Oh, U., Hirsh, J., Kernan, M. J., and Kim, C. (2004). Two interdependent TRPV channel subunits, inactive and Nanchung, mediate hearing in Drosophila. *J Neurosci* **24**, 9059-9066.

Govere, J., Durrheim, D. N., Baker, L., Hunt, R., and Coetzee, M. (2000). Efficacy of three insect repellents against the malaria vector Anopheles arabiensis. *Med Vet Entomol* **14**, 441-444.

Guo, S., and Kim, J. (2007). Molecular evolution of Drosophila odorant receptor genes. *Mol Biol Evol* **24**, 1198-1207.

Guo, W., Wang, X., Ma, Z., Xue, L., Han, J., Yu, D., and Kang, L. (2011). CSP and Takeout Genes Modulate the Switch between Attraction and Repulsion during Behavioral Phase Change in the Migratory Locust. *PLoS Genet* **7**, e1001291.

Hall, D. R., Beevor, P. S., Cork, A., Nesbitt, B. F., and Vale, G. A. (1984). 1-octen-3-ol, a potent olfactory stimulant and attractant for tsetse isolated from cattle odours. *Insect Sci. Appl.* **5**, 335-339.

Hallem, E., Ho, M. G., and Carlson, J. R. (2004). The Molecular Basis of Odor Coding in the Drosophila Antenna. *Cell* **117**, 965-979.

Hallem, E. A., and Carlson, J. R. (2006). Coding of odors by a receptor repertoire. *Cell* **125**, 143-160.

Hallem, E. A., Dahanukar, A., and Carlson, J. R. (2006). Insect odor and taste receptors. *Annu Rev Entomol* **51**, 113-135.

Hallem, E. A., Nicole Fox, A., Zwiebel, L. J., and Carlson, J. R. (2004). Olfaction: mosquito receptor for human-sweat odorant. *Nature* **427**, 212-213.

Harraca, V., Syed, Z., and Guerin, P. M. (2009). Olfactory and behavioural responses of tsetse flies, Glossina spp., to rumen metabolites. *J Comp Physiol A Neuroethol Sens Neural Behav Physiol* **195**, 815-824.

Hekmat-Scafe, D. S., Scafe, C. R., McKinney, A. J., and Tanouye, M. A. (2002). Genome-wide analysis of the odorant-binding protein gene family in Drosophila melanogaster. *Genome Res* **12**, 1357-1369.

Hildebrand, J. G., and Shepherd, G. M. (1997). Mechanisms of olfactory discrimination: converging evidence for common principles across phyla. *Annu Rev Neurosci* **20**, 595-631.

Hill, C. A., Fox, A. N., Pitts, R. J., Kent, L. B., Tan, P. L., Chrystal, M. A., Cravchik, A., Collins, F. H., Robertson, H. M., and Zwiebel, L. J. (2002). G protein-coupled receptors in Anopheles gambiae. *Science* **298**, 176-178.

Hill, S. R., Hansson, B. S., and Ignell, R. (2009). Characterization of antennal trichoid sensilla from female southern house mosquito, Culex quinquefasciatus Say. *Chem Senses* **34**, 231-252.

Hittinger, C. T., Johnston, M., Tossberg, J. T., and Rokas, A. (2010). Leveraging skewed transcript abundance by RNA-Seq to increase the genomic depth of the tree of life. *Proc Natl Acad Sci U S A* **107**, 1476-1481.

Howell, P. I., and Knols, B. G. (2009). Male mating biology. *Malar J* **8 Suppl 2**, S8.

Hughes, D. T., Pelletier, J., Luetje, C. W., and Leal, W. S. (2010). Odorant receptor from the southern house mosquito narrowly tuned to the oviposition attractant skatole. *J Chem Ecol* **36**, 797-800.

Isenberg, H. D., and Sundheim, L. H. (1958). Indole reactions in bacteria.

J Bacteriol **75**, 682-690.

Ismail, I. A. (1964). Comparative Study of Sense Organs in the Antennae of Culicine and Anopheline Female Mosquitoes. *Acta Trop* **21**, 155-168.

Jeanbourquin, P., and Guerin, P. M. (2007). Chemostimuli implicated in selection of oviposition substrates by the stable fly Stomoxys calcitrans. *Med Vet Entomol* **21**, 209-216.

Jones, W. D., Nguyen, T.-A. T., Kloss, B., Lee, K. J., and Vosshall, L. B. (2005). Functional conservation of an insect odorant receptor gene across 250 million years of evolution. *Current Biology* **15**, R119-R121.

Justice, R. W., Dimitratos, S., Walter, M. F., and Biessmann, H. (2003). Sexual Dimorphic Expression of Putative Antennal Carrier Protein Genes in the Malaria Vector *Anopheles gambiae*. *Insect Molecular Biology* **12**, 581-594.

Kaissling, K. E. (2009). Olfactory perireceptor and receptor events in moths: a kinetic model revised. *J Comp Physiol A Neuroethol Sens Neural Behav Physiol* **195**, 895-922.

Katz, T. M., Miller, J. H., and Hebert, A. A. (2008). Insect repellents: historical perspectives and new developments. *J Am Acad Dermatol* **58**, 865-871.

Kim, J., Chung, Y. D., Park, D. Y., Choi, S., Shin, D. W., Soh, H., Lee, H. W., Son, W., Yim, J., Park, C. S., Kernan, M. J., and Kim, C. (2003). A TRPV family ion channel required for hearing in Drosophila. *Nature* **424**, 81-84.

Kim, M. S., Repp, A., and Smith, D. P. (1998). LUSH odorant-binding protein mediates chemosensory responses to alcohols in Drosophila melanogaster. *Genetics* **150**, 711-721.

Kim, M. S., and Smith, D. P. (2001). The invertebrate odorant-binding protein LUSH is required for normal olfactory behavior in Drosophila. *Chem Senses* **26**, 195-199.

Kiszewski, A. E., and Darling, S. T. (2010). Estimating a mosquito repellent's potential to reduce malaria in communities. *J Vector Borne Dis* **47**, 217-221.

Koonin, E. V. (2005). Orthologs, paralogs, and evolutionary genomics. *Annu Rev Genet* **39**, 309-338.

Krautwurst, D., Yau, K. W., and Reed, R. R. (1998). Identification of ligands for olfactory receptors by functional expression of a receptor library. *Cell* **95**, 917-926.

Krieger, J., Grosse-Wilde, E., Gohl, T., Dewer, Y. M., Raming, K., and Breer, H. (2004). Genes encoding candidate pheromone receptors in a moth (Heliothis virescens). *Proc Natl Acad Sci U S A* **101**, 11845-11850.

Krieger, J., Klink, O., Mohl, C., Raming, K., and Breer, H. (2003). A candidate olfactory receptor subtype highly conserved across different insect orders. *J Comp Physiol A Neuroethol Sens Neural Behav Physiol* **189**, 519-526.

Kruse, S. W., Zhao, R., Smith, D. P., and Jones, D. N. (2003). Structure of a specific alcohol-binding site defined by the odorant binding protein LUSH from Drosophila melanogaster. *Nat Struct Biol* **10**, 694-700.

Krzywinski, J., Wilkerson, R. C., and Besansky, N. J. (2001). Toward understanding Anophelinae (Diptera, Culicidae) phylogeny: insights from nuclear single-copy genes and the weight of evidence. *Syst Biol* **50**, 540-556.

Kwon, H. W., Lu, T., Rutzler, M., and Zwiebel, L. J. (2006). Olfactory responses in a gustatory organ of the malaria vector mosquito Anopheles gambiae. *Proc Natl Acad Sci U S A* **103**, 13526-13531.

Kwon, J. Y., Dahanukar, A., Weiss, L. A., and Carlson, J. R. (2007). The molecular basis of CO2 reception in Drosophila. *Proc Natl Acad Sci U S A* **104**, 3574-3578.

Kwon, Y., Kim, S. H., Ronderos, D. S., Lee, Y., Akitake, B., Woodward, O. M., Guggino, W. B., Smith, D. P., and Montell, C. (2010). Drosophila TRPA1 channel is required to avoid the naturally occurring insect repellent citronellal. *Curr Biol* **20**, 1672-1678.

Kyorku, C., Brightwell, R., and Dransfield, R. D. (1990). Traps and odour baits for the tsetse fly, *Glossina longipennis* (Diptera: Glossinidae). *Bulletin of Entomological Research. 1990;* **80**, 405-415.

Laissue, P. P., Reiter, C., Hiesinger, P. R., Halter, S., Fischbach, K. F., and Stocker, R. F. (1999). Three-dimensional reconstruction of the antennal lobe in Drosophila melanogaster. *J Comp Neurol* **405**, 543-552.

Larsson, M. C., Domingos, A. I., Jones, W. D., Chiappe, M. E., Amrein, H., and Vosshall, L. B. (2004). Or83b encodes a broadly expressed odorant receptor essential for Drosophila olfaction. *Neuron* **43**, 703-714.

Lee, M. H., and Salvaterra, P. M. (2002). Abnormal chemosensory jump 6 is a positive transcriptional regulator of the cholinergic gene locus in Drosophila olfactory neurons. *J Neurosci* **22**, 5291-5299.

Lee, Y., Kim, S. H., and Montell, C. (2010). Avoiding DEET through insect gustatory receptors. *Neuron* **67**, 555-561.

Li, J., Riehle, M. M., Zhang, Y., Xu, J., Oduol, F., Gomez, S. M., Eiglmeier, K., Ueberheide, B. M., Shabanowitz, J., Hunt, D. F., Ribeiro, J. M., and Vernick, K. D. (2006). Anopheles gambiae genome reannotation through synthesis of ab initio and comparative gene prediction algorithms. *Genome Biol* **7**, R24.

Lindh, J. M., Kannaste, A., Knols, B. G., Faye, I., and Borg-Karlson, A. K. (2008). Oviposition responses of Anopheles gambiae s.s. (Diptera: Culicidae) and identification of volatiles from bacteria-containing solutions. *J Med Entomol* **45**, 1039-1049.

Lindsay, S. W., and Janneh, L. M. (1989). Preliminary field trials of personal protection against mosquitoes in The Gambia using deet or permethrin in soap, compared with other methods. *Med Vet Entomol* **3**, 97-100.

Liu, C., Pitts, R. J., Bohbot, J. D., Jones, P. L., Wang, G., and Zwiebel, L. J. (2010). Distinct olfactory signaling mechanisms in the malaria vector mosquito Anopheles gambiae. *PLoS Biol* **8**,

Lu, T., Qiu, Y. T., Wang, G., Kwon, J. Y., Rutzler, M., Kwon, H. W., Pitts, R. J., van Loon, J. J., Takken, W., Carlson, J. R., and Zwiebel, L. J. (2007). Odor coding in the maxillary palp of the malaria vector mosquito Anopheles gambiae. *Curr Biol* **17**, 1533-1544.

Macdonald, G. (1957) *The Epidemiology and Control of Malaria*, Oxford University Press, London

Mackenzie, J. S., Gubler, D. J., and Petersen, L. R. (2004). Emerging flaviviruses: the spread and resurgence of Japanese encephalitis, West Nile and dengue viruses. *Nat Med* **10**, S98-109.

Mackie, R. I., Stroot, P. G., and Varel, V. H. (1998). Biochemical identification and biological origin of key odor components in livestock waste. *J Anim Sci* **76**, 1331-1342.

Maibeche-Coisne, M., Jacquin-Joly, E., Francois, M. C., and Nagnan-Le Meillour, P. (2002). cDNA cloning of biotransformation enzymes belonging

to the cytochrome P450 family in the antennae of the noctuid moth Mamestra brassicae. *Insect Mol Biol* **11**, 273-281.

Marinotti, O., Calvo, E., Nguyen, Q. K., Dissanayake, S., Ribeiro, J. M., and James, A. A. (2006). Genome-wide analysis of gene expression in adult Anopheles gambiae. *Insect Mol Biol* **15**, 1-12.

Marinotti, O., Nguyen, Q. K., Calvo, E., James, A. A., and Ribeiro, J. M. (2005). Microarray analysis of genes showing variable expression following a blood meal in Anopheles gambiae. *Insect Mol Biol* **14**, 365-373.

Masse, N. Y., Turner, G. C., and Jefferis, G. S. (2009). Olfactory information processing in Drosophila. *Curr Biol* **19**, R700-713.

Mboera, L. E. G., and Takken, W. (1997). Carbon dioxide chemotropism in mosquitoes (Diptera: Culicidae) and its potential in vector surveillance and management programmes. *Rev. Med. Vet. Entomol.* **85**, 355-368.

Mboera, L. E. G., Takken, W., Mdira, K. Y., Chuwa, G. J., and Pickett, J. A. (2000). Oviposition and Behavioral Responses of Culex quinquefasciatus to Skatole and Synthetic Oviposition Pheromone in Tanzania. *Journal of Chemical Ecology* **26**, 1193-1203.

McBride, C. S. (2007). Rapid evolution of smell and taste receptor genes during host specialization in Drosophila sechellia. *Proc Natl Acad Sci U S A* **104**, 4996-5001.

McIver, S. B. (1982). Sensilla mosquitoes (Diptera: Culicidae). *J Med Entomol* **19**, 489-535.

McKenna, M. P., Hekmat Scafe, D. S., Gaines, P., and Carlson, J. R. (1994). Putative Drosophila pheromone-binding proteins expressed in a subregion of the olfactory system. *J Biol Chem* **269**, 16340-16347.

Meijerink, J., Braks, M. A., Braak, A. A., Adam, W., Dekker, T., Posthumus, M. A., Beek, T. A., and Van Loon, J. J. A. (2000). Identification of olfactory stimulants for *Anopheles gambiae* from human sweat samples. *Journal of Chemical Ecology* **26**, 1367-1382.

Meijerink, J., Braks, M. A., and Van Loon, J. J. (2001). Olfactory receptors on the antennae of the malaria mosquito Anopheles gambiae are sensitive to ammonia and other sweat-borne components. *J Insect Physiol* **47**, 455-464.

Meijerink, J., Braks, M. A. H., Brack, A. A., Adam, W., Dekker, T.,

Posthumus, M. A., Van Beek, T. A., and Van Loon, J. J. A. (2000). Identification of Olfactory Stimulants for Anopheles gambiae from Human Sweat Samples. *Journal of Chemical Ecology* **26**, 1367-1382.

Meijerink, J., Braks, M. A. H., and van Loon, J. J. A. (2001). Olfactory receptors on the antennae of the malaria mosquito *Anopheles gambiae* are sensitive to ammonia and other sweat-borne components. *Journal of Insect Physiology* **47**, 455-464.

Melo, A. C., Rutzler, M., Pitts, R. J., and Zwiebel, L. J. (2004). Identification of a chemosensory receptor from the yellow fever mosquito, Aedes aegypti, that is highly conserved and expressed in olfactory and gustatory organs. *Chem Senses* **29**, 403-410.

Meola, S. M., and Sittertz-Bhatkar, H. (2002). Neuroendocrine modulation of olfactory sensory neuron signal reception via axo-dendritic synapses in the antennae of the mosquito, Aedes aegypti. *J Mol Neurosci* **18**, 239-245.

Meola, S. M., Sittertz-Bhatkar, H., Pendleton, M. W., Meola, R. W., Knight, W. P., and Olson, J. (2000). Ultrastructural analysis of neurosecretory cells in the antennae of the mosquito, Culex salinarius (Diptera: Culicidae). *J Mol Neurosci* **14**, 17-25.

Millar, G. J., Chaney, J. D., Beehler, J. W., and Mulla, M. S. (1994). Interaction of the *Culex quinquefasciatus* egg raft pheromone with a natural chemical associated with oviposition sites. *Journal of the American Mosquito Control Association* **10**, 374-379.

Mombaerts, P. (1999). Molecular biology of odorant receptors in vertebrates. *Annu. Rev. Neurosci.* **22**, 487-509.

Mombaerts, P. (2004). Odorant receptor gene choice in olfactory sensory neurons: the one receptor–one neuron hypothesis revisited. *Curr Opin Neurobiol* **14**, 31-36.

Moore, S. J., Darling, S. T., Sihuincha, M., Padilla, N., and Devine, G. J. (2007). A low-cost repellent for malaria vectors in the Americas: results of two field trials in Guatemala and Peru. *Malar J* **6**, 101.

Moore, S. J., Davies, C. R., Hill, N., and Cameron, M. M. (2007). Are mosquitoes diverted from repellent-using individuals to non-users? Results of a field study in Bolivia. *Trop Med Int Health* **12**, 532-539.

Moore, S. J., Lenglet, A., and Hill, N. (2002). Field evaluation of three plant-based insect repellents against malaria vectors in Vaca Diez Province, the Bolivian Amazon. *J Am Mosq Control Assoc* **18**, 107-110.

Mortazavi, A., Williams, B. A., McCue, K., Schaeffer, L., and Wold, B. (2008). Mapping and quantifying mammalian transcriptomes by RNA-Seq. *Nat Methods* **5**, 621-628.

Muller, H. M., Catteruccia, F., Vizioli, J., della Torre, A., and Crisanti, A. (1995). Constitutive and blood meal-induced trypsin genes in Anopheles gambiae. *Exp Parasitol* **81**, 371-385.

Nakagawa, T., Sakurai, T., Nishioka, T., and Touhara, K. (2005). Insect sex-pheromone signals mediated by specific combinations of olfactory receptors. *Science* **307**, 1638-1642.

Neira-Oviedo, M., Tsyganov-Bodounov, A., Lycett, G. J., Kokoza, V., Raikhel, A. S., and Krzywinski, J. (2010). The RNA-Seq approach to studying the expression of mosquito mitochondrial genes. *Insect Mol Biol*

Neuhaus, E. M., Gisselmann, G., Zhang, W., Dooley, R., Stortkuhl, K., and Hatt, H. (2005). Odorant receptor heterodimerization in the olfactory system of Drosophila melanogaster. *Nat Neurosci* **8**, 15-17.

Niemann, S., Spehr, N., Van Aken, H., Morgenstern, E., Peters, G., Herrmann, M., and Kehrel, B. E. (2004). Soluble fibrin is the main mediator of Staphylococcus aureus adhesion to platelets. *Circulation* **110**, 193-200.

Nozawa, M., and Nei, M. (2007). Evolutionary dynamics of olfactory receptor genes in Drosophila species. *Proc Natl Acad Sci U S A* **104**, 7122-7127.

O'Gower, A. K. (1963). Environmental stimuli and the oviposition behaviour of Aedes aegypti var. queenslandis Theobald (Diptera, Culicidae). *Animal Behaviour* **11**, 189-197.

Ohara, H., Nikaido, M., Date-Ito, A., Mogi, K., Okamura, H., Okada, N., Takeuchi, Y., Mori, Y., and Hagino-Yamagishi, K. (2009). Conserved repertoire of orthologous vomeronasal type 1 receptor genes in ruminant species. *BMC Evol Biol* **9**, 233.

Olsen, S. R., and Wilson, R. I. (2008). Lateral presynaptic inhibition mediates gain control in an olfactory circuit. *Nature* **452**, 956-960.

Paluch, G., Bartholomay, L., and Coats, J. (2010). Mosquito repellents: a review of chemical structure diversity and olfaction. *Pest Manag Sci* **66**, 925-935.

Pelletier, J., Guidolin, A., Syed, Z., Cornel, A. J., and Leal, W. S. (2010). Knockdown of a mosquito odorant-binding protein involved in the sensitive detection of oviposition attractants. *J Chem Ecol* **36**, 245-248.

Pelletier, J., Hughes, D. T., Luetje, C. W., and Leal, W. S. (2010). An odorant receptor from the southern house mosquito Culex pipiens quinquefasciatus sensitive to oviposition attractants. *PLoS One* **5**, e10090.

Pennetier, C., Warren, B., Dabire, K. R., Russell, I. J., and Gibson, G. (2010). "Singing on the wing" as a mechanism for species recognition in the malarial mosquito Anopheles gambiae. *Curr Biol* **20**, 131-136.

Pitts, R. J., Fox, A. N., and Zwiebel, L. J. (2004). A highly conserved candidate chemoreceptor expressed in both olfactory and gustatory tissues in the malaria vector Anopheles gambiae. *Proc Natl Acad Sci U S A* **101**, 5058-5063.

Pitts, R. J., and Zwiebel, L. J. (2006). Antennal sensilla of two female anopheline sibling species with differing host ranges. *Malar J* **5**, 26.

Ponnusamy, L., Xu, N., Nojima, S., Wesson, D. M., Schal, C., and Apperson, C. S. (2008). Identification of bacteria and bacteria-associated chemical cues that mediate oviposition site preferences by Aedes aegypti. *Proc Natl Acad Sci U S A* **105**, 9262-9267.

Poonam, S., Paily, K. P., and Balaraman, K. (2002). Oviposition attractancy of bacterial culture filtrates: response of Culex quinquefasciatus. *Mem Inst Oswaldo Cruz* **97**, 359-362.

Qiu, Y. T., Smallegange, R. C., Hoppe, S., van Loon, J. J., Bakker, E. J., and Takken, W. (2004). Behavioural and electrophysiological responses of the malaria mosquito Anopheles gambiae Giles sensu stricto (Diptera: Culicidae) to human skin emanations. *Med Vet Entomol* **18**, 429-438.

Robertson, H. M., Gadau, J., and Wanner, K. W. (2010). The insect chemoreceptor superfamily of the parasitoid jewel wasp Nasonia vitripennis. *Insect Mol Biol* **19 Suppl 1**, 121-136.

Robertson, H. M., and Kent, L. B. (2009). Evolution of the gene lineage encoding the carbon dioxide receptor in insects. *J Insect Sci* **9**, 19.

Robertson, H. M., and Wanner, K. W. (2006). The chemoreceptor superfamily in the honey bee, Apis mellifera: expansion of the odorant, but not gustatory, receptor family. *Genome Res* **16**, 1395-1403.

Robinson, M. D., and Oshlack, A. (2010). A scaling normalization method

for differential expression analysis of RNA-seq data. *Genome Biol* **11**, R25.

Roche-King, J., Christensen, T. A., and Hildebrand, J. G. (2000). Response characteristics of an identified, sexually dimorphic olfactory glomerulus. *Journal of Neuroscience* **20**, 2391-2399.

Rogers, M. E., Jani, M. K., and Vogt, R. G. (1999). An olfactory-specific glutathione-S-transferase in the sphinx moth Manduca sexta. *J Exp Biol* **202**, 1625-1637.

Rutzler, M., and Zwiebel, L. (2005). Molecular biology of insect olfaction:recent progress and conceptual models. *J Comp Physiol A Neuroethol Sens Neural Behav Physiol* 1-14.

Sachs, J., and Malaney, P. (2002). The economic and social burden of malaria. *Nature* **415**, 680-685.

Sarov-Blat, L., So, W. V., Liu, L., and Rosbash, M. (2000). The Drosophila takeout gene is a novel molecular link between circadian rhythms and feeding behavior. *Cell* **101**, 647-656.

Sato, K., Pellegrino, M., Nakagawa, T., Nakagawa, T., Vosshall, L. B., and Touhara, K. (2008). Insect olfactory receptors are heteromeric ligand-gated ion channels. *Nature*

Sato, K., and Touhara, K. (2009). Insect olfaction: receptors, signal transduction, and behavior. *Results Probl Cell Differ* **47**, 121-138.

Schmelz, E. A., Alborn, H. T., Engelberth, J., and Tumlinson, J. H. (2003). Nitrogen deficiency increases volicitin-induced volatile emission, jasmonic acid accumulation, and ethylene sensitivity in maize. *Plant Physiol* **133**, 295-306.

Schmiedeberg, K., Shirokova, E., Weber, H. P., Schilling, B., Meyerhof, W., and Krautwurst, D. (2007). Structural determinants of odorant recognition by the human olfactory receptors OR1A1 and OR1A2. *J Struct Biol* **159**, 400-412.

Schymura, D., Forstner, M., Schultze, A., Krober, T., Swevers, L., Iatrou, K., and Krieger, J. (2010). Antennal expression pattern of two olfactory receptors and an odorant binding protein implicated in host odor detection by the malaria vector Anopheles gambiae. *Int J Biol Sci* **6**, 614-626.

Sharakhova, M. V., Hammond, M. P., Lobo, N. F., Krzywinski, J., Unger, M. F., Hillenmeyer, M. E., Bruggner, R. V., Birney, E., and Collins, F. H.

(2007). Update of the Anopheles gambiae PEST genome assembly. *Genome Biol* **8**, R5.

Siju, K. P., Hansson, B. S., and Ignell, R. (2008). Immunocytochemical localization of serotonin in the central and peripheral chemosensory system of mosquitoes. *Arthropod Struct Dev* **37**, 248-259.

Siju, K. P., Hill, S. R., Hansson, B. S., and Ignell, R. (2010). Influence of blood meal on the responsiveness of olfactory receptor neurons in antennal sensilla trichodea of the yellow fever mosquito, Aedes aegypti. *J Insect Physiol* **56**, 659-665.

Singh, A. K., Gupta, S., Barnes, A., Carlson, J. M., and Ayers, J. K. (2007). Red blood cell erythropoietin, not plasma erythropoietin, concentrations correlate with changes in hematological indices in horses receiving a single dose of recombinant human erythropoietin by subcutaneous injection. *J Vet Pharmacol Ther* **30**, 175-178.

Smallegange, R. C., Qiu, Y. T., van Loon, J. J., and Takken, W. (2005). Synergism between ammonia, lactic acid and carboxylic acids as kairomones in the host-seeking behaviour of the malaria mosquito Anopheles gambiae sensu stricto (Diptera: Culicidae). *Chem Senses* **30**, 145-152.

Smallegange, R. C., Verhulst, N. O., and Takken, W. (2011). Sweaty skin: an invitation to bite? *Trends Parasitol*

Smart, R., Kiely, A., Beale, M., Vargas, E., Carraher, C., Kralicek, A. V., Christie, D. L., Chen, C., Newcomb, R. D., and Warr, C. G. (2008). Drosophila odorant receptors are novel seven transmembrane domain proteins that can signal independently of heterotrimeric G proteins. *Insect Biochem Mol Biol* **38**, 770-780.

Smith, B. H., and Getz, W. M. (1994). Nonpheromonal Olfactory Processing in Insects. *Annual Review of Entomology* **39**, 351-375.

Snow, R. W., Guerra, C. A., Noor, A. M., Myint, H. Y., and Hay, S. I. (2005). The global distribution of clinical episodes of Plasmodium falciparum malaria. *Nature* **434**, 214-217.

Spehr, J., Spehr, M., Hatt, H., and Wetzel, C. H. (2004). Subunit-specific P2X-receptor expression defines chemosensory properties of trigeminal neurons. *Eur J Neurosci* **19**, 2497-2510.

Spehr, M., and Hatt, H. (2004). hOR17-4 as a potential therapeutic target. *Drug News Perspect* **17**, 165-171.

Spehr, M., Schwane, K., Heilmann, S., Gisselmann, G., Hummel, T., and Hatt, H. (2004). Dual capacity of a human olfactory receptor. *Curr Biol* **14**, R832-833.

Spehr, M., Schwane, K., Riffell, J. A., Barbour, J., Zimmer, R. K., Neuhaus, E. M., and Hatt, H. (2004). Particulate adenylate cyclase plays a key role in human sperm olfactory receptor-mediated chemotaxis. *J Biol Chem* **279**, 40194-40203.

Sumba, L. A., Guda, T. O., Deng, A. L., Ahmed, H., Beier, J. C., and Knols, B. G. J. (2004). Mediation of oviposition site selection in the African malaria mosquito *Anopheles gambiae* (Diptera: Culicidae) by semiochemicals of microbial origin. *International Journal of Tropical Insect Science. 2004;* **24**, 260-265.

Sutcliffe, J. F. (1994). Sensory bases of attractancy: morphology of mosquito olfactory sensilla- - a review. *J Am Mosq Control Assoc* **10**, 309-315.

Syed, Z., and Leal, W. S. (2008). Mosquitoes smell and avoid the insect repellent DEET. *Proc Natl Acad Sci U S A* **105**, 13598-13603.

Syed, Z., and Leal, W. S. (2009). Acute olfactory response of Culex mosquitoes to a human- and bird-derived attractant. *Proc Natl Acad Sci U S A* **106**, 18803-18808.

t Hoen, P. A., Ariyurek, Y., Thygesen, H. H., Vreugdenhil, E., Vossen, R. H., de Menezes, R. X., Boer, J. M., van Ommen, G. J., and den Dunnen, J. T. (2008). Deep sequencing-based expression analysis shows major advances in robustness, resolution and inter-lab portability over five microarray platforms. *Nucleic Acids Res* **36**, e141.

Takken, W. (1991). The Role of Olfaction in Host-Seeking of Mosquitoes: A Review. *Insect Science Applications* **12**, 287-295.

Takken, W., and Knols, B. G. (1999). Odor-mediated behavior of Afrotropical malaria mosquitoes. *Annu Rev Entomol* **44**, 131-157.

Takken, W., van Loon, J. J., and Adam, W. (2001). Inhibition of host-seeking response and olfactory responsiveness in Anopheles gambiae following blood feeding. *J Insect Physiol* **47**, 303-310.

Tamura, K., Dudley, J., Nei, M., and Kumar, S. (2007). MEGA4: Molecular Evolutionary Genetics Analysis (MEGA) software version 4.0. *Mol Biol Evol* **24**, 1596-1599.

Tichy, A. L., Ray, A., and Carlson, J. R. (2008). A new Drosophila POU gene, pdm3, acts in odor receptor expression and axon targeting of olfactory neurons. *J Neurosci* **28**, 7121-7129.

Touhara, K., and Vosshall, L. B. (2009). Sensing odorants and pheromones with chemosensory receptors. *Annu Rev Physiol* **71**, 307-332.

Trigg, J. K. (1996). Evaluation of a eucalyptus-based repellent against Anopheles spp. in Tanzania. *J Am Mosq Control Assoc* **12**, 243-246.

van den Berg, H. (2009). Global status of DDT and its alternatives for use in vector control to prevent disease. *Environ Health Perspect* **117**, 1656-1663.

van der Goes van Naters, W., and Carlson, J. R. (2006). Insects as chemosensors of humans and crops. *Nature* **444**, 302-307.

Verhulst, N. O., Takken, W., Dicke, M., Schraa, G., and Smallegange, R. C. (2010). Chemical ecology of interactions between human skin microbiota and mosquitoes. *FEMS Microbiol Ecol* **74**, 1-9.

Vogt, R. G., and Riddiford, L. M. (1981). Pheromone binding and inactivation by moth antennae. *Nature* **293**, 161-163.

Vogt, R. G., and Riddiford, L. M. (1981). Pheremone binding and inactivation by moth antennae. *Nature* **293**, 161-163.

Vosshall, L. B. (2000). Olfaction in Drosophila. *Curr Opin Neurobiol* **10**, 498-503.

Vosshall, L. B., Amrein, H., Morozov, P. S., Rzhetsky, A., and Axel, R. (1999). A spatial map of olfactory receptor expression in the Drosophila antenna. *Cell* **96**, 725-736.

Vosshall, L. B., and Stocker, R. F. (2007). Molecular architecture of smell and taste in Drosophila. *Annu Rev Neurosci* **30**, 505-533.

Vosshall, L. B., Wong, A. M., and Axel, R. (2000). An olfactory sensory map in the fly brain. *Cell* **102**, 147-159.

Wang, G., Carey, A. F., Carlson, J. R., and Zwiebel, L. J. (2010). Molecular basis of odor coding in the malaria vector mosquito Anopheles gambiae. *Proc Natl Acad Sci U S A* **107**, 4418-4423.

Wang, Z., Gerstein, M., and Snyder, M. (2009). RNA-Seq: a revolutionary tool for transcriptomics. *Nat Rev Genet* **10**, 57-63.

Warr, E., Aguilar, R., Dong, Y., Mahairaki, V., and Dimopoulos, G. (2007). Spatial and sex-specific dissection of the Anopheles gambiae midgut transcriptome. *BMC Genomics* **8**, 37.

Weissenbock, H., Hubalek, Z., Bakonyi, T., and Nowotny, N. (2010). Zoonotic mosquito-borne flaviviruses: worldwide presence of agents with proven pathogenicity and potential candidates of future emerging diseases. *Vet Microbiol* **140**, 271-280.

Wistrand, M., Kall, L., and Sonnhammer, E. L. (2006). A general model of G protein-coupled receptor sequences and its application to detect remote homologs. *Protein Sci* **15**, 509-521.

Xia, Y., Wang, G., Buscariollo, D., Pitts, R. J., Wenger, H., and Zwiebel, L. J. (2008). The molecular and cellular basis of olfactory-driven behavior in Anopheles gambiae larvae. *Proc Natl Acad Sci U S A* **105**, 6433-6438.

Xia, Y., and Zwiebel, L. J. (2006). Identification and characterization of an odorant receptor from the West Nile virus mosquito, Culex quinquefasciatus. *Insect Biochem Mol Biol* **36**, 169-176.

Xu, P., Atkinson, R., Jones, D. N., and Smith, D. P. (2005). Drosophila OBP LUSH is required for activity of pheromone-sensitive neurons. *Neuron* **45**, 193-200.

Xu, P. X., Zwiebel, L. J., and Smith, D. P. (2003). Identification of a distinct family of genes encoding atypical odorant-binding proteins in the malaria vector mosquito, Anopheles gambiae. *Insect Mol Biol* **12**, 549-560.

Zdobnov, E. M., and Bork, P. (2007). Quantification of insect genome divergence. *Trends Genet* **23**, 16-20.

Zhainazarov, A. B., Spehr, M., Wetzel, C. H., Hatt, H., and Ache, B. W. (2004). Modulation of the olfactory CNG channel by Ptdlns(3,4,5)P3. *J Membr Biol* **201**, 51-57.

Zwiebel, L. J., and Takken, W. (2004). Olfactory regulation of mosquito-host interactions. *Insect Biochem Mol Biol* **34**, 645-652.